Flying Wing UAV for Surveillance and Object Tracking

Team: Kennesaw High Altitude Lightweight Inspection Device

Authors:

Paul Horne: Technical Aircraft Expert

Jared Lasley: Data Analyst, Mathematician

Kristen Padgett: Project Manager, Systems Engineer

Scott Semmelink: Project Coordinator, Technical Reviewer

Advisors:

Dr. Adeel Khalid, Professor in Aerospace Engineering

John Witzigreuter, Inspired Products, LLC

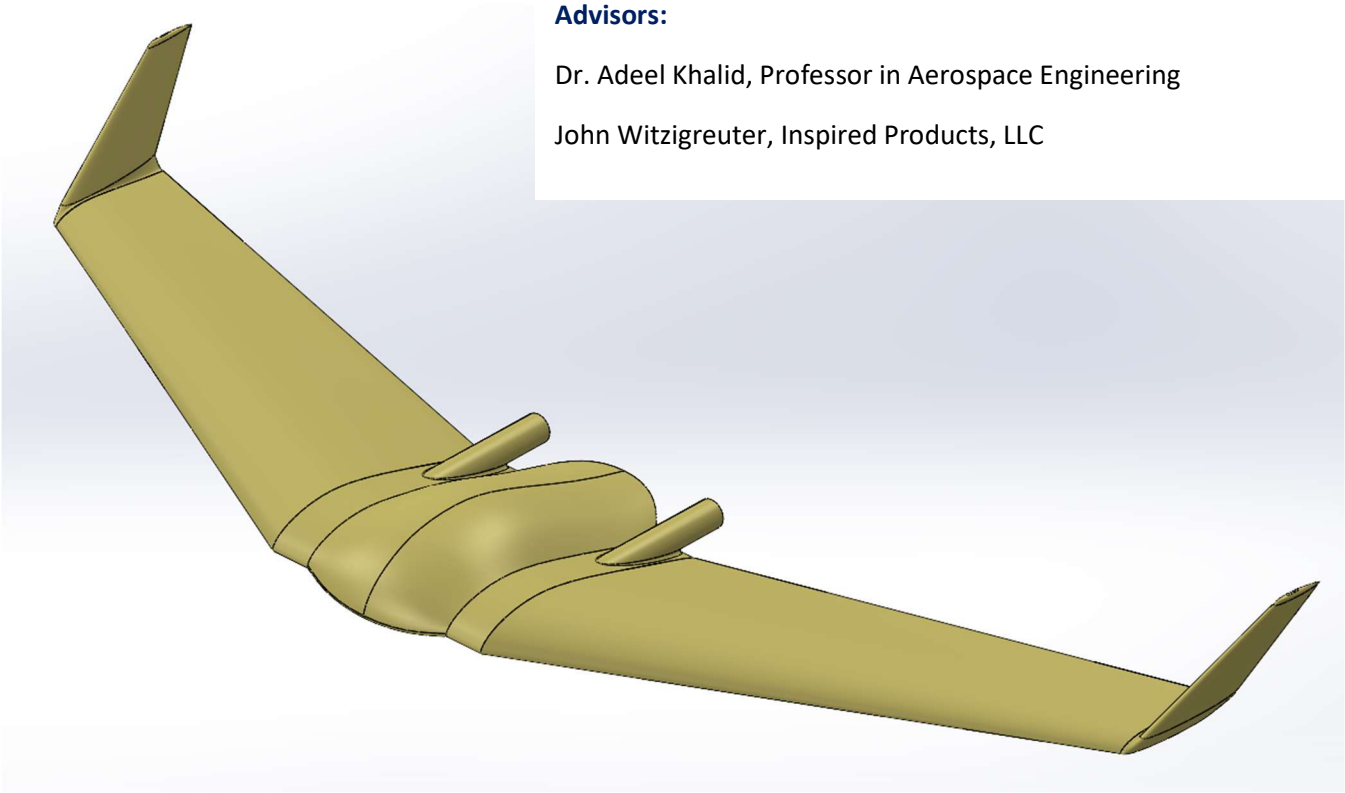

Executive Summary:

Unmanned aerial vehicles (UAV) have become ubiquitous in recent years due to their adaptability and ease of use. Surveillance UAVs in particular have seen increased interest and usage by law enforcement, civilian security, surveying, and federal services. The increased interest has led to the development of UAVs with increased endurance and payload capacity. Further as many of the applications of surveillance drones involve heightened security requirements, an aircraft of domestic make is preferential to many organizations.

With this demand in mind, Inspired Products, LLC put forth a request for assistance in the design and testing of a surveillance UAV. More specifically, Inspired Products, LLC has mandated that the UAV be of a flying wing configuration in order to increase endurance. This flying wing UAV must be able to remain aloft for extended periods while also possessing a payload capacity which is sufficient to carry cameras and other sensory equipment. Additionally, the UAV must possess removable wings which remain within a given span as set forth in the requirements given below (Section 3.1: Requirements).

The development of the Flying Wing UAV was an iterative process in which various areas were considered and analyzed. The Flying Wing UAV's fuselage is 3D-printed to allow for rapid prototyping and reconfiguration to allow for testing of different payload configurations in short order. The wings and winglets are constructed of high-density foam to preserve weight and provide sufficient durability (Figure 72). Initial airfoil testing was performed utilizing computational fluid dynamics (CFD) initially in the xflr5 software (Chapter 4: Airfoil Selection) and then further analyzed in Solidworks (Chapter 5: Airfoil Analysis). After analysis, the Eppler 344 was selected as the root airfoil and the Eppler 325 as the tip airfoil. The winglets are a GOE 330 airfoil. Analysis of the final model was performed utilizing CFD in solid works (Chapter 8: Final Aircraft design) and it was found to be sufficient to satisfy the requirements. Confirmation of the CFD results were obtained via the testing of a scale model in the Kennesaw State University sub-sonic wind tunnel (Chapter 10: Wind Tunnel Testing). The results of these test confirmed those obtained through CFD.

Other aspects were also considered in the course of the project such as budgetary considerations and avionics selection. The total calculated cost of the aircraft comes out to $978.69 for the materials and components required (Section 3.6: Budget). The cost of fabricating the aircraft was generously covered by our company sponsor. The avionics for the UAV selected were selected primarily by the sponsor. The UAV will utilize a receiver and transmitter with built in telemetry to provide guidance. Additionally, the aircraft utilizes two 10,000 mAh batteries and retractable propellors to allow for belly landings (Section 9.2: Avionics Selection).

The development of this Flying Wing UAV will provide organizations around the nation with a UAV platform that improves upon current offerings via incrementally iteration in both endurance and payload capacity. This has been achieved through the use of the theoretical and practical skills we have gained as Aerospace Engineering students at Kennesaw State University, whether it be through hand calculations, use of computational fluid dynamics capable software, or wind-tunnel experimentation.

Table of Contents

List of Figures

List of Tables

Chapter 1: Flying Wing UAV for Surveillance and Object Tracking

1.1) Introduction:

The goal of this project is to design, build, and test a flying wing unmanned aerial vehicle (UAV) prototype that will replace a traditional high-wing twin motor airframe. This UAV will be further developed and used for surveillance and object tracking. Although there are existing, foreign-made models that can meet the requirements for the UAV, this design will fulfill the desire for end-users to purchase an American-made product.

The UAV will consist of three major parts—the fuselage, and the left and right wings. The fuselage will hold the battery, motors, communication equipment, and payload. Although there is an existing design for the fuselage, supplied by the client, it has been changed slightly to meet the requirements of the aircraft. The wings can be removed and reattached to the UAV for ease of transportation in a field environment. The wings, elevons, and winglets are the focus of the design, per the client's request. The wings have been analyzed, using both flow analysis and wind tunnel testing. Construction of the prototype was in the initial schedule, but due to limited time we were not able to complete construction and field testing of the UAV before the submission of this project.

1.2) System Overview:

The client provided us with the description of their product as follows: The central fuselage is printed from polylactic acid (PLA) utilizing a 3D printer. Internal components such as the batteries, receivers, and all other flight electronics are placed into the fuselage. The top and bottom half of the wings are cut from high density foam using a foam cutter. The wings then have a carbon fiber rod inserted between the two halves before being sealed together using a bonding agent and tape to seal the seams. The control surfaces are cut from high density foam using a foam cutter. The control surfaces are then attached to the main wing using plastic hinges and to the controlling servo via a control arm. Finally, the wings are attached to the main fuselage via the carbon fiber rod embedded in the wing.

1.3) Objective:

The primary objectives of this project are to design, 3D print, and wind tunnel test our flying wing UAV. To be qualified as successful the design must meet design requirements as outlined in section 3.2. These requirements include but are not limited to a maximum wingspan of 6 feet, a maximum gross weight of 15 lbs., and minimum payload of 3 lbs.

1.4) Justification:

There are several motivations behind the design of this UAV. A primary concern of our customer is the country of origin of the aircraft. Currently one of the most popular aerial photography UAV platforms is the Believer, which is designed and manufactured in China. While the Believer is a capable surveying aircraft there are multiple applications of a sensitive nature such as national security, military operations, or law enforcement which require a domestically produced solution. In addition to

customers which require a domestically produced product for security concerns, there is a large subset of Americans which support the “Buy American” movement. In a poll of 2,201 U.S. adults by Morning Consult 84% of respondents indicated that they would purchase an American made product over a foreign manufactured product of the same quality. Further 52% of respondents indicated that they would be willing to pay 66% more for an American produced product than for a foreign produced product of equivalent quality [17].

In addition to designing a domestically produced product it is the goal of this aircraft to improve upon current market offerings in terms of endurance and payload capacity. This effort to improve upon the characteristics of UAVs of similar purpose such as the Believer is what led to the development of requirements as stated in section 3.2.

1.5) Mission Profile

The Flying Wing UAV has a mission profile consisting of launch and climb, cruise to target area, conduct surveillance over the target, cruise home, descent, and landing. The mission profile is represented visually in the figure below.

Table 1: Aircraft Performance Parameters

Parameter	Performance Value
Cruise Speed	20 m/s
Climb Rate	18.25 m/s
Range	123.12 km
Endurance	1.71 hr

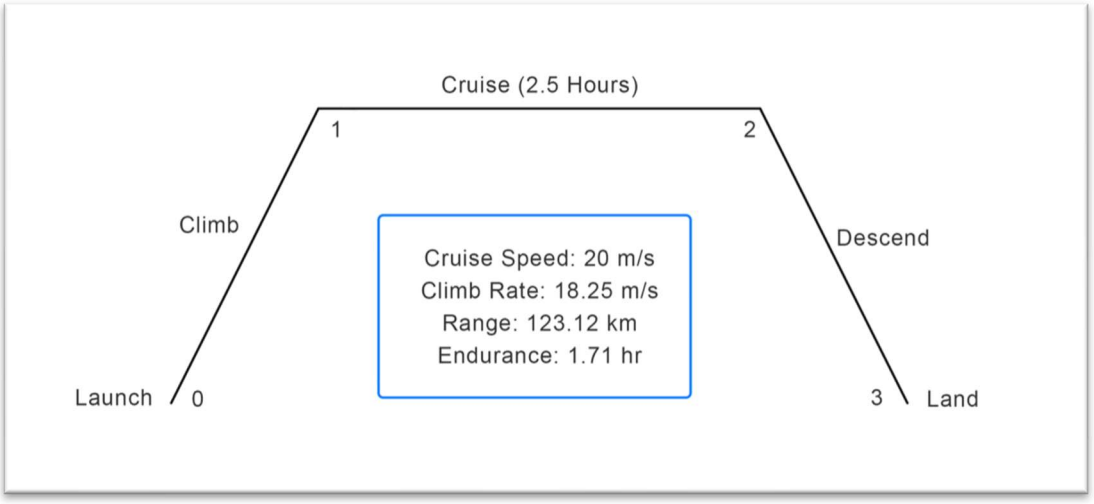

Figure 1: Mission Profile of the Proposed Unmanned Aerial Vehicle

Chapter 2: Literature Review

2.1) US Patent 9550567

One of the challenges faced during this project has been determining the most feasible method for takeoff and landing. US Patent 9550567 is a UAV design established by Amazon Technologies, Inc. to deliver packages from distribution centers to customers [7]. This design has overcome the need for any hand launch or bungee launch mechanism buy utilizing a vertical-takeoff-and-landing (VTOL) design. The uniqueness of this design is its folding concept. The wing and tail fold in to allow for quadrocopter style control for takeoff and landing while still allowing the craft to fly on a fixed wing during cruising conditions.

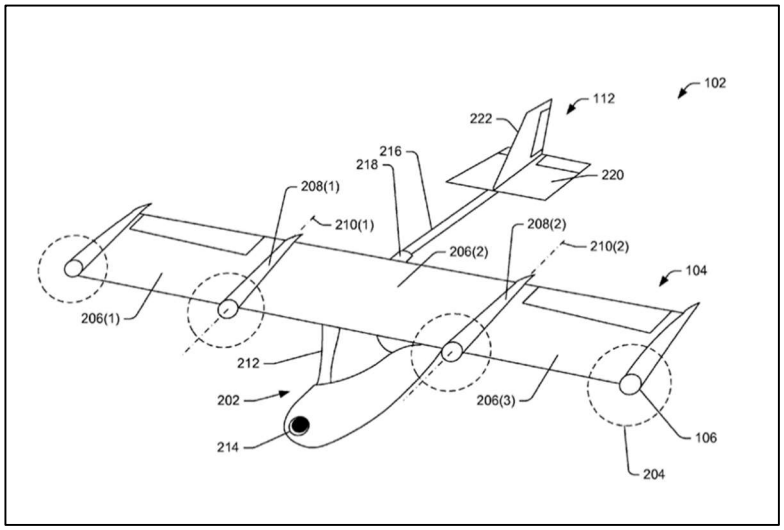

Figure 2: Folding UAV Design [7]

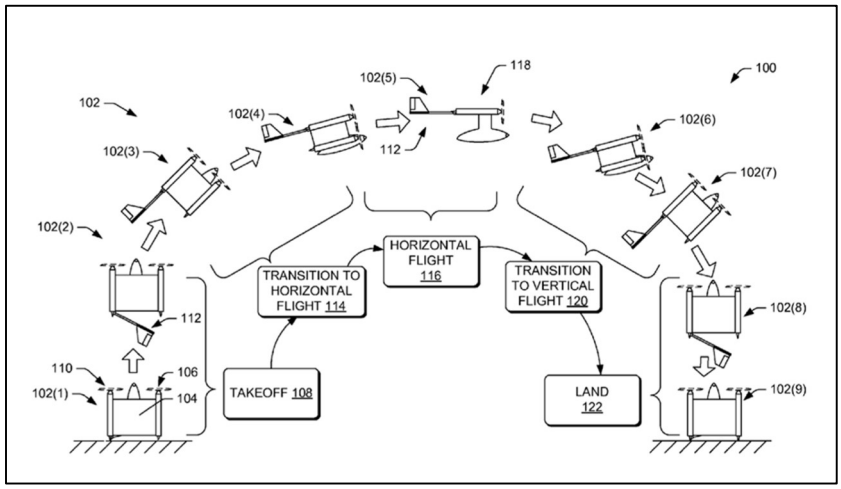

Figure 3: Folding UAV - VTOL Transitions [7]

2.2) Penguin C UAS

The most challenging design requirement encountered thus far has been that of the 2.5-hour endurance. The team at UAV Factory developed the Penguin C UAS specifically for high endurance missions. The Penguin C is rated for an endurance of up to 20 hours and holds a world record for achieving a 54.5-hour flight in 2012 [23]. While the Penguin C is a much larger aircraft at a wingspan of 3.3 meters and a maximum takeoff weight of 50.7 lbs, the primary factor in its ability to achieve such a long endurance is the propulsion system. The Penguin has an electronic fuel injected combustion engine that runs on 98 octane gasoline. This fuel has a much higher energy density than that of lithium-polymer batteries to allow for greater thrust-to-weight ratio and lower wing loading.

Figure 4: Penguin C UAS [23]

2.3) C-Astral Bramor mSX

The Bramor mSX from C-Astral, a UAV targeted at the agricultural industry, is very similar in specification to the design goals of this project. With a 1.55-meter wingspan, a 15 m/s cruise velocity, a 30 m/s maximum velocity, and a maximum endurance of 3 hours, the Bramor mSX is a great example aircraft for our project. While C-Astral has not released much information in regard to the electronics used in the aircraft, the clear advantage comes from the airframe design. A composite of carbon fiber and kevlar results in an airframe that is very lightweight with a very smooth exterior to reduce drag.

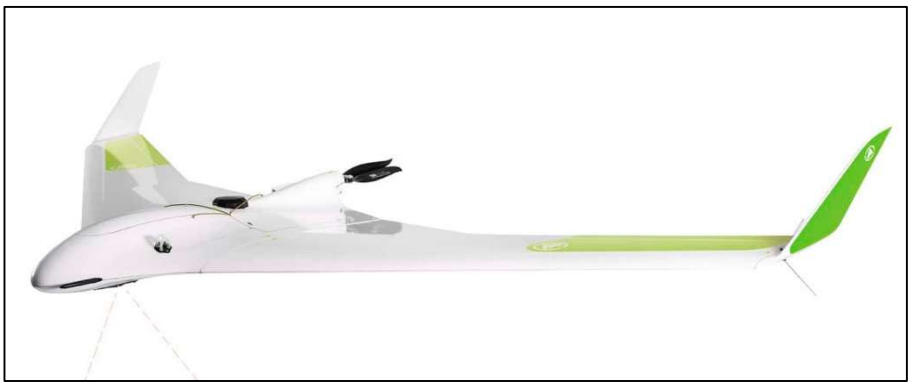

Figure 5: C-Astral Bramor mSX [4]

Figure 6: C-Astral Bramor mSX - Top View [4]

2.4) senseFly eBee X

The senseFly eBee X is a mapping drone with a 90-minute maximum endurance. The UAV is made of foam and has a 1.16m wingspan. The maximum takeoff weight of 3.6 lbs is very lightweight with respect to the size of UAV. This results in a very low wing loading which allows for increased endurance. The very low payload capacity and 4900mah 4s lithium-polymer battery attribute to the low weight of the aircraft. The eBee X is also limited in its camera and sensor options due to its belly-landing requirements.

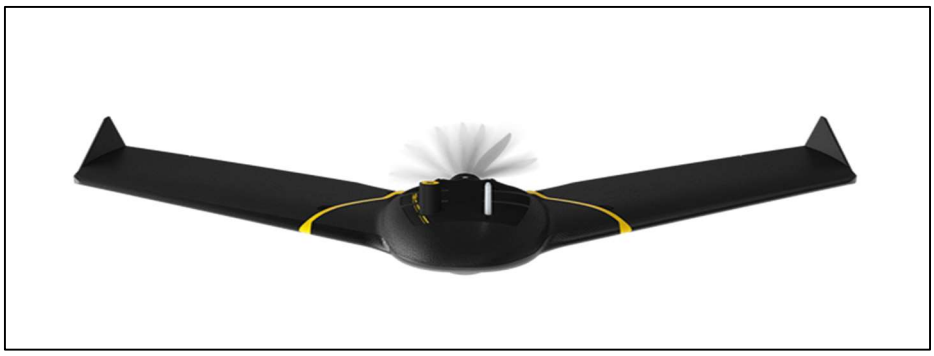

Figure 7: senseFly eBee X Front View [6]

Figure 8: senseFly eBee X Top View [6]

2.5) Nest of Dragons:

Koen Van de Kerckhove is a Belgian flight hobbyist and overall tinkerer who has an interest in all machines unusual. Koen is also a webmaster who created and runs the website http://www.nestofdragons.net/. He has gathered a lot of information on flying wings in general, but has a section dedicated to the Horten flying wings. He even has an excel tool, designed for his site by Marko Stamenovic, that will assist in the design of a Horten style flying wing [24]. This website provided the knowledge that inspired us to design the first wing configuration that achieved the 15-pound lift requirement.

2.6) MH Aerotools:

Dr. Martin Hepperle has a PhD in Aerospace Engineering and operates a website dedicated to the aerodynamics of model aircraft. He has a good bit of information on flying wings, reflex airfoils and the

stability of a flying wing. His website, https://www.mh-aerotools.de/airfoils/index.htm [11], was very helpful in directing us to what characteristics to look for when selecting an airfoil for a flying wing.

2.7) Design and Construction of a Remote Piloted Flying Wing:

Design and Construction of a Remote Piloted Flying Wing was a bachelors thesis written by eight students of the Worcester Polytechnic Institute in 1994. It was a useful tool in seeing the design process of a flying wing [5]. Although a little outdated as far as lacking newer flying wing airfoil developments, it was still very relative to the flying wing design process today.

2.8) Design, Build and Fly a Flying Wing:

This was a recently published article in the *Athens Journal of Technology and Engineering* in 2018. The article documents, the design, build and flight of a flying wing, as implied by the title. This was useful as a starting point for our design as it was a recent effort of college students with similar levels of experience in the field of aerospace engineering [10].

2.9) Aircraft Winglet Design: Increasing the Aerodynamic Efficiency of a Wing:

This was a student published thesis that contained their CFD based analysis of different wing tip designs and their effectiveness. Devices examined were split-tip, spiroid, blended, fenced, and sharklet designs. The sharklet design proved to be the most beneficial, however, it did not fit our design due to the large tip chord on our design [9].

Chapter 3: Project Management

3.1) Requirements:

Table 2 shows the contractual level requirements that were provided by the customer. On the far left, CON ID is a value given to each contractual requirement to provide a means of identifying and linking requirements as they are developed. Once our team received the contractual requirements, we were then able to develop the high-level systems requirements. The high-level systems requirements were broken up into different categories—Performance, Design, Safety, Functional, and Physical Constraints. Performance requirements are those that define how well a task is to be performed. Design requirements are essential limitations in the aircraft design and composition. They are often known as "Physical Requirements" as well because they describe the physical boundaries of the system. Safety Requirements are developed to ensure that any potential risk of harm to an individual is mitigated during the design, fabrication, and test phases of the project. Functional requirements define the qualities that the product must have and are typically derived from customer objectives and requirements. Lastly, physical constraints are requirements that define any limitations in the physical design that could be due to test equipment, environmental conditions, design equipment, or other limiting factors that arise during the design process [8]. Each of these requirements can be seen in Tables 2 through 6 below.

Table 8 shows action items that will need to be resolved. Action items are used to provide clarification on systems requirements that are unclear or may pose an issue. For example, the first action item, AI0001 in Table 8, is listed to obtain information about which axis the velocity of 30 m/s is in given from the contractual requirement.

Risk items, represented by RI, are objects that pose a risk in being successful when tested. Each risk item is given a value represented by RI ID. A risk level is also associated with each RI object, which can be low, medium, or high. A risk would mean that there is potential that the current design would not meet the contractual or system requirement(s). Below are the probabilities associated to each risk ranking. Let X represent the probability of failure.

- Low: $X \leq 25\%$
- Medium: $25\% < X < 90\%$
- High: $X \geq 90\%$

An example of a risk item can be seen in Table 9 object RI0001. There is a possibility that neither the hand launch nor bungee launch will work. A medium risk has been designated to this object and a risk reduction effort has been added. Because the customer requirement has stated either a hand or bungee launch, there is a chance that the contractual requirement may not be met.

It is important to note that the requirements have changed throughout the design process, specifically the high-level systems requirements. There have also been adjustments in requirements at the contractual level. Writing requirements is an iterative process so the requirements have changed over the course of the project.

Table 2: Contractual Requirements

CON REQ ID	Requirement	AI ID Assoc.	RI ID Assoc.	Notes
CON0001	The UAV aircraft shall be a flying wing design.			A flying wing is a tailless fixed-wing aircraft that has no definite fuselage, with its crew, payload, fuel, and equipment housed inside the main wing structure.
CON0002	The flying wing aircraft shall obtain speeds up to 30 m/s in the longitudinal axis.	**AI0001**		
CON0003	The flying wing aircraft shall operate in cruising speed for a maximum of 2.5 hours.			In aviation, endurance is the maximum length of time that an aircraft can spend in cruising flight.
CON0004	The flying wing aircraft shall be launched using surgical tubing.	**AI0002**	**RI0001**	
CON0004	The flying wing aircraft shall perform a belly landing.			
CON0005	The flying wing aircraft control surfaces shall operate within +3G's and -2G's.			Maunverability is the window of when your control surfaces will function properly.
CON0006	The flying wing aircraft shall have a payload of less than 3 lbs.	**AI0003**		The maximum weight at which the pilot is allowed to attempt to take off, due to structural or other limits. Assumption: Payload is included in max gross weight.
CON0007	The flying wing aircraft shall not exceed a maximum gross weight of 15 lbs.			
CON0008	The flying wing aircraft shall have a distance of 6 ft between each wingtip.			The wingspan (or just span) of a bird or an airplane is the distance from one wingtip to the other wingtip.
CON0009	The flying wing aircraft shall be powered by a motor pusher design.			
CON0010	The flying wing aircraft shall be powered by 2 motors.			
CON0011	The flying wing aircraft shall have winglets.			

Table 3: High Level Systems Requirements: Performance

SYS REQ ID	Requirement	AI ID Link	RI ID Link	Notes
Performance Requirements				
PR0001	The flying wing aircraft shall have a distance of 18 inches between the leading and trailing edge at the root of the wing.			Chord length: Distance between leading and trailing edge.
PR0002	The flying wing aircraft shall have a distance of 6 inches between the leading and trailing edge at the tip of the wing.	AI0004		Chord length: Distance between leading and trailing edge.
PR0003	The flying wing aircraft wings shall be twisted at -3 degrees to the horizontal.			Recommended starting point for twist given in the aircraft design textbook.
PR0004	The leading edge of the flying wing aircraft wings shall be swept back at an angle of 30 degrees relative to the lateral axis.	AI0005		
PR0005	The flying wing aircraft shall have a winglet height of 6 inches.	AI0006		
PR0006	The flying wing aircraft shall have winglets with a cant angle of 45 degrees to the horizontal.	AI0007		
PR0007	The flying wing aircraft shall have a root to tip ratio of 0.3.			Taper ratio: ratio of root to tip.

Table 4: High Level Systems Requirements: Design

SYS REQ ID	Requirement	AI ID Link	RI ID Link	Notes
Design Requirements				
DR0001	The flying wing aircraft shall be a blended body wing and fuselage design.			
DR0002	The flying wing aircraft shall have servos mounted in the root of the wing.			
DR0003	The flying wing aircraft shall have two 12x10 folding propellers.		RI0002	
DR0004	The flying wing aircraft shall have a monokote skin covering.			
DR0005	The flying wing aircraft wings shall be composed of XPS foam cuttings.	AI0008		
DR0006	The flying wing aircraft shall have hollow tubes inside the wings.			The hollow tube design helps reduce weight and increases efficiency.
DR0007	The flying wing aircraft shall be controlled using a DX6E 6-Channel DSMX Transmitter.			
DR0008	The flying wing aircraft shall have two MN4012 KV480 motors.			
DR0009	The flying win aircraft shall be powered by two Turnigy 10 amp 4S batteries.		RI0003	
DR0010	The flying wing aircraft shall have two 150oz-in micro servos.			
DR0011	The flying wing aircraft shall have four 24" servo extension leads.			
DR0012	The flying wing aircraft shall have the two motors mounted within the fuselage.			
DR0013	The flying wing aircraft shall have the two batteries mounted within the fuselage.			
DR0014	The flying wing aircraft shall have the surveillance gear mounted within the fuselage.	AI0009		
DR0015	The flying wing aircraft shall have the servo extension leads mounted within the fuselage.			

Table 5: High Level Systems Requirements: Safety

SYS REQ ID	Requirement	AI ID Link	RI ID Link	Notes
Safety Requirements				
SR0001	The flying wing aircraft shall be a two-man hand launch.			Safety concern: Propellers cutting launcher's hands.
SR0002	The flying wing aircraft fabricated design shall be tested at Cobb County RC Field located in Acworth, GA.			To ensure a safe flying envrionment that will not disturb other aircraft or potentiall harm individuals on the ground.

Table 6: High Level Systems Requirements: Functional

SYS REQ ID	Requirement	AI ID Link	RI ID Link	Notes
Functional Requirements				
FR0001	The flying wing aircraft shall perform surveillance and object tracking.			
FR0002	The flying wing aircraft shall have a low drag and high lift configuration.			
FR0003	The flying wing aircraft shall have CFD analysis performed on the overall design.			
FR0004	The flying wing aircraft wing design shall be cut using sponsor provided foam cutter.			Originally, we were going to use KSU aero lab foam cutter but adjustments were made to use a foam cutter from sponsor.
FR0006	The flying wing aircraft shall be tested in the KSU aero lab wind-tunnel.			
FR0007	The flying wing aircraft shall have a successful test flight.		RI0004	

Table 7: High Level Systems Requirements: Physical Constraints

SYS REQ ID	Requirement	AI ID Link	RI ID Link	Notes
Physical Constraints				
PC0002	The flying wing aircraft shall be 3D printed as a scale model for wind tunnel testing.			Full size UAV design is too large for testing.
PC0003	The flying wing aircraft 3D model shall be no larger than 1 ft x 1 ft in size.			Limitation of wind tunnel size.

Table 8: Action Items

AI ID	Assigned To	Date Assigned	Reference REQ	Action Item	Resolution	Date Resolved
AI0001	Kristen	1/25/2021	**CON0002**	Determine axis of velocity (assumed longitudual).	Velocity is in the logitudinal	2/4/2021
AI0002	Kristen	1/25/2021	**CON0004**	Determine most feasible method for launch (bungee/hand launch)	Hand Launch: Only one battery used for field testing	4/18/2021
AI0003	Kristen	1/25/2021	**CON0006**	Determine if max weight will include payload of less than 3 lbs.	Max weight does include payload.	2/4/2021
AI0004	Scott/Paul	2/20/2021	**PR0002**	Determine if 6 inches of chord length is appropriate for our design.	See Wing Design	3/22/2021
AI0005	Scott/Paul	2/21/2021	**PR0004**	Determine if sweep angle is appropriate for our design.	See Wing Design	3/22/2021
AI0006	Jared	2/21/2021	**PR0005**	Determine if winglet sizing is appropriate for our design.	See Winglet Design	3/22/2021
AI0007	Jared	2/21/2021	**PR0006**	Determine if cant angle for winglet is appropriate for our design.	See Winglet Design	3/22/2021
AI0008	Team	2/21/2021	**DR0005**	Determine the best type of foam to use for our wing design.	Foma Type: FOAMULAR 150 2 in. x 4 ft. x 8 ft. R-10 Scored Squared Edge Rigid Foam Board Insulation Sheathing	3/22/2021
AI0009	Team	2/21/2021	**DR0014**	Determine placement of fuselage equipment.	Sponsor has taken on this task.	4/18/2021

Table 9: Risk Items

RI ID	Risk Level	Reference REQ	Risk Item	Risk Reduction Efforts	Risk Status
RI0001	Medium	**CON0004**	Bungee and Hand Launch Failure	Perform Test on 15 lb weight launched with surgical tubing	Field testing moved to after FDR
RI0002	Medium	**DR0003**	Chosen propeller may not be best suited for aircraft design.	Perform a tradestudy on propeller options.	Field testing moved to after FDR
RI0003	Medium	**DR0009**	Potential risk that battery weight will cause weight requirement to be exceeded (when entire aircraft is composed).	May have to run off of one battery (two batteries are included in model)	Field testing moved to after FDR
RI0004	High	**FR0007**	Behind schedule - May not get to field testing	Fabricating design in conjunction with wind tunnel testing	Field testing moved to after FDR

3.2) Minimum Success Criteria:

The success of this project is dependent on the completion of a working prototype aircraft that meets the mission requirements and constraints listed below. In addition to the completion of a prototype aircraft, a successful project includes the authoring of a final report and presentation.

Mission Requirements:

- Sustainable Velocity: 30 m/s
- Endurance: 2.5 hours
- Hand and/or Bungee Launch
- In-Flight Forces: +3Gs, - 2Gs
- Payload: 3 lbs or more

Constraints:

- Max Gross Weight: 15 lbs
- Max Wingspan: 6 ft
- Propulsion: 2-Motor Pusher

3.3) Gantt Chart

Figure 9 shows the overall project schedule in the Gantt Chart. The completion of each item is indicated by the black bar within the block. Some of the items in the Gantt Chart are not filled to completion with the black bar. This is because during our initial schedule planning, we anticipated performing field testing on a final, fabricated model. However, due to limited time, and extensive time spent during the initial design phase, we will not be able to complete field testing. The final marking of our project is wind tunnel testing and analyzing the results of the test. It is notable that some of the fabrication process has been started, as shown in the Gantt Chart, and that is because the field testing will still be completed but is will not be included in this report due to time limitations.

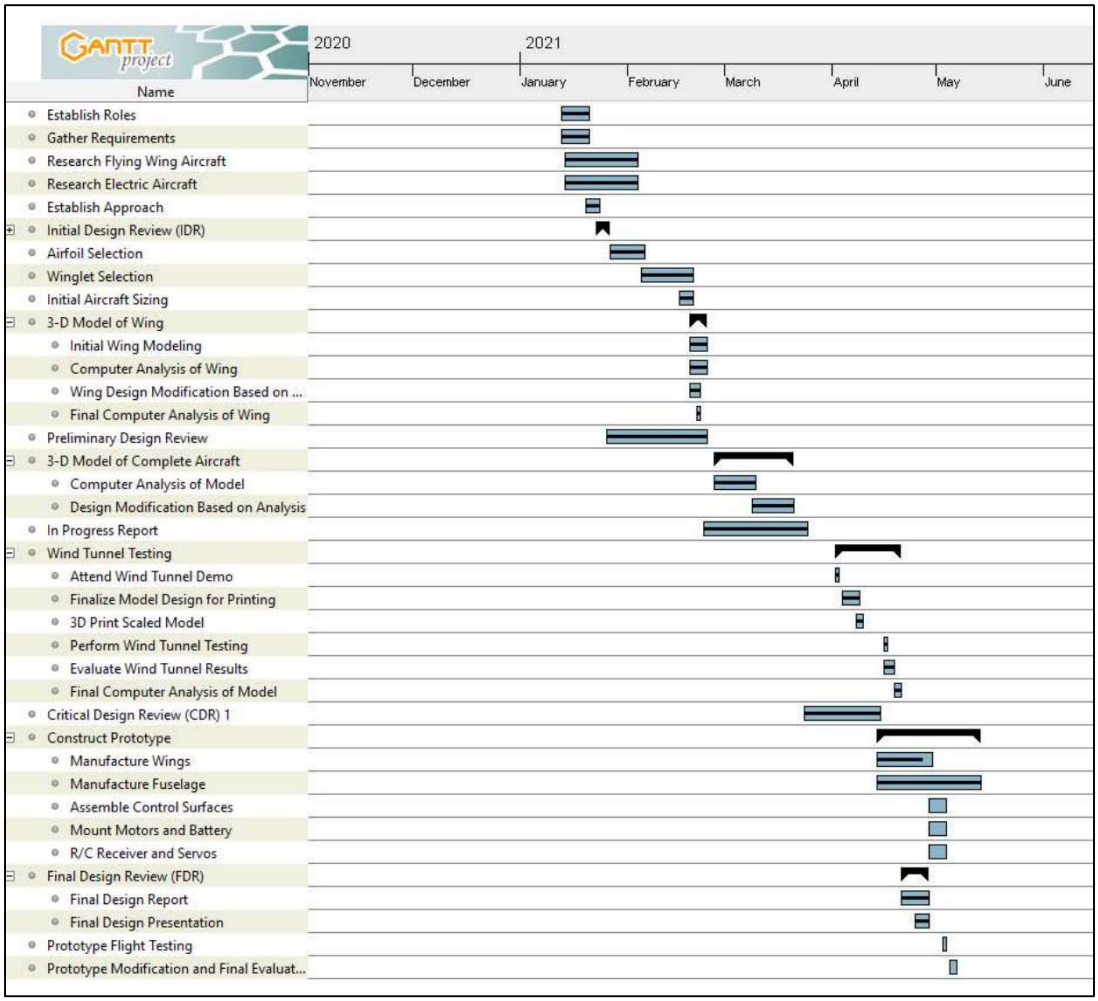

Figure 9: Gantt Chart with Percentage Complete (Indicated by Black Bar)

3.4) Flow Chart

Figure 10 and Figure 11 show the block diagram that is being used to design the flying wing UAV. The block diagram can be read left to right and top to bottom. The arrows indicate the flow of the design process and designate a “yes” or “no”, which is used to determine which path to follow.

Starting from the top left, the first step is to define the requirements. The requirements are crucial to the overall project design because they outline the parameters that need to be met during aircraft development. Once the requirements are defined, the next path leads to fuselage development, which in our case was already completed by the sponsor. After the fuselage has been developed, the next step is to work on the wing design. As shown in Figure 1, the first step to the wing design is to determine the best airfoil based on our requirements. Once an airfoil is selected and basic aerodynamic tests are done on the airfoil, the control surfaces can then be determined. At this point, the focus is on the wing geometry, which includes twist, sweep, angle of incidence, taper ratio, ailerons, elevator, and winglets. More aerodynamic calculations then need to be performed to ensure control surface selection is sufficient given the requirements.

Following Figure 1, next is detailed weight and sizing calculations for the UAV with the wing geometry and other equipment (electronics and surveillance gear within the fuselage) included. Then preliminary design sketches can be done in SolidWorks or AutoCAD. At this point, test procedures and requirement updates need to be completed. Test procedures are based on the requirements themselves. Essentially, test procedures are used to verify that a requirement is met. Each procedure also includes a pass/fail criterion to be used to determine if the test is a success.

After the test procedures are developed, the materials required for wind tunnel testing and field testing can be obtained. This would include materials to fabricate the aircraft as well. Once the aircraft is fabricated, wind tunnel tests can be performed. In Figure 11, following the wind tunnel test is a series of questions regarding whether the test was successful. The test is deemed successful based on the test procedures that were developed prior to testing. If the test is unsuccessful, the diagram walks through what caused the failure and how to go back through the process of testing once it has been resolved.

After wind-tunnel testing, field testing can be conducted, which is also based on the test procedures. Once the field test is deemed successful, the aircraft becomes a working prototype. Note—as stated in previous section, this last step has been omitted in our final project and report.

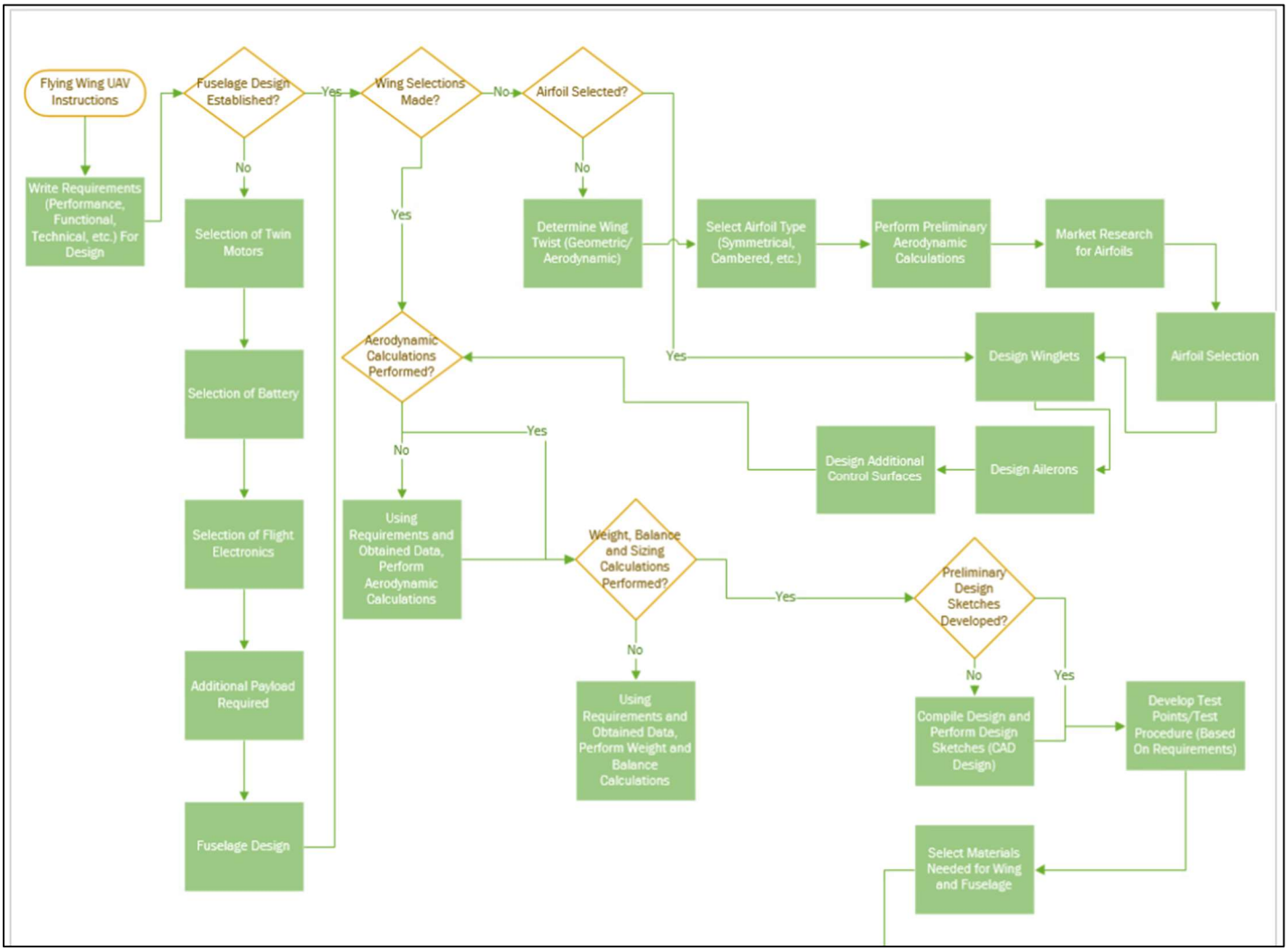

Figure 10: Block Diagram Part 1

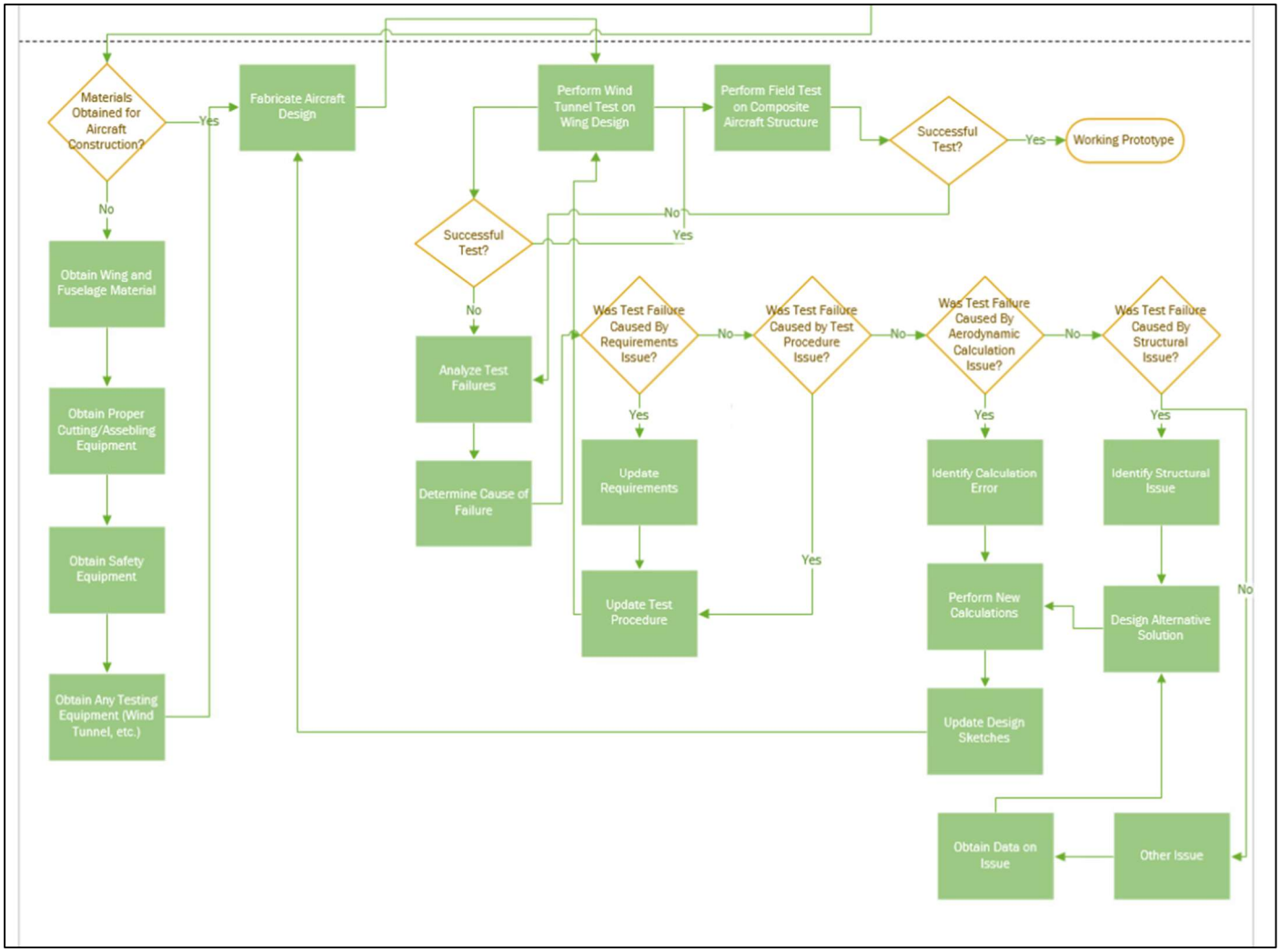

Figure 11: Block Diagram Part 2

3.5) Schedule and Responsibilities:

The key schedule deadlines can be seen below in Table 10. These dates are hard deadlines that must be met. Table 11 shows tasking for our project and how it was broken up.

Table 10: Key Deadlines

January 15, 2021	Group members and topic selected.
January 27, 2021	Initial Design Review (IDR)
February 24, 2021	Preliminary Design Review (PDR)
March 24, 2021	In Progress Review (IPR)
April 14, 2021	Critical Design Review (CDR)
April 28, 2021	Final Design Review (FDR)

Table 11: Group Tasks List

Task	Assigned To	Status	Notes
Topic Selected	Team	Complete	Due January 15
Initial Requirements Defined	Project Manager	Complete	
Initial Design Review	Team	Complete	Due January 27
Baseline Parameters Defined (for initial calculations)	Team	Complete	
Airfoil Market Research/Narrow down Airfoil Selections	Systems Engineer/Data Analyst	Complete	
XFLR5 Airfoil Analysis	Data Analyst and Technical Reviewer	Complete	
Integrating Potential Airfoil Selections Into Solidworks Working Design	Technical Aircraft Expert and Technical Reviewer	Complete	
Update Requirements/Define High Level Systems Requirements	Systems Engineer	Complete	
Sizing/Initial Weight Calculations	Technical Reviewer	Complete	
SolidWorks Testing/Analysis for Baseline Wing Geometry Parameters	Technical Aircraft Expert and Technical Reviewer	Complete	
Preliminary Design Review	Team	Complete	Due February 24
Iterate Design Parameters in Solidworks to Find Optimized Parameters	Technical Aircraft Expert and Technical Reviewer	Complete	
Perform Winglet Research/Sizing	Mathematician	Complete	
Perform Additional Control Surface Sizing	Technical Aircraft Expert	Complete	
Design Scaled Model of UAV in SolidWorks for Testing	Technical Aircraft Expert and Technical Reviewer	Complete	Due March 28
In Progress Review	Team	Complete	Due March 24
3D Print Model (with Paul's 3D Printer)	Technical Aircraft Expert	Complete	Due March 31
Develop Test Procedure for Wind Tunnel Testing	Systems Engineer	Complete	
Critical Design Review	Team	Complete	Due April 14
Perform Wind Tunnel Testing	Team/Sponsor	Complete	Testing on April 16
Analyze Test Results	Team/Sponsor	Complete	
Obtain Materials Required Design Fabrication	Team/Sponsor	Complete	
Final Design Review	Team	Complete	Due April 28
Contruct Aircraft	Team/Sponsor	NA	
Perform Field Testing	Team/Sponsor	NA	
Analyze Test Results	Team/Sponsor	NA	

3.6) Budget:

The majority of the expense for this project have been covered by the project sponsor. The overall project budget can be seen in Table 12 below.

Table 12: Budget for Student and Sponsor Portion

Overall Project Budget			
Item	**Price (each)**	**Quantity**	**Total Price**
FOAMULAR 150 2 in. x 4 ft. x 8 ft. R-10 Scored Squared Edge Rigid Foam Board Insulation Sheathing	$37.83	2	$75.66
Control Linkages			$15
Bungee Launch System			$30
3-D Model Printing Supplies			$0.30
Other General Assembly Supplies			$25
DX6e 6-Channel DSMX Transmitter with AR620	$243.77	1	$243.77
AR620 DSMX Receiver		1	
Props 12x10 +spinners	$30	2	$60
MN4012 KV480 Motors	$100	2	$200
4S 10 amp hour battery pack	$89.48	2	$178.96
Servos	$61	2	$122
Servo Extension	$7	4	$28
Foam Wire Cutter			
Total Cost			**$978.69**

3.7) Required Materials:

The resources required for this project will be listed below. The list is divided into two categories. The first category will be the resources of which the project sponsor has agreed to provide. The second category is a list of resources expected to be supplied by the team and/or KSU.

Sponsor Provided Resources:

- 3D Printer (for large components)
- 3D Printing Filament
- Transmitter
- Receiver
- Propellors/Attachment Components
- Motors
- Electronic Speed Controllers (ESCs)
- Servos
- Servo Extension Cables
- Battery
- Battery Charger
- Telemetry/Data Collection System

Team/KSU Provided Resources:

- SolidWorks (CFD Testing)
- Wind Tunnel
- 3D Printer (for scaled model)
- 3D Printing Filament

- Hot Wire Foam Cutter
- Foam
- Assembly Supplies (tape, glue, etc.)
- Control Linkages
- Bungee Launch System

3.8) Resources Available

There have been many resources available for our UAV design project. First, the library and online library catalog were useful for market research and development. Additionally, the KSU aerospace lab was used for testing our design in the wind tunnel that is available for student use. One of the students in the group has a 3D printer, which was used to print our scaled model for wind tunnel testing. The program sponsor put together a hot wire foam cutter that was to be used in fabrication of the wings. He also purchased a large 3D printer for printing the fuselage.

Chapter 4: Airfoil Selection

4.1) Airfoil Research

After conducting initial research, eight different airfoils were selected for further analysis. These airfoils were examined using the program XFLR5, which uses XFOIL to analyze airfoil characteristics. For sake of brevity, only the top three choices will include graphs. The airfoils not chosen for further analysis will be displayed with a brief explanation of why they were not chosen. Most of these airfoils could be found on the *Airfoil Tools* website [3], except for the HS 522 airfoil, which was found on the *Airfoil Database for Tailless and Flying Wings* website [19].

4.2) PW-51 Airfoil

The first airfoil examined was the PW-51 (Figure 12). It is described as good for speed, but it is suited for gliders so it might not be feasible for our design. The airfoil performance at various Reynold's numbers can be seen in Figures 14 through 17).

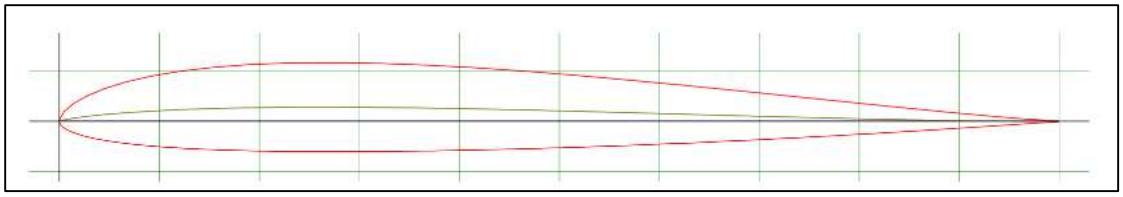

Figure 12: PW-51 Airfoil

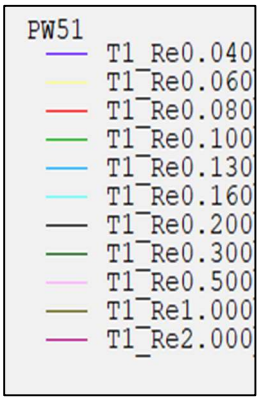

Figure 13: PW 51 Graph Legend (Re x 1,000,000)

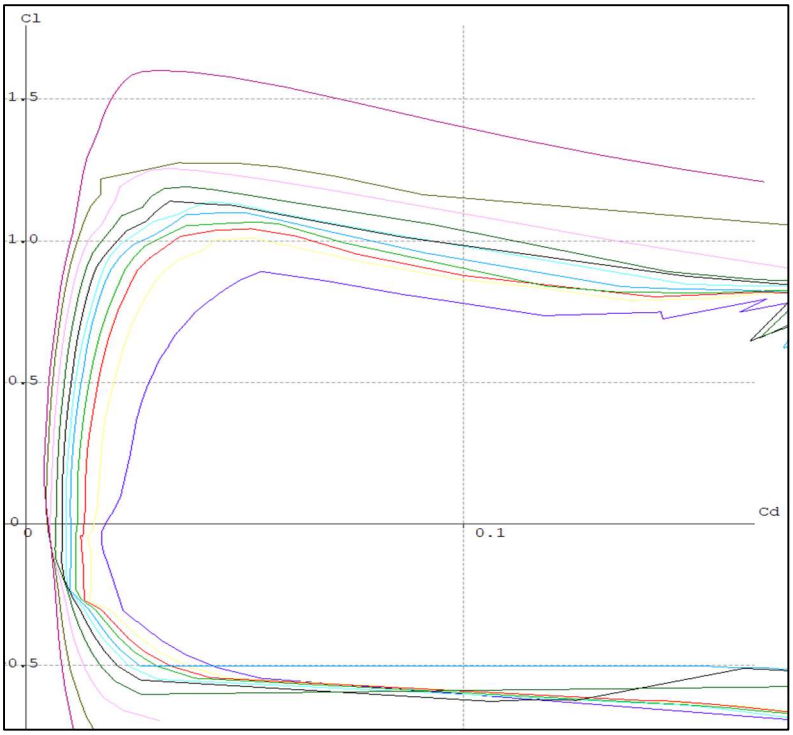

Figure 14: PW-51 Drag Polar

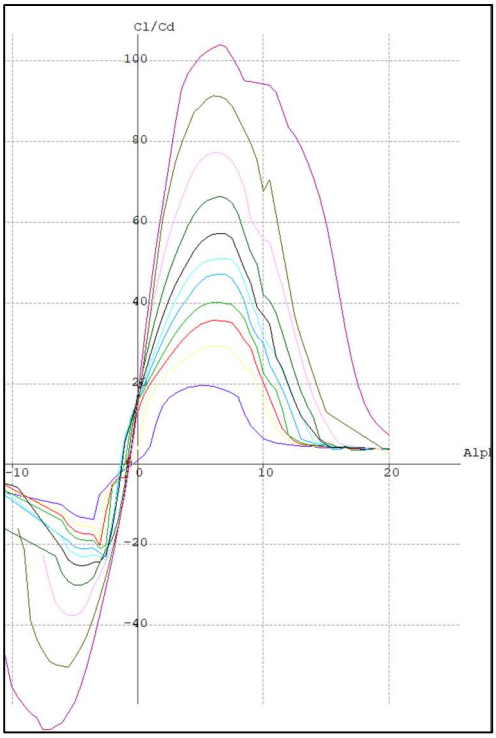

Figure 15: PW-51 Cl/Cd vs Alpha

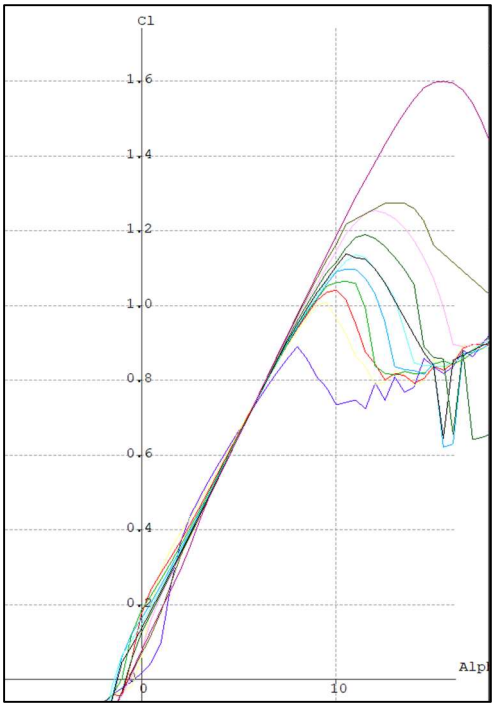

Figure 16: PW-51 Cl vs Alpha

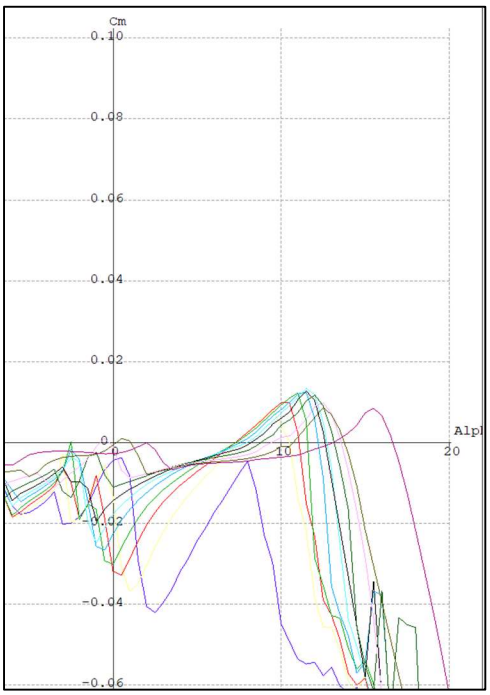

Figure 17: PW-51 Moment vs Alpha

This airfoil reached a max Cl/Cd at about 6 degrees alpha for all the Reynolds numbers in question. This airfoil has a very low negative moment when operating at max Cl/Cd, but the moment becomes more negative when alpha approaches 0 degrees. The effect was greater at lower Reynold's numbers.

4.3) PW-75 Airfoil

The second airfoil that was examined was the PW-75. Described as good for all around flying, it is a modified PW-51, but with more reflex (Figure 18). The airfoil performance at various Reynold's numbers can be seen in Figures 20 through 23).

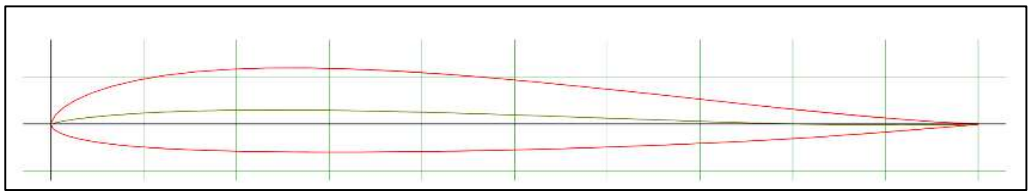

Figure 18: PW-75 Airfoil

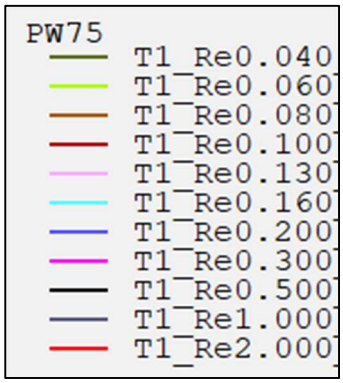

Figure 19: PW-75 Graph Legend (Re x 1,000,000)

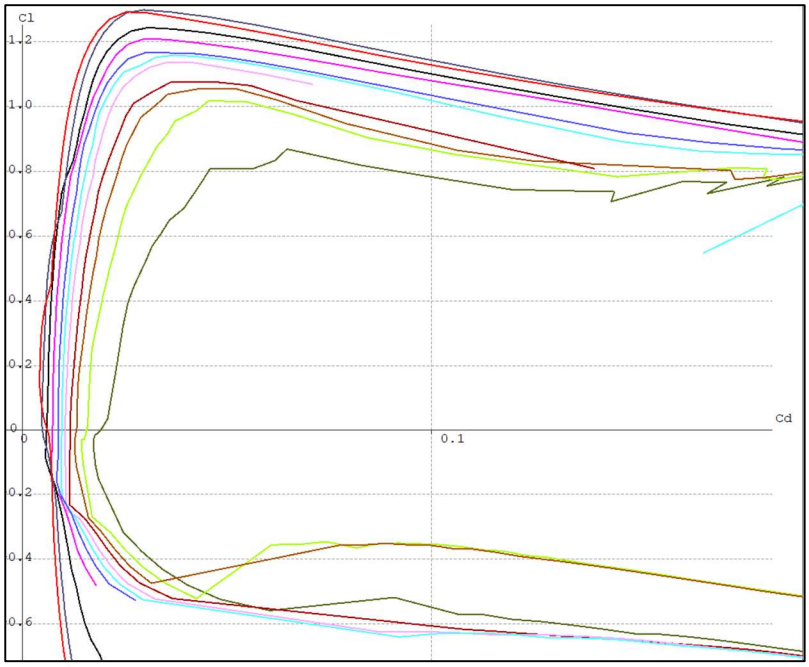

Figure 20: PW-75 Drag Polar

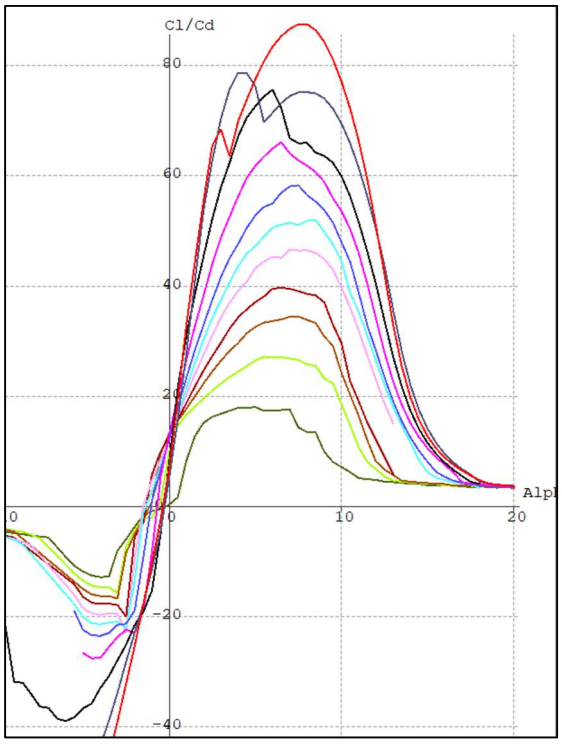

Figure 21: PW-75 Cl/Cd vs Alpha

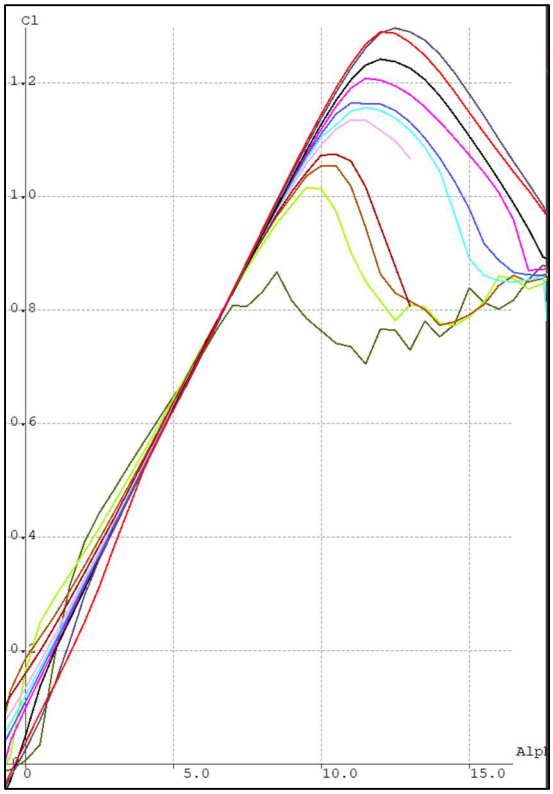

Figure 22: PW-75 Cl vs Alpha

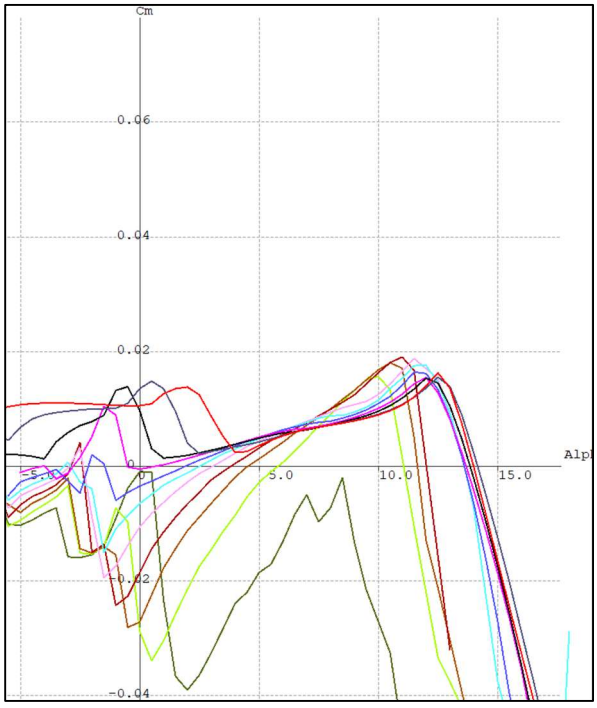

Figure 23: PW-75 Moment vs Alpha

This airfoil reached a max Cl/Cd at between 5 and 8 degrees alpha for the Reynolds numbers in question. The max Cl/Cd ratio was rather low, but this was the only airfoil with a positive moment, meaning a tendency to pitch up, which might be useful.

4.4) PW-106 Airfoil

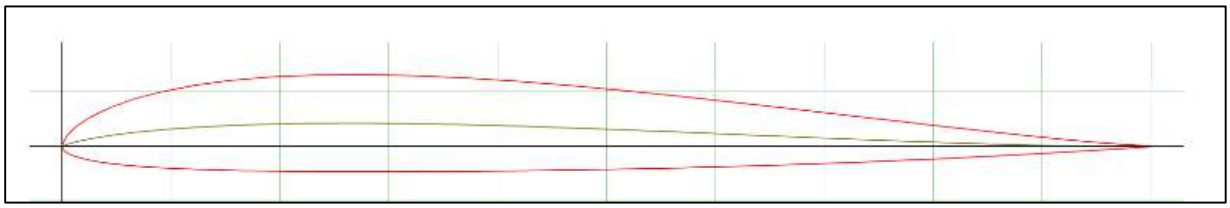

Figure 24: PW-106 Airfoil

The PW-106 Airfoil (Figure 24) had a high camber and high Cl_{max}. This airfoil reached a max C_l/C_d at about 6 degrees alpha for all the Reynolds numbers in question, with the exception being at Re=1,000,000. The max C_l/C_d ratio was higher than the PW-75 and about the same as the PW-51. This airfoil has a low negative moment when operating at max C_l/C_d, but the moment becomes more negative when the alpha approaches 0 degrees. The moment was greater than the PW-51 and its effect was greater at lower Reynold's Numbers. This airfoil was not selected for further analysis.

4.5) MH-60 Airfoil

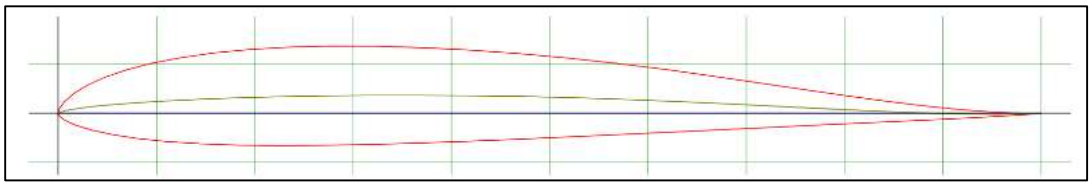

Figure 25: MH-60 Airfoil

The MH-60 Airfoil (Figure 25) has been used successfully in F3B tailless model planes. This airfoil reached a max C_l/C_d at about 6 degrees alpha for all the Reynolds numbers in question. The max C_l/C_d ratio was slightly higher than the PW series, while maintaining similar C_l/C_d at low to mid-range Re numbers. This airfoil has a low negative moment when operating at max C_l/C_d, but the moment becomes more negative when the alpha approaches 0 degrees, even more than the PW-106. The effect is greater at lower Reynold's numbers. This airfoil was not selected for further analysis.

4.6) Eppler 339 Airfoil

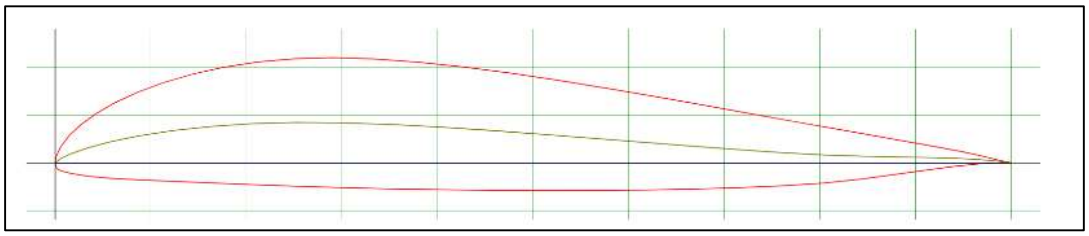

Figure 26: Eppler 339 Airfoil

The Eppler 339 airfoil (Figure 26) reached a max C_l/C_d at about 0 degrees alpha for a Reynolds number of 40,000 and increased rather linearly with Reynolds number to a maximum at about 10 degrees alpha at a Re of 1,000,000. The max C_l/C_d ratio was higher than the PW series by about 30-35%. However, this airfoil experienced a large loss of C_l/C_d at low to mid-range Re numbers when compared to the other airfoils. This airfoil had a large negative moment when operating at max C_l/C_d, but the moment became more negative rather quickly when the alpha approached 0 degrees. The effect was greater at lower Reynold's numbers and this airfoil produced the largest negative moment of all eight airfoils that were examined. This airfoil was not selected for further analysis due to lack of performance at low to mid Reynold's numbers and an extraordinarily high moment.

4.7) Eppler 334 Airfoil

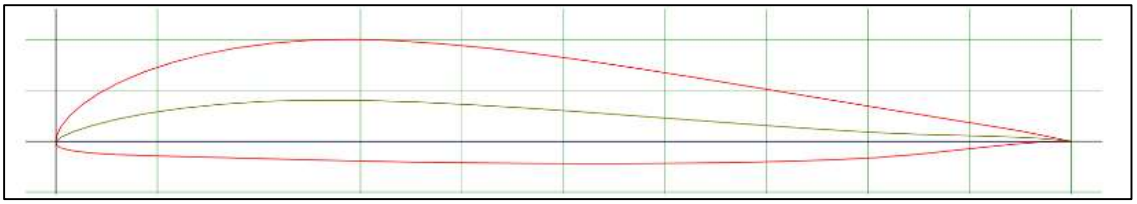

Figure 27: Eppler 334 Airfoil

The EPPLER-334 airfoil (Figure 27) had a high lift coefficient with low Reynold's numbers. This seemed to be the most common airfoil selection for a flying wing UAV with a similar wingspan as our current design. This airfoil reached a max C_l/C_d at about 0 degrees alpha at a Reynold's number of 40,000 and increased somewhat linearly with Reynold's number to a maximum at about 8 degrees angle of attack (AOA) at a Reynold's number of 1,000,000. The max C_l/C_d ratio is higher than the PW series by about 40%. However, this airfoil experiences a large loss of Cl/Cd at low to mid-range Re numbers when

compared to the other airfoils, but not as large of a loss as the EPPLER 339. This airfoil has a large negative moment when operating at max C_l/C_d, but the moment becomes more negative rather quickly when alpha approaches 0 degrees. The effect is greater at lower Reynold's numbers and this airfoil produced the second largest negative moment of all eight airfoils that were examined. This airfoil was not selected for further analysis due to lack of performance at low to mid Reynold's numbers and a high moment.

4.8) Eppler 333 Airfoil

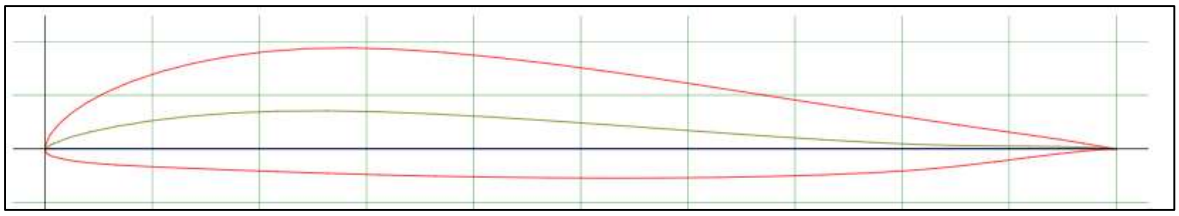

Figure 28: Eppler 333 Airfoil

In comparison to the MH airfoils the EPPLER 333 airfoil (Figure 28) had an increased C_l, however C_d increased slightly between the angles of attack of -5 and 15 degrees and greatly increased beyond that. This airfoil reached a max C_l/C_d at about 0 degrees alpha at a Reynold's number of 40,000. This increased somewhat linearly with Reynold's number to a maximum at about 8 degrees alpha at a Re of 1,000,000. The maximum C_l/C_d ratio was the least of the EPPLER series, but more than any PW series airfoil. However, this airfoil experienced a large loss of C_l/C_d at low to mid-range Re numbers when compared to the other airfoils, but not as large of a loss as the EPPLER 339. This airfoil had a large negative moment when operating at max C_l/C_d, but the moment becomes more negative gradually when alpha approached 0 degrees. The effect was greater at lower Reynold's numbers and this airfoil produced the third largest negative moment of all eight airfoils that were examined. This airfoil was not selected for further analysis due to lack of performance at low to mid Reynold's numbers and a high moment.

4.9) HS 522 Airfoil

The HS 522 airfoil (Figure 29) is one of the most popular airfoils for swept wings due to low drag and very low Reynold's numbers you need to generate lift. This airfoil has also successfully been used on tailless model aircraft. The airfoil performance at various Reynold's numbers can be seen in Figures 31 through 34.

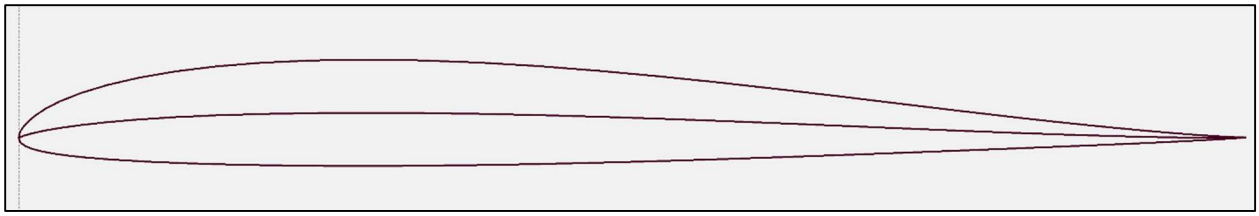

Figure 29: HS 522 Airfoil

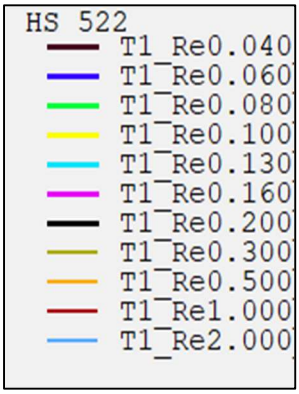

Figure 30: HS 522 Graph Legend (Re x 1,000,000)

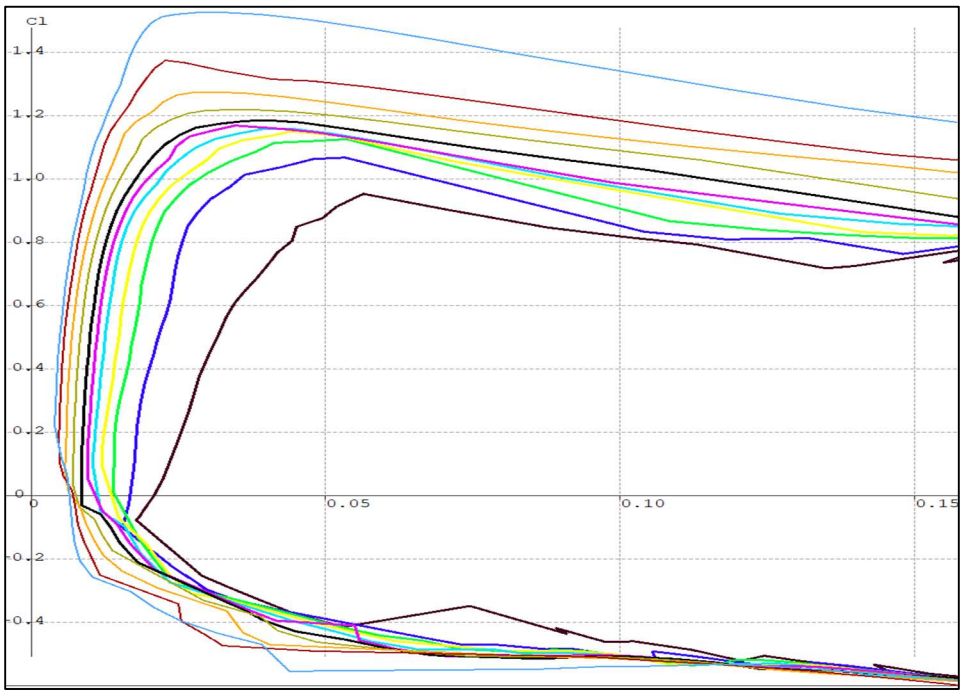

Figure 31: HS 522 Drag Polar

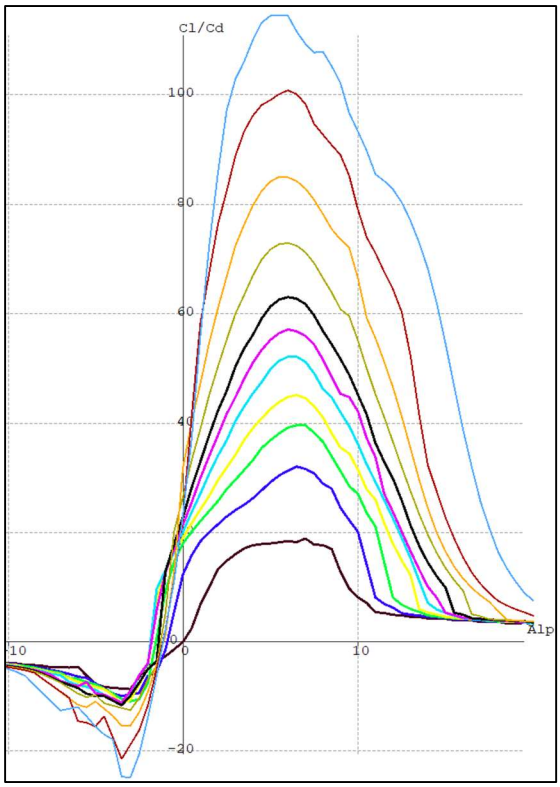

Figure 32: HS 522 Cl/Cd vs Alpha

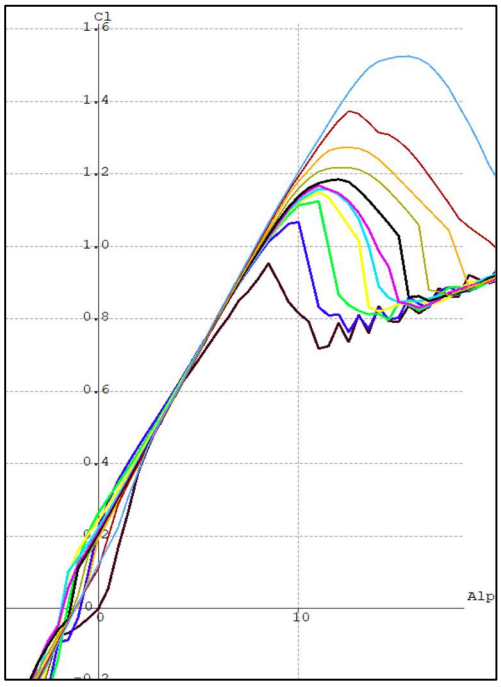

Figure 33: HS 522 Cl vs Alpha

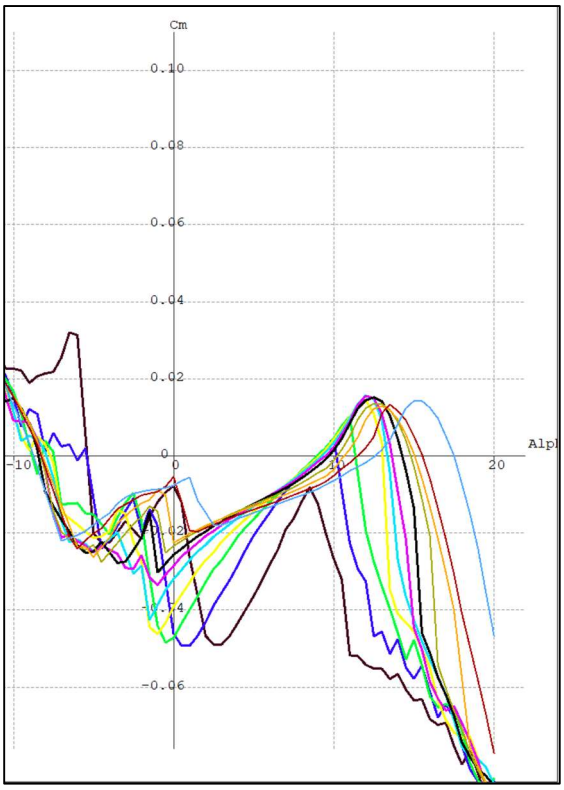

Figure 34: HS 522 Moment vs Alpha

This airfoil reached a maximum C_l/C_d at about 6 degrees alpha for all Reynold's numbers in question. The max C_l/C_d ratio was respectable, more than any PW series, but less than any airfoil in the EPPLER series. This airfoil did not experience a large loss of C_l/C_d at low to mid-range Re numbers when compared to the other airfoils. It showed similar performance to the PW series airfoils and greater performance than any EPPLER series airfoil at those lower Reynold's numbers. This airfoil had a small to moderate negative moment when operating at max C_l/C_d, but the moment became more negative when alpha approached 0 degrees. The effect was greater at lower Reynold's numbers. This airfoil seemed to be the best combination of low and high Reynold's number performance as well as possessing a moment that was not too severe.

4.10) Winglet Airfoil Research

After conducting initial research on the optimal design of winglets 6 airfoils were selected for additional analysis. These airfoils were analyzed utilizing the XFLR5 software's wing and plane design function (Figure 35). Each winglet was analyzed combined with the main wing to determine its effect on the freestream velocity required to produce the required 15lbs of lift. Additionally, several other parameters which affect the performance of the wing were analyzed such as the coefficient of lift, coefficient of

drag, moment coefficient, and lift to drag ratio. Each winglet was analyzed at with a length equal to the chord and a length of ½ of the chord.

No Winglet Wing					
CL	CD	Cl/CD	Cm	Vinf (m/s)	
0.447	0.023	19.431	0.081	24.57	

Winglet Height=Chord						
Winglet Airfoil	CL	CD	CL/CD	Cm	Vinf (m/s)	Vinf %Difference
NACA 0011	0.469	0.024	19.362	0.097	24.16	-1.67%
PSU-90	0.475	0.025	19.303	0.095	24	-2.32%
PSU-94	0.477	0.025	19.274	0.089	23.94	-2.56%
GOE 602	0.477	0.025	19.224	0.089	23.95	-2.52%
GOE 450	0.479	0.026	18.586	0.088	23.91	-2.69%
GOE 330	0.479	0.026	18.202	0.089	23.89	-2.77%

Winglet Height=1/2 Chord						
Winglet Airfoil	CL	CD	CL/CD	Cm	Vinf (m/s)	Vinf %Difference
NACA 0011	0.466	0.024	19.555	0.087	24.21	-1.47%
PSU-90	0.469	0.024	19.494	0.086	24.14	-1.75%
PSU-94	0.47	0.024	19.398	0.083	24.12	-1.83%
GOE 602	0.47	0.024	19.416	0.083	24.12	-1.83%
GOE 450	0.471	0.025	18.903	0.082	24.11	-1.87%
GOE 330	0.471	0.025	18.73	0.083	24.1	-1.91%

Table 13: Results of Winglet Analysis at 0 degrees AOA

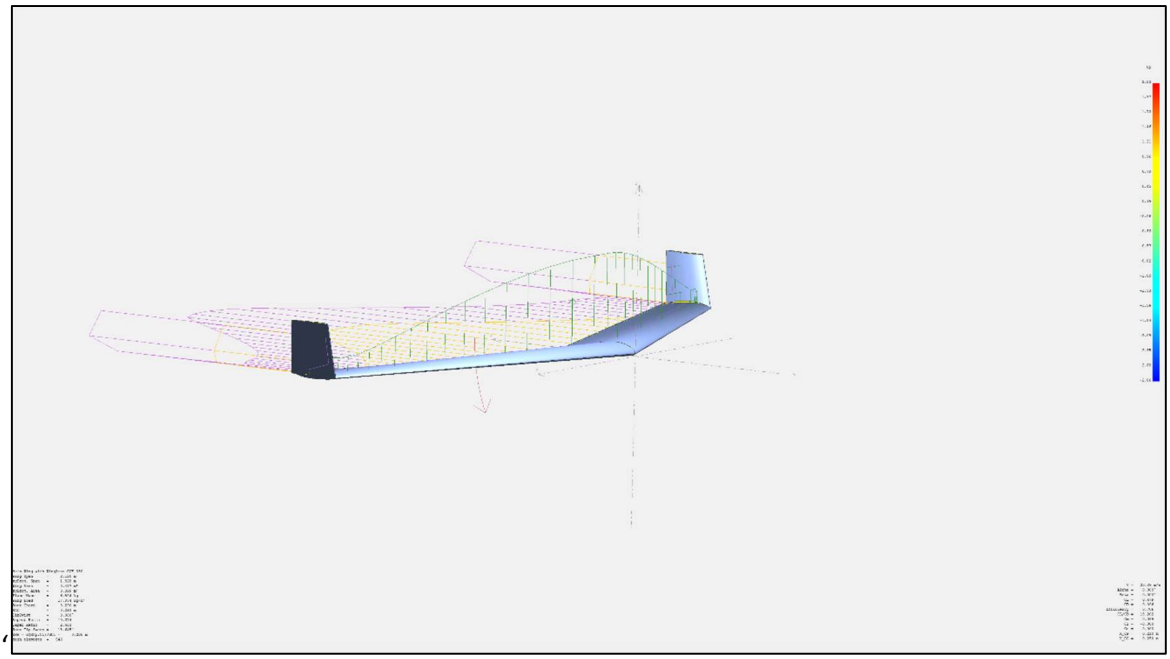

Figure 35:XFLR5 Wing and Plane Design with GOE 330 Winglets

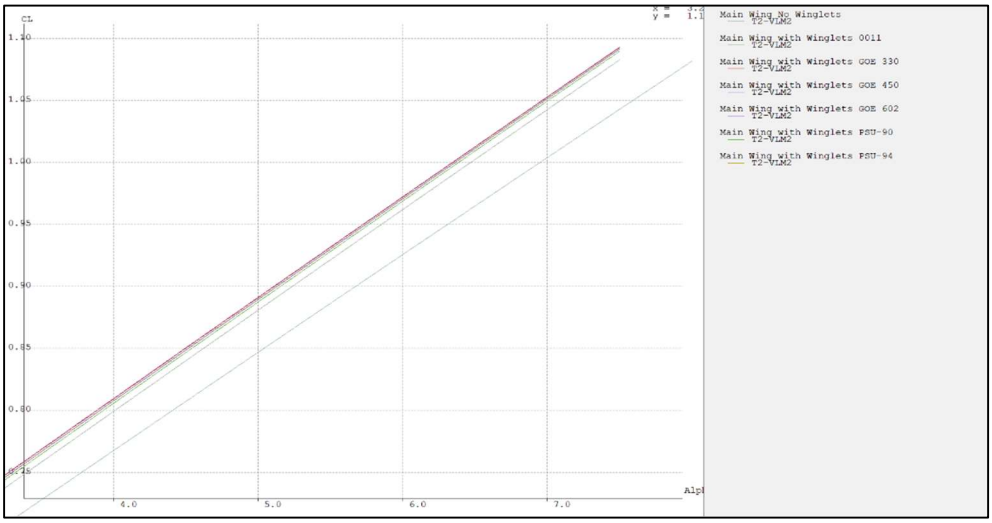

Figure 36: Winglet CL vs. Alpha

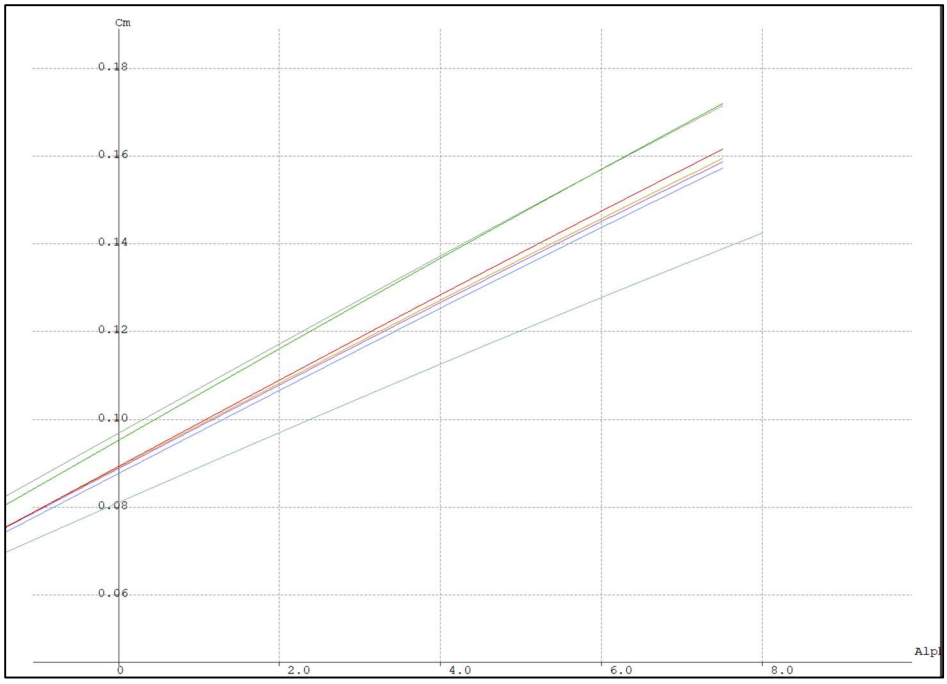

Figure 37: Winglet Cm vs. Alpha

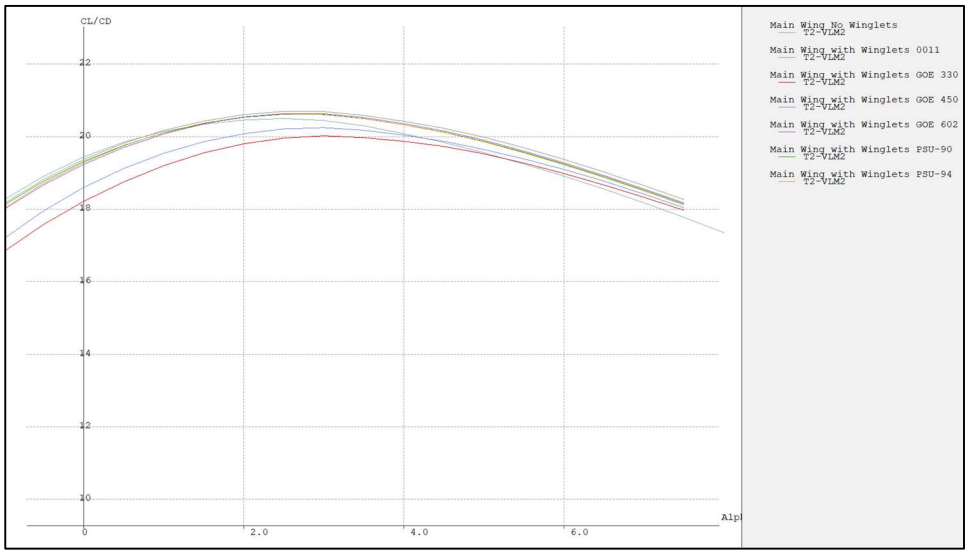

Figure 38: CL/CD Ratio Vs. Alpha

The results of the winglet analyses are displayed above (Table 12). After analyzing the 6 winglet airfoils the GOE 330 was determined to provide the greatest increase in the coefficient of lift of the wing (Figure 36). Analysis of the performance of this winglet indicates a decrease of 2.5% in the freestream velocity required to maintain 15 lbs. of lift at 0 degrees AOA with a winglet height equal to the chord. In analysis of the winglets the parameter of highest importance was increasing the lift generated by the wing. As a result, the winglet height is selected to be equal to the chord. The GOE 330's main drawbacks are its lift to drag ratio (Figure 38) and coefficient of drag. With a CD of 0.026 at 0 degrees AOA drag on the wing is increased by 13% consequently this increase in drag is the cause of the low lift to drag ratio of this

winglet configuration. Other airfoils such as NACA 0011 accel is both aforementioned categories, however the primary parameter to be optimized was lift generation. Finally, the GOE 330 has the second lowest increase in pitching moment which is ideal for a flying wing due to the lack of a tail (Figure 37). Therefore, we have selected the GOE 330 with a height equal to the chord for optimum performance.

Chapter 5: Airfoil Analysis

5.1) SolidWorks Analysis Setup

Once the three best airfoils were selected, a 30-degree swept wing was created for each airfoil using the program SolidWorks. These wings were created with a taper ratio of 0.33 and -3.00-degree twist. These characteristics were selected based on historical designs and analysis[12]. Since the focus was on selecting the best wing design, no large payload carrying wing section that would normally house the batteries and avionics were included in the simulations. The simulations were run at average condition found at 1000 ft above sea level at a speed of 65.6 ft/s (20 m/s), which is the design goal for cruise speed. The pressure was 2040.85 lbf/ft^2 (14.17 psi) and the temperature was 55.43 °F (13 °C). The CFD settings can be viewed in Figures 39-41, below.

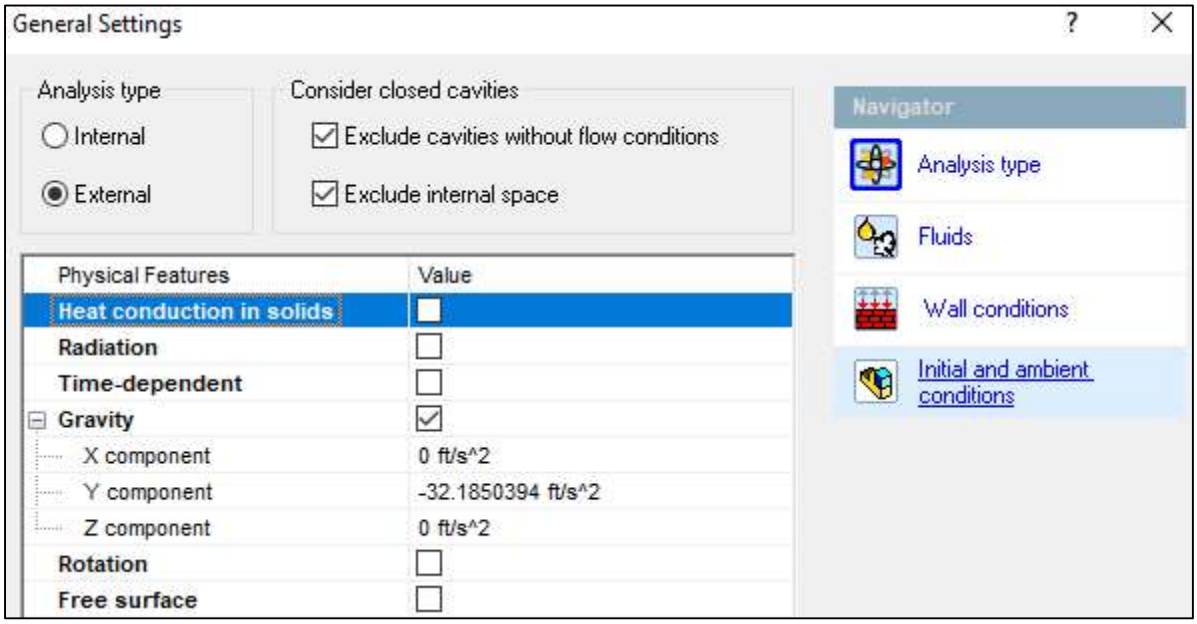

Figure 39: Solidworks Flow Simulation Conditions

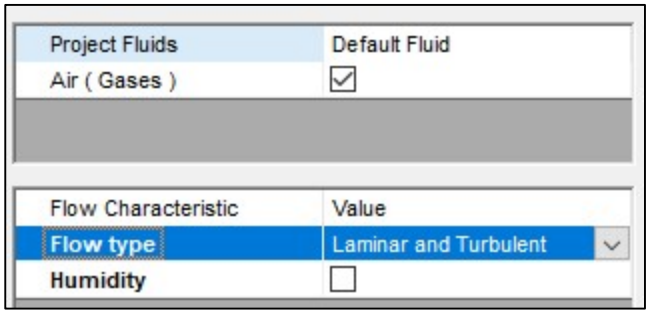

Figure 40: Solidworks Flow Simulation Conditions (Cont. 1)

Parameter	Value
Parameter Definition	User Defined
Thermodynamic Parameters	
Parameters	Altitude
Altitude	1000 ft
Pressure	2040.85361 lbf/ft^2
Pressure potential	☑
Refer to the origin	☐
Temperature	55.434011 °F
Temperature deviation	0 °F
Velocity Parameters	
Parameter	Velocity
Defined by	3D Vector
Velocity in X direction	65.6167979 ft/s
Velocity in Y direction	0 ft/s
Velocity in Z direction	0 ft/s
Turbulence Parameters	
Parameters	Turbulence intensity and length
Turbulence intensity	0.1 %
Turbulence length	0.00152388528 ft

Figure 41: Solidworks Flow Simulation Conditions (Cont. 2)

The freestream air flowed in a direction parallel to the positive x-axis, which meant the drag force also acted in the direction of the positive x-axis. Gravity acted in the negative y-axis direction, while lift acted in the positive y-axis direction. In the Solidworks screen capture figures, the air velocity vector is depicted by a large blue arrow that is collocated with the simulation space reference axes (green). Each wing was examined at the following angles of attack: zero degrees and whole degree increments between 5 and 12 degrees. Angles of attack of less than 5 degrees were not examined because the lift values were too low to be useful for this design. To save space in this report, a graph of the data for all angles of attack will be presented, along with the pressure contours and flow streams for only the angle of attack that produced the greatest lift. However, angles of attack greater than 12 degrees were not explored at this time because the analysis was focused on examining the wings during normal flight conditions. Angles of attack greater than 12 degrees were deemed out of desirable level flight conditions, which historically fall between 2- and 5-degrees angle of attack.

It is believed that the moment data from the simulation is incorrect. It does not match up with historical airfoil behavior. This is most likely due to human error in the use of the Solidworks Flow Simulation software. The current solution is to research exactly where the model needs to be placed inside the simulation, or if there is another way to define where the moment is calculated to determine the moment properly.

5.2) Solidworks Analysis on the PW-75 Airfoil

The first wing to be examined used the PW-75 airfoil. The unique characteristic about this wing is that it produced a positive moment. This wing produced its greatest lift at 11 degrees at 9.8 lbs (Figure 42). but was most efficient at a 9-degree angle of attack, where the L/D ratio was 4.1 and it produced 8.3 lbs. of lift (Figure 43).

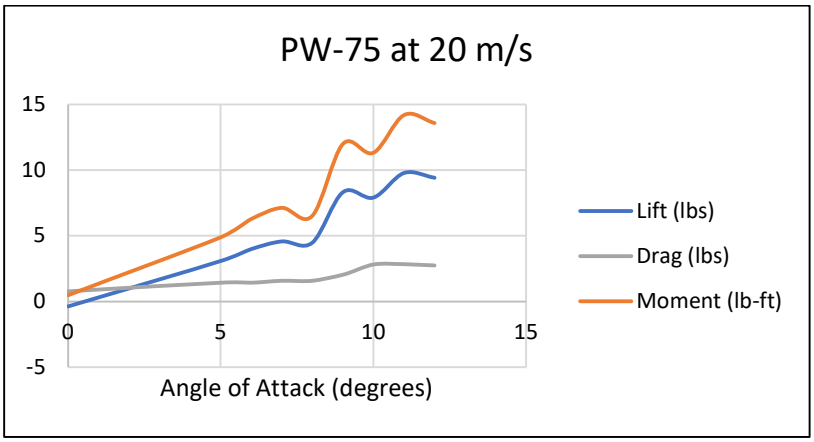

Figure 42: Lift, Drag, and Moment vs Angle of Attack for the PW-75 Wing at 20 m/s Airspeed.

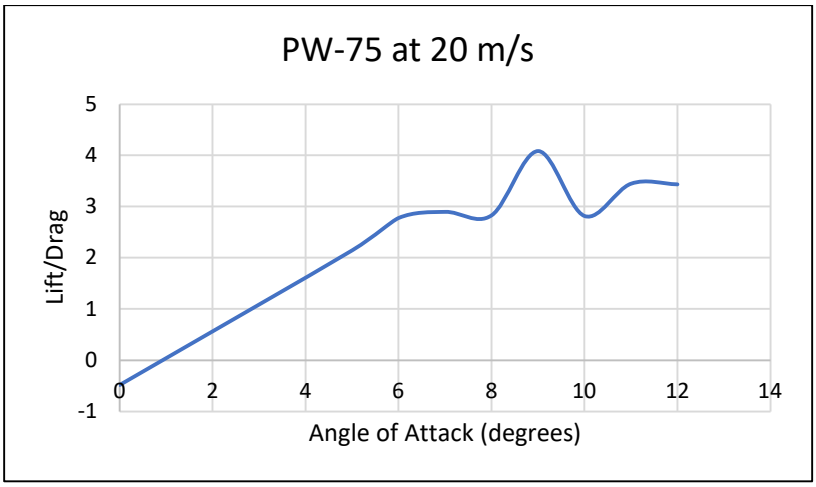

Figure 43: L/D Ratio vs Angle of Attack for the PW-75 Wing at 20 m/s Airspeed.

The PW-75 Wing simulation views shown below all have an angle of attack of 11 degrees.

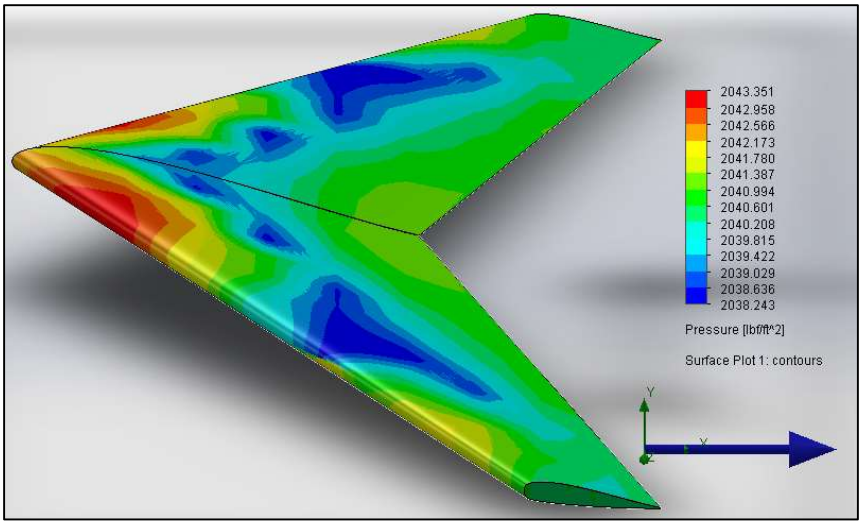

Figure 44: PW-75 Wing Surface Pressure, Top Oblique

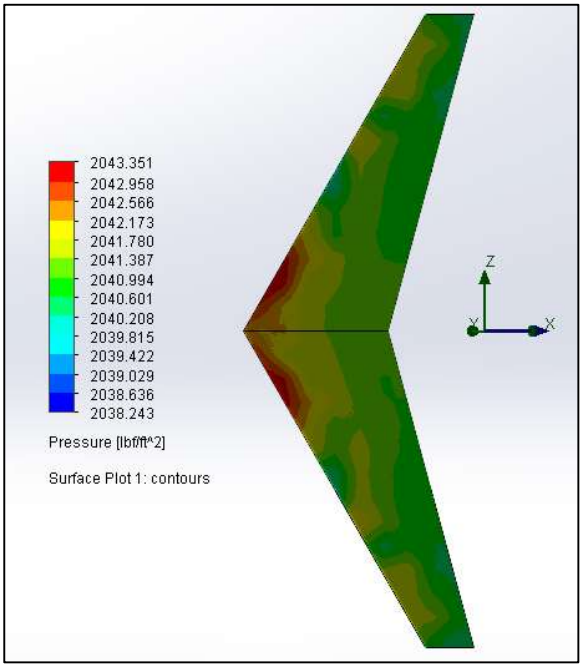

Figure 45: PW-75 Wing Surface Pressure, Bottom

When comparing the top (Figure 44) and bottom (Figure 45) surface pressure views of the PW-75 wing, the generation of lift can really be visualized. The lifting force come from the difference in pressure at the surface of the wing. The top surface of the wing shows areas of low to middling pressures, whereas the bottom surface shows high to middling pressures. This higher pressure acting on the bottom of the wing is not completely balanced by the relatively lower pressure acting on the top surface of the wing.

This difference in pressure, acting over the surface of the wing, provides the lift force. The lift force is only derived from the components of force acting parallel to the y-axis.

Likewise, the drag forces are visualized in the same way, but as the difference in pressures between the leading edge and trailing edge of the wing. The drag force is only the portion of the force acting parallel to the x-axis.

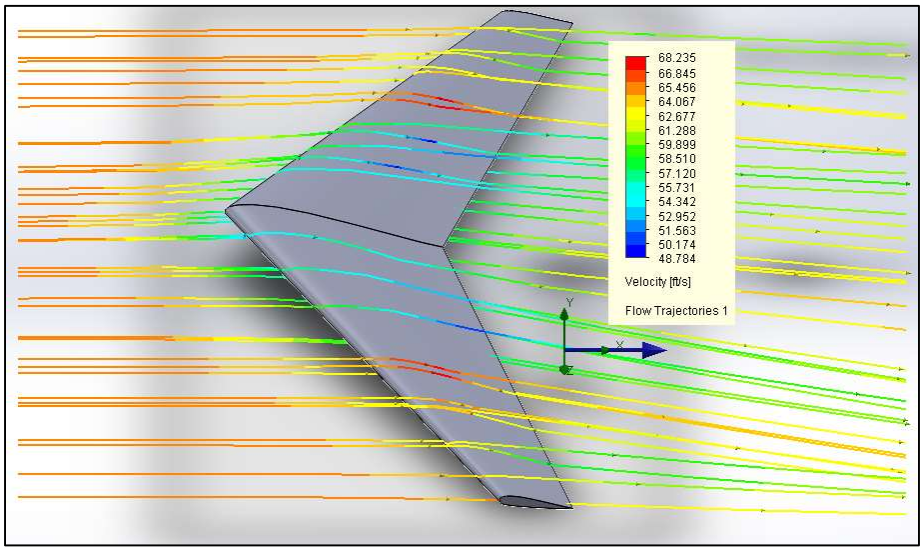

Figure 46: PW-75 Wing Velocity Flow Lines, Top Oblique

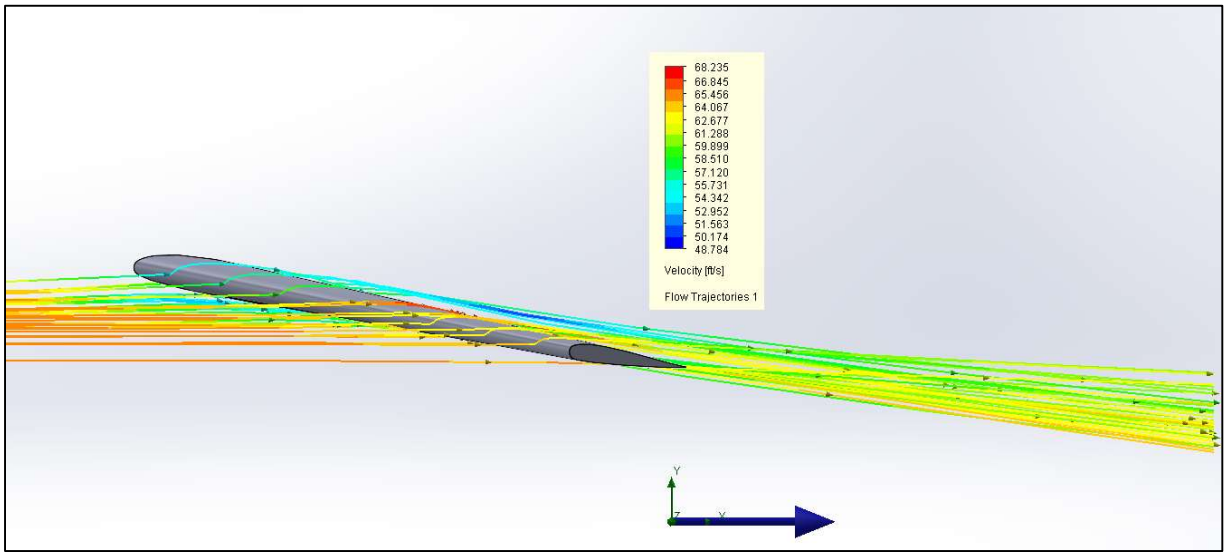

Figure 47: PW-75 Wing Velocity Flow Lines, Profile

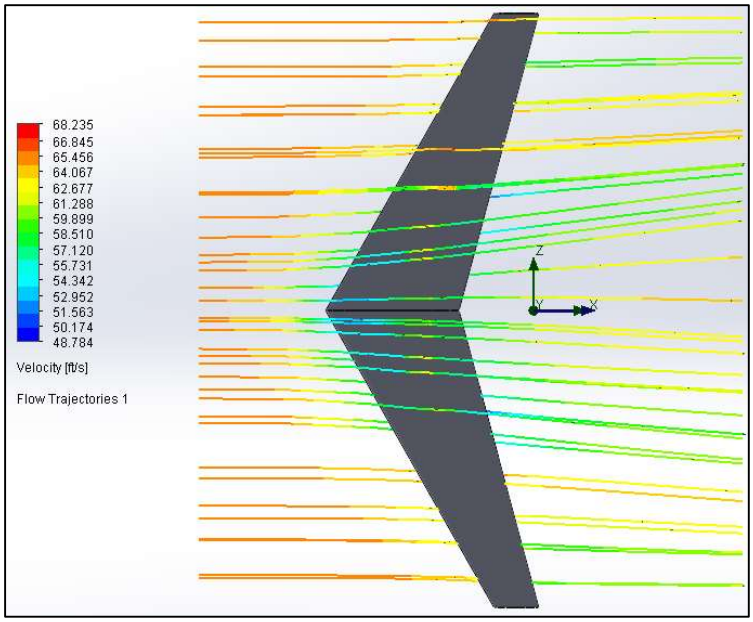

Figure 48: PW-75 Wing Velocity Flow Lines, Bottom

The velocity flow lines (Figures 46-48) show two things. First, they show the path of the air around the wing. Second, they show how the velocity of the air varies as it passes around the wing. If the velocity flow lines are compared with the surface pressures, a clear relationship can be drawn between the two. Areas of lower surface pressure occur where the air velocity over the surface is higher. Likewise, areas of higher surface pressure occur with lower air velocity over the surface.

5.3) SolidWorks Analysis on the PW-51 Airfoil

The second wing to be examined used the PW-51 airfoil. This wing produced its greatest lift at 12 degrees angle of attack at 9.7 lbs (Figure 49). It was at its most efficient at an 8-degree angle of attack (Figure 50), where the maximum L/D ratio was 4.5 and it achieved 7.7 lbs. of lift.

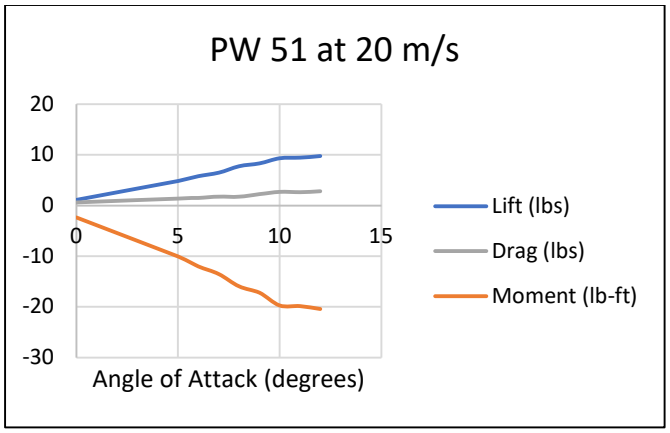

Figure 49: Lift, Drag, and Moment vs Angle of Attack for the PW-51 Wing at 20 m/s Airspeed

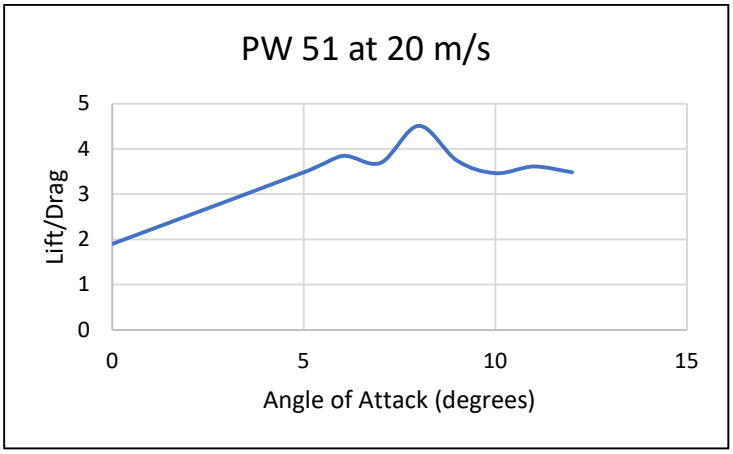

Figure 50: L/D Ratio vs Angle of Attack of the PW-51 Wing at 20 m/s Airspeed

The PW-51 Wing simulation views shown below all have an angle of attack of 12 degrees.

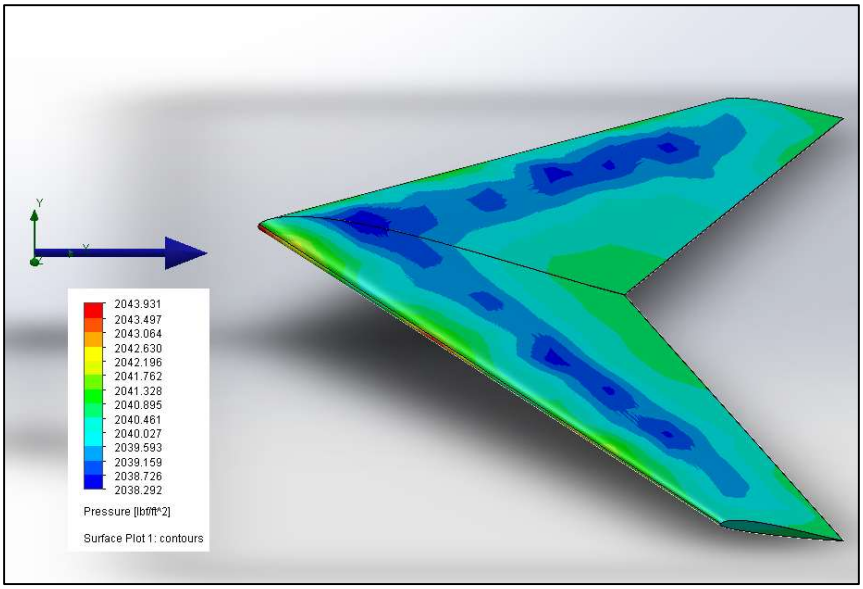

Figure 51: PW-51 Wing Surface Pressure, Top Oblique

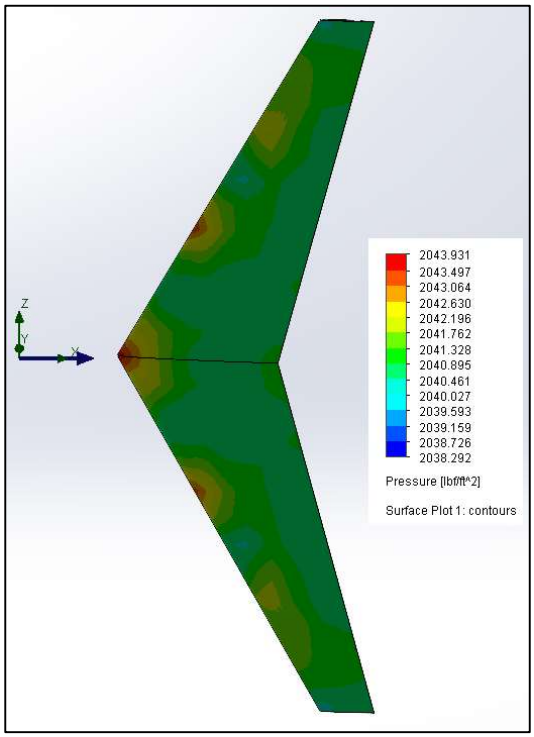

Figure 52: PW-51 Wing Surface Pressure, Bottom

The PW-51 surface pressures appear much lower on top (Figure 51) than the PW-75. However, this does not amount to more lift for the wing because the pressures on the bottom (Figure 52) of the wing were also lower, meaning that the pressure difference was not that great. Since lift is based on the difference

in pressures, this amounted to similar lift between both the P-51 and P-75 wings. The velocity flow lines for the PW-51 can be seen in Figures 53 through 55.

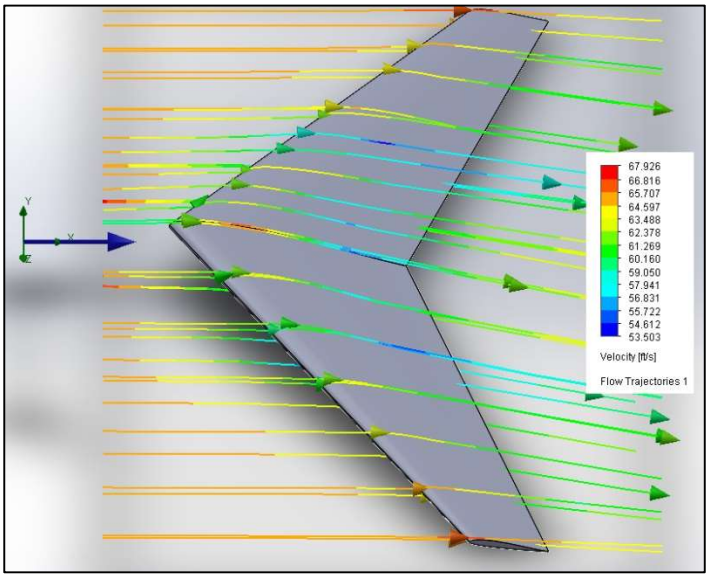

Figure 53: PW-51 Wing Velocity Flow Lines, Top Oblique.

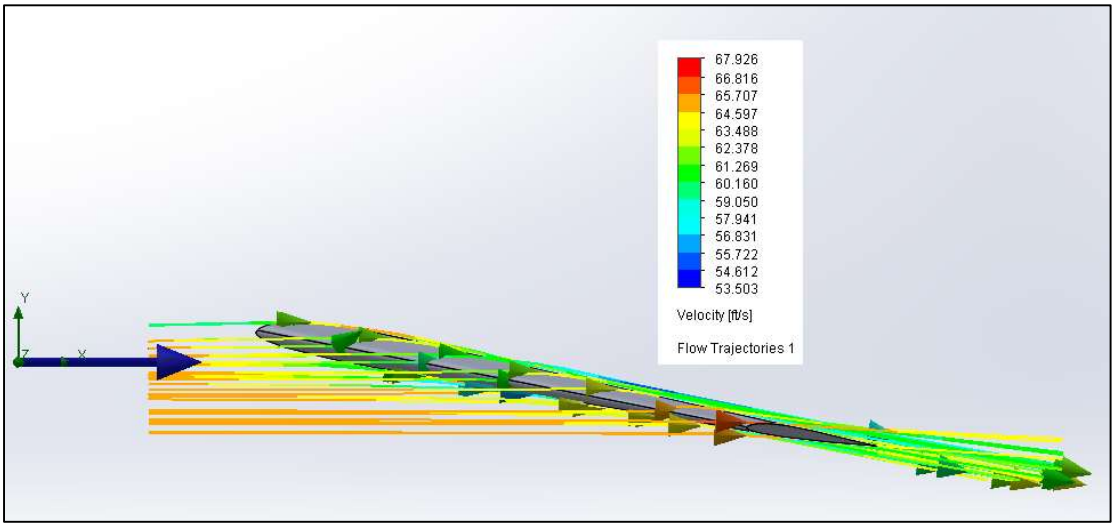

Figure 54: PW-51 Wing Velocity Flow Lines, Profile.

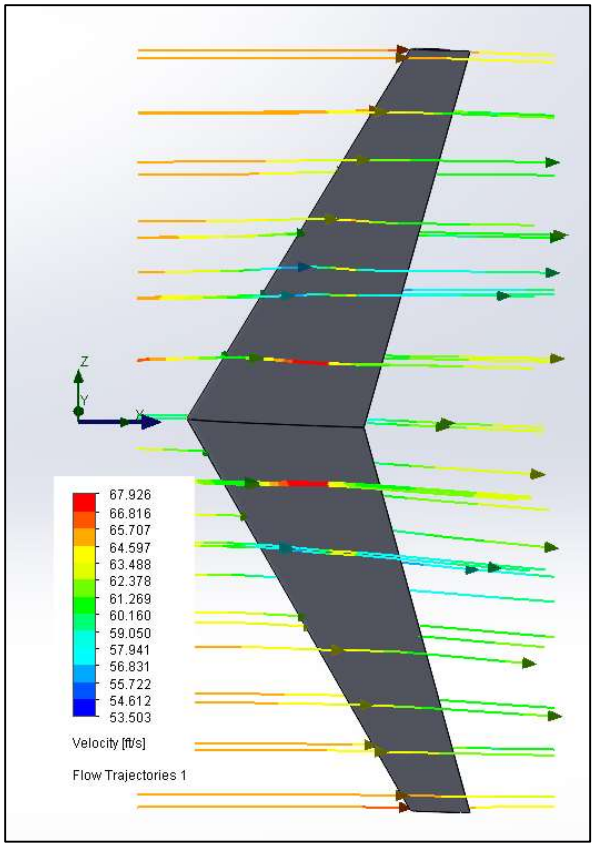

Figure 55: PW-51 Wing Velocity Flow Lines, Bottom.

5.4) SolidWorks Analysis on the HS 522 Airfoil

The third wing to be examined used the HS 522 airfoil. This wing produced its greatest lift at 11 degrees angle of attack at 13.6 lbs (Figure56). It was at its most efficient at a 5-degree angle of attack (Figure 57), where the maximum L/D ratio was 8.0, but it only achieved 5.9 lbs. of lift. Of the three wings, the wing based on the HS 522 airfoil produced the most efficient wing and the most lift at all angles of attack below 12 degrees.

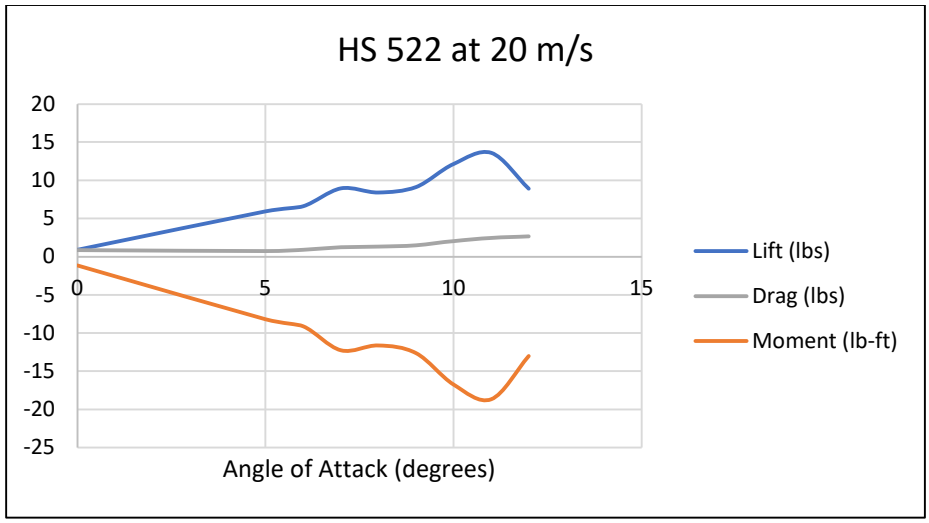

Figure 56: Lift, Drag, and Moment vs Angle of Attack for the HS 522 Wing at 20 m/s Airspeed

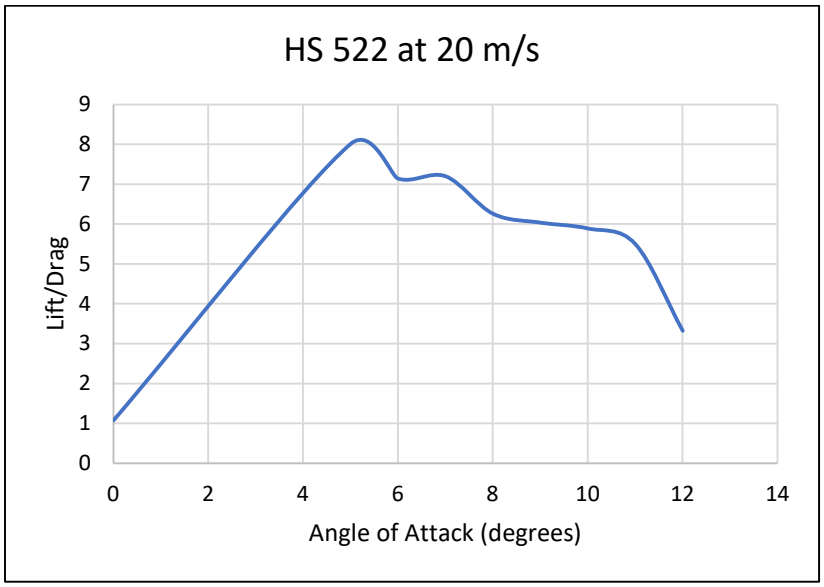

Figure 57: L/D Ratio vs Angle of Attack of the HS 522 Wing at 20 m/s Airspeed

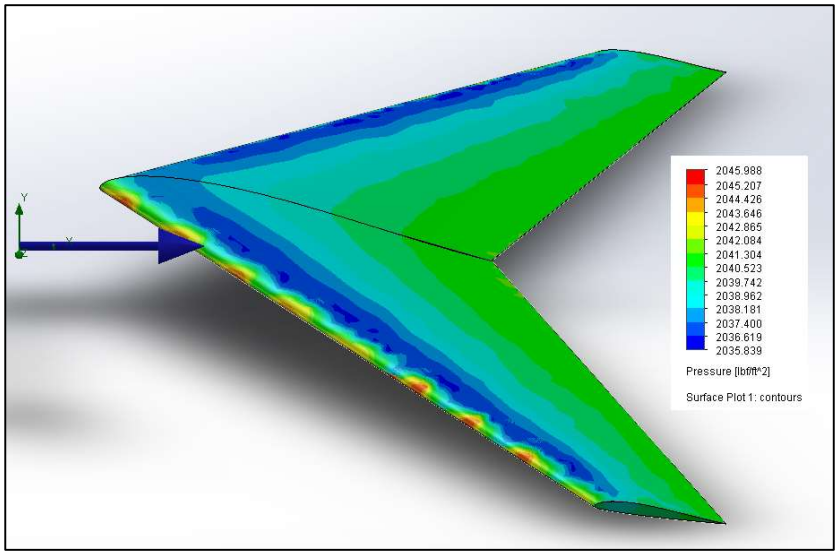

Figure 58: HS 522 Wing Surface Pressure, Top Oblique

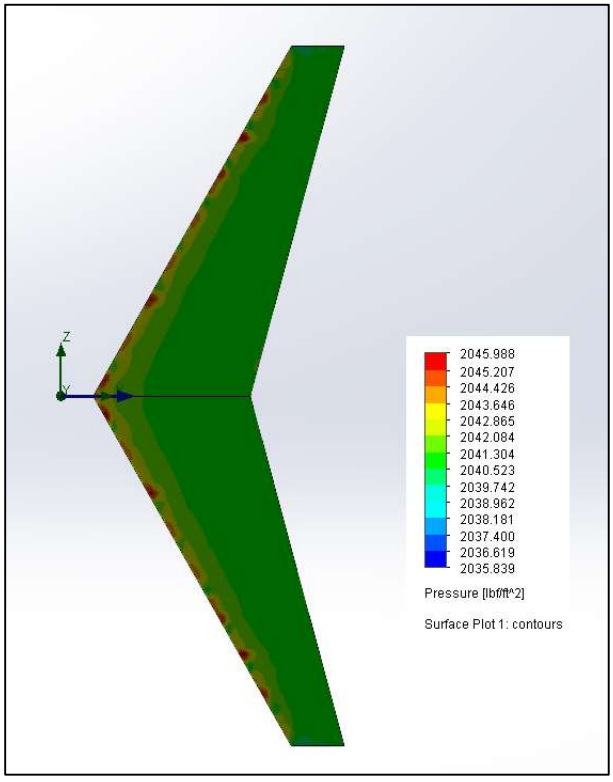

Figure 59: HS 522 Wing Surface Pressure, Bottom

The HS 522 based wing produced the most uniform surface pressure gradients across the entire wing when compared to the two PW series wings (Figures 58-59). This, when viewed alongside the flowlines (Figures 60-62), gives the impression of an efficient wing. The L/D data backs that up, as the HS 522

based wing is nearly twice as efficient when compared to the other wings at their high lift angles of attack.

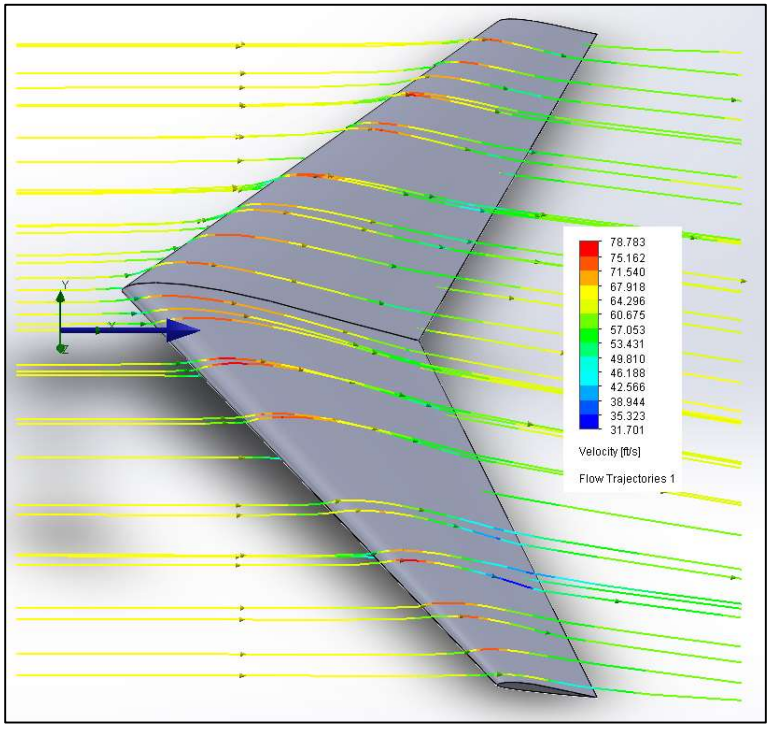

Figure 60: HS 522 Wing Velocity Flow Lines, Top Oblique

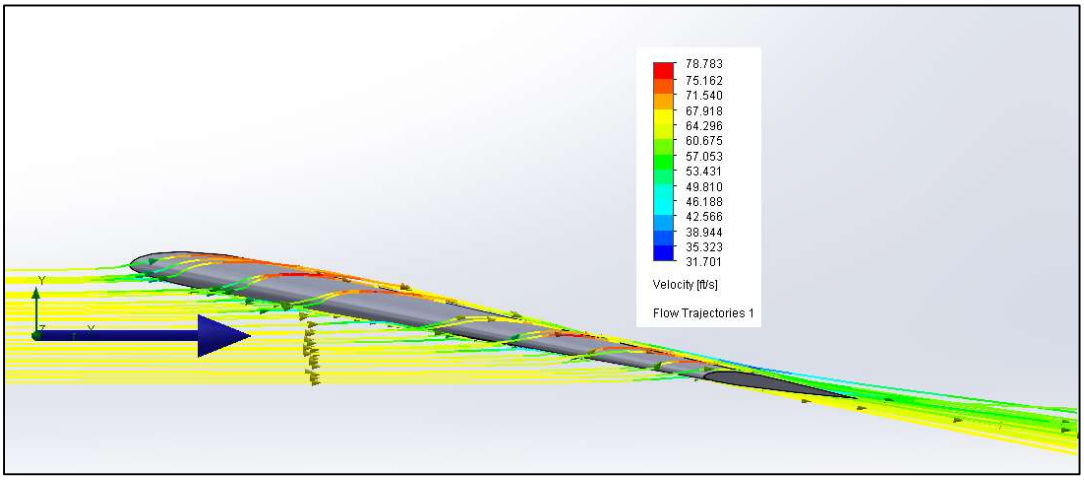

Figure 61: HS 522 Wing Velocity Flow Lines, Profile

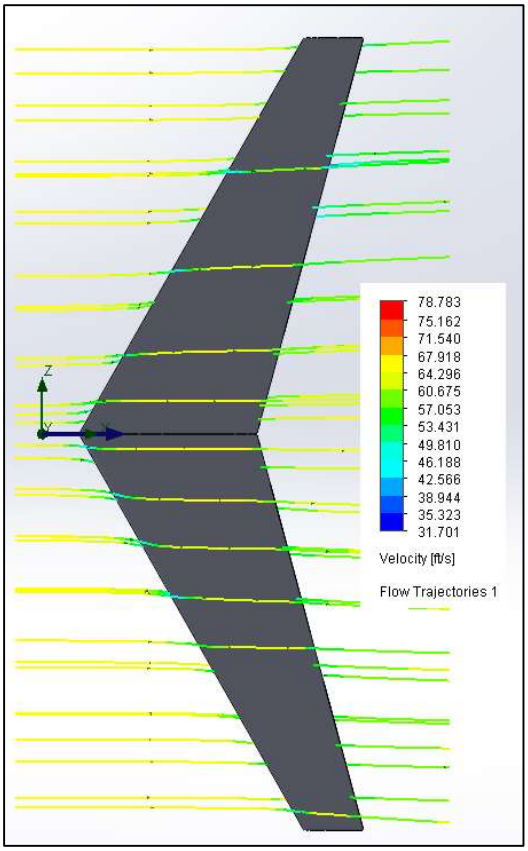

Figure 62: HS 522 Wing Velocity Flow Lines, Bottom

Chapter 6: Wing Composition and Modeling

Even though the HS 522 performed quite well, the airfoil, in its current configuration, would never provide enough lift to meet the customer's 15-pound gross takeoff weight requirement. The team had already discussed using a thicker, high-lift airfoil, but that would have the side effect of producing a significant negative moment. To counter that moment, it was decided that a different airfoil, with a positive moment, would need to be used for the wing tips. Since a model had already been set up in Solidworks, it was relatively simple to quickly test additional airfoils in combination with each other. It was decided that the Eppler 344 airfoil (Figure 63) would be used for the root of the wing and the Eppler 325 airfoil (Figure 64) would be used for the tip of the wing. The same negative 3-degree twist was used as before. There was similar overall lift when compared to the HS 522 wing, but with greater drag, yet also with very little moment (Figures 65 and 66).

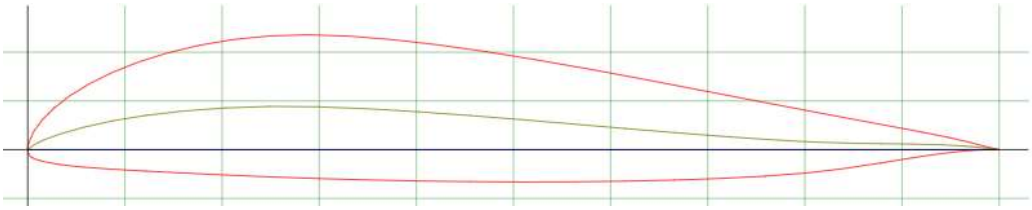

Figure 63: Eppler 344 Airfoil.

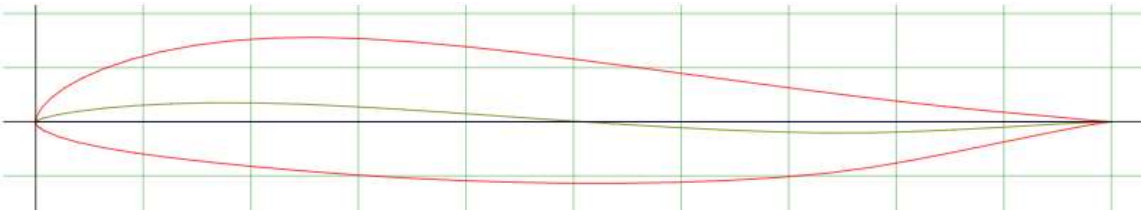

Figure 64: Eppler 325 Airfoil.

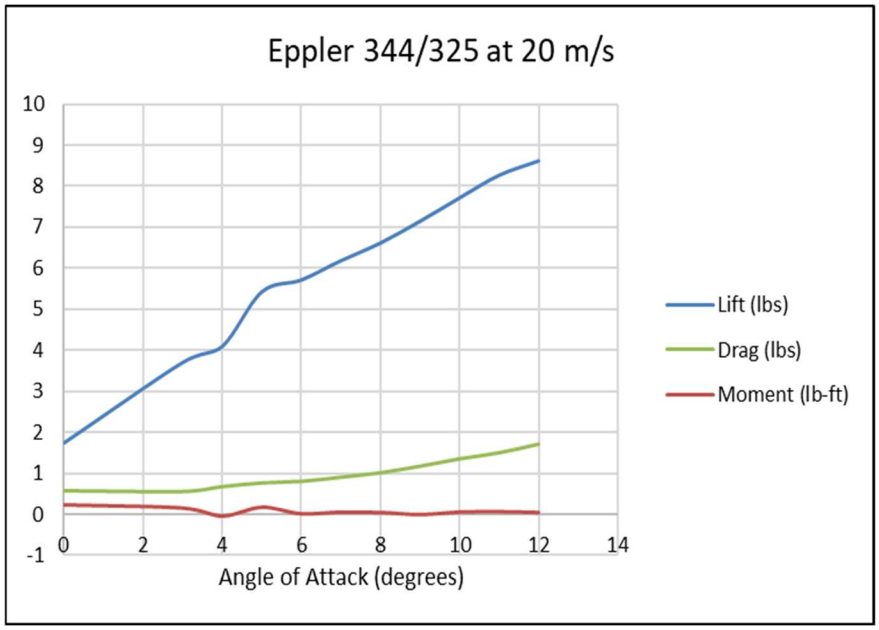

Figure 65: Eppler 344/325 Wing Performance

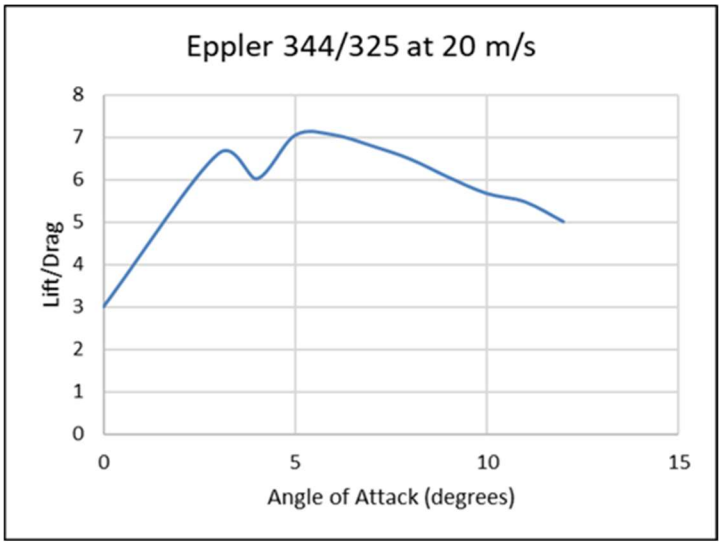

Figure 66: Eppler 344/325 Wing Lift/Drag Ratio

However, during initial simulations, it was quickly apparent that this would not be enough to obtain the required lift of 15 pounds.

While scouring the internet for more information, the website http://www.nestofdragons.net/ [24] was discovered in a last-ditch effort to meet this requirement. This website was created by a hobbyist with a taste for unorthodox aircraft and machines. He had a significant amount of information on flying wings, including work done by the Horten brothers of Germany. One of their methods was to have a high initial

wing incidence, moving to an even greater incidence at about 1/3 of the way between the root and the tip of the wing, before finally a large amount of negative twist (washout) to the tip. This washout equated to 5 degrees from the root and 6 degrees from the point on greatest wing incidence (Figure 67).

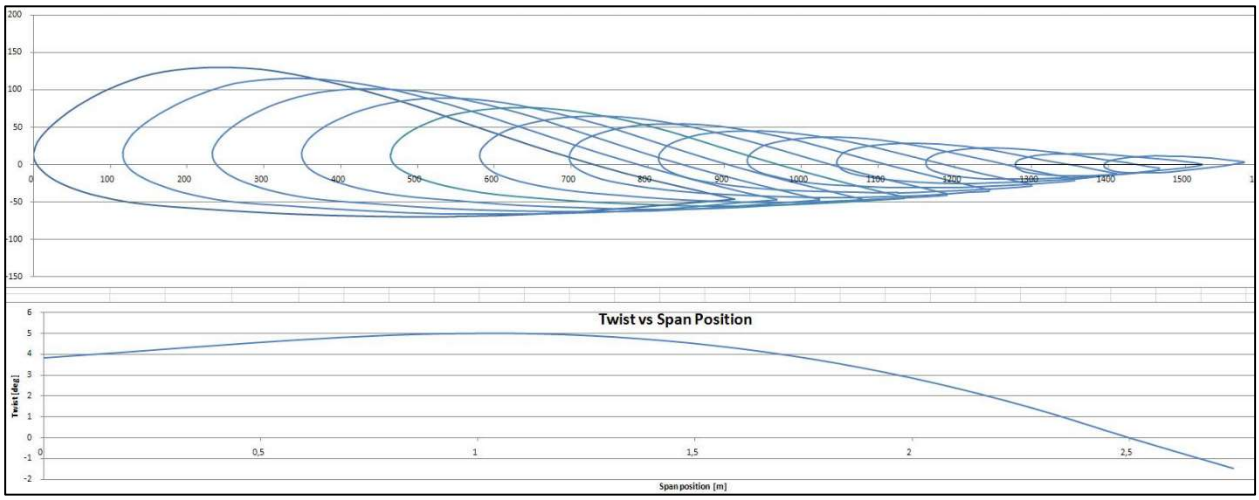

Figure 67: Horten Wing Twist vs Span [24]

Unfortunately, this type of wing, with alternating twist along the span, could not be manufactured by this team using currently available resources. Instead, a model was created in Solidworks using a high initial angle of incidence with a linear negative twist between the root and the tip. The Eppler 344/325 root/tip airfoils were kept in this initial build. At this point a “fuselage”/lifting body was created to house the electronics, battery, etc. This was necessitated not only by the need to house the aircraft components but an immediate need to have something to mount a wing with incidence to. A model of the battery was created in the model to ensure the body would be roomy enough to accommodate it. An Eppler 344 airfoil was used as the basis for the body with the idea that the body should be modeled as closely as possible to an airfoil in the hope of generating more lift. The Eppler 344 airfoil below the chord line went unchanged, but a spline was created above the chord line that ran from the leading edge to the trailing edge that became the top of the airfoil, and hence the center profile of the body. The body was then formed by lofting the body airfoil to the root airfoil. The body central airfoil chord was longer than the root chord, which facilitated a rounded front and rear to the body. The root airfoils were aligned with an incidence of 5 degrees with respect to the body’s central airfoil chord. The wings have a short section of plank airfoil at the root to allow space for the motor mounts. The wings then have a taper ratio of 0.5 from the end of the plank section to the tip airfoil chords, which have 6 degrees of washout with respect to the root chord. The motor mounts are two cylinders, equal in diameter to the motor, joined to the plank section of the wings with a filet.

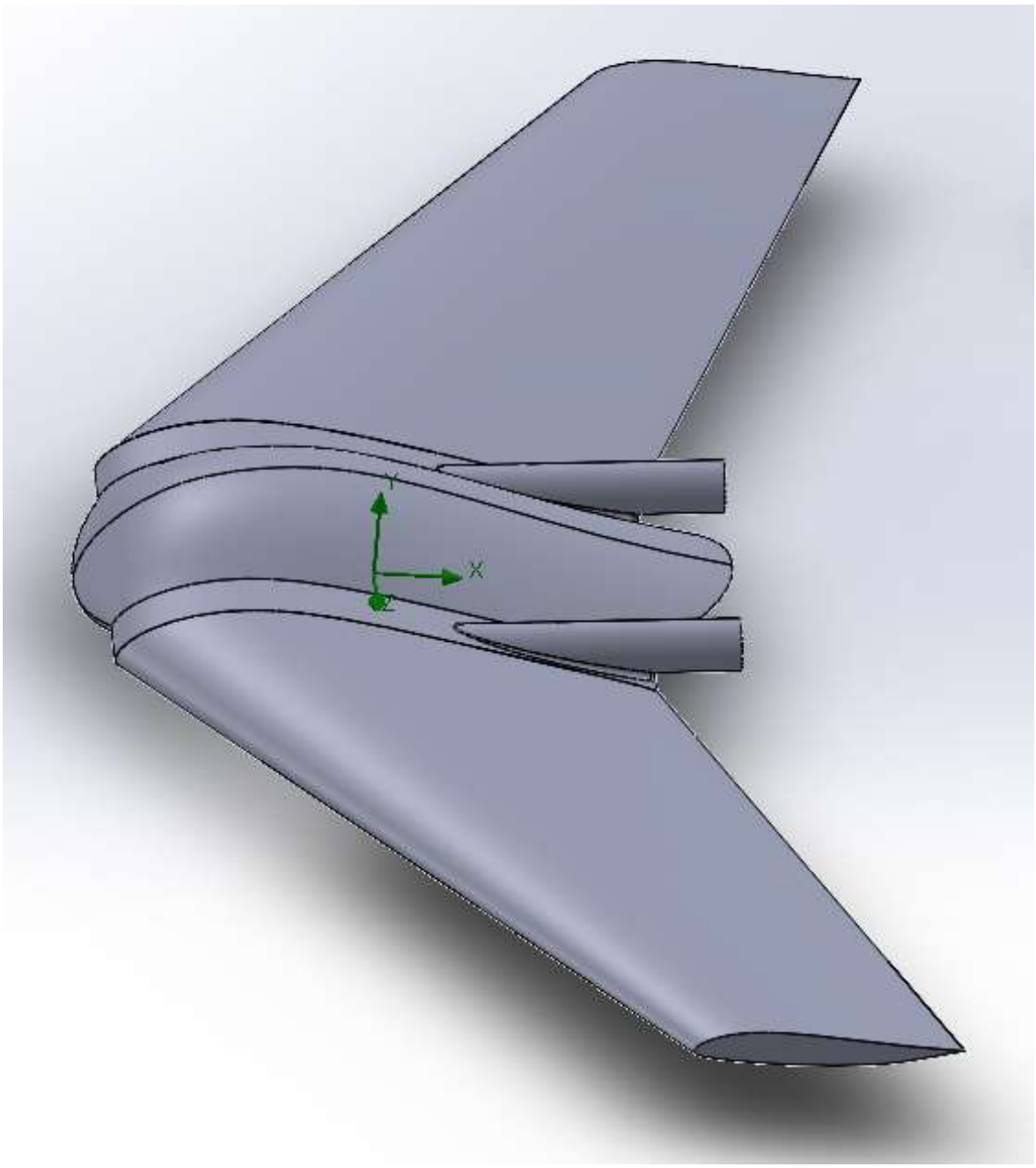

Figure 68: Early 3-D Model of Project Flying Wing Aircraft

With the current aircraft setup (Figure 68), the first simulation produced very promising results, with lift values close to 15 pounds at a five-degree angle of attack (Figure 69). The L/D ratio nearly reaches 6, at an AOA of 4 degrees (Figure 70). Initial moment values were of concern since they ranged from positive to over 4 lb-ft of negative torque, however this was due to the model not being centered in the simulation space at its aerodynamic center. Through an iterative process of simulations, the model was simulated with the simulation space origin located at variable locations on the central body airfoil chord. Starting at an origin location 0.32m from the nose of the aircraft, the simulation was run every 0.02m, moving the nose closer to the origin. Eventually the change in moments between simulations shifted at

0.24m. The location of the aerodynamic center was then narrowed down to approximately 0.255m from the nose of the aircraft, along the chord line of the central body airfoil. This location is of great importance to aircraft stability and for placing the center of gravity of the aircraft by manipulating the placement of components and/or ballast.

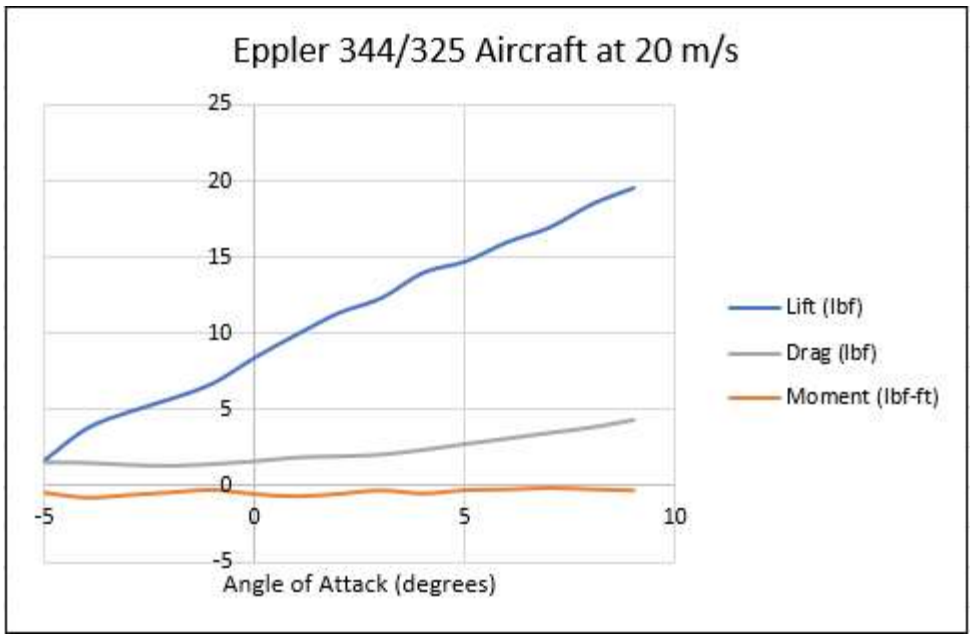

Figure 69: Lift, Drag and Moment vs Angle of Attack of the Initial Aircraft Model

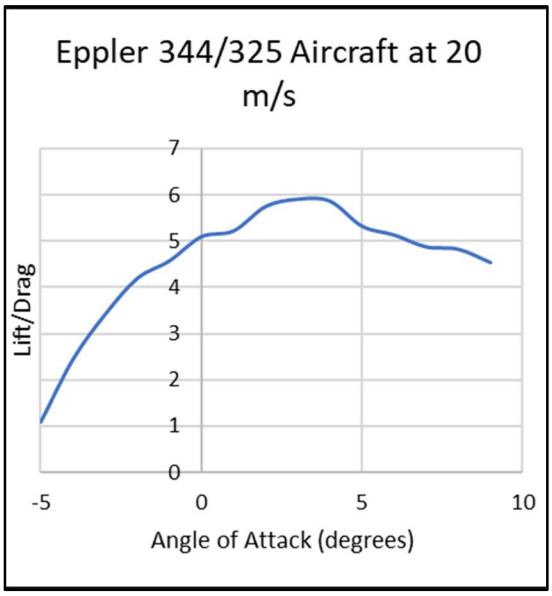

Figure 70: Lift to Drag Ratio vs Angle of Attack of the Initial Aircraft Model

Due to time constraints and the difficulty in getting to this point in the design process, it was decided to move forward with the current airfoil and aircraft layout since it currently meets the lift and size requirements. We do believe that both the airfoil and wing design can be improved in future iterations.

Chapter 7: Weight and Sizing

7.1) Initial Sizing:

The sizing for this aircraft was challenging in two different ways. The first reason was the flying wing design. The sizing methods that from Dr. Daniel P. Raymer's book, *Aircraft Design: A Conceptual Approach* [18], were largely based on existing aircraft and empirical data. However, flying wings were not really discussed and references in the charts provided in the book largely did not explicitly list data for flying wings. Therefore, a best educated estimate was often used during sizing. The second reason that sizing was a challenge was the introduction of electric powered aircraft, which complete mission segments without losing fuel weight.

Traditional sizing methods were followed except for weight fractions. Weight fractions were replaced by a factor called battery mass fraction (BMF). The BMF serves the equivalent role as weight fractions during the sizing process. Chapter 20 in *Aircraft Design: A Conceptual Approach* covered electrical aircraft, and section 20.11 covered electrical aircraft sizing methods.

Sizing began with the desired mission profile (See Figure 1) of an assisted launch using either human or bungie power, a climb to 1,000 ft AGL, a 2.5-hour cruise period, and then a descent to belly landing. A payload of 3 pounds was considered.

A general appearance and form of the aircraft was already given, so the next step in the sizing process was to determine the empty weight fraction. Existing sizing equations did not work, either due to the small size of the aircraft, the fact that it was electric, or possibly a combination of factors. This was not initially discovered until the iteration process. To solve the problem, several different small electric flying wings were researched, and their takeoff weight and empty weight fraction data were plotted (Table 14). From this data, a sizing equation was derived (Figure 71).

Table 14: Historical Weight Data for Small Electric Aircraft [15][16][20][27].

Historical Raw Data		
Plane	Wo (lb)	We/Wo
Phantom FPV Flying Wing	1.98	0.58
Zeta FX-79 Buffalo FPV Flying Wing	4.96	0.53
Believer	12.13	0.4
Skywalker X8 Flying Wing	3	0.558

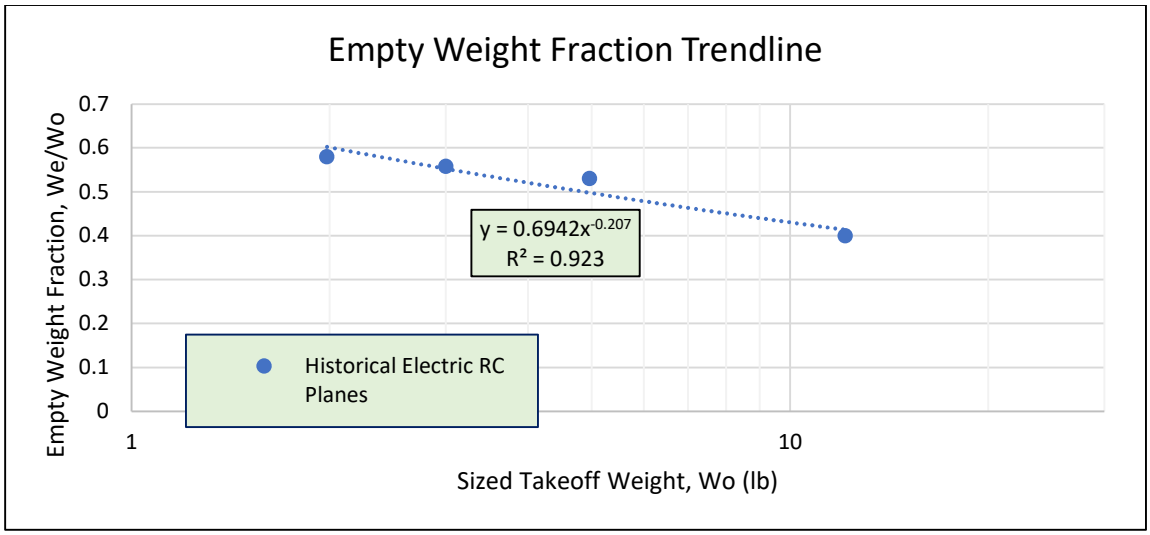

Figure 71: Trendline and Sizing Equation Development.

We were then able to use the historical S_{wet}/S_{ref} of a B-49 flying wing bomber, along with our estimated aspect ratio of 6.56 to calculate our wetted aspect ratio of approximately 3. The K_{LD} of 11, for retractable geared prop aircraft, was used to calculate the $(L/D)_{max}$ of approximately 19. From there, traditional sizing methods were set aside for electrical aircraft sizing methods [18].

First, some factors were known, as the motors and battery have already been selected by our sponsor, Mr. Witzigreuter. The maximum motor power at the batter voltage of 22.2v, according to manufacturer data, was 870 watts per motor (2 motors) [14]. The battery energy density could also be calculated by taking the battery total energy capacity in watt-hours and dividing it by its mass. This produced an energy density of 168.18 Wh/kg. The propeller efficiency was assumed to be 0.8, which matched up with initial market research for 12-inch diameter propellers. The efficiency from battery to motor shaft was assumed to be 0.931, based off historical data presented in Dr. Raymer's book.

Once those values were determined, BMF values could begin to be determined. To determine the BMF for the initial climb after launch, the vertical velocity was first calculated. Since this calculation was dependent on the sizing weight guess, it was built into the excel sizing spreadsheet (Table 15). A velocity of 76% of cruise velocity was used as the most efficient speed for climb. The vertical velocity was then used to calculate the climb BMF. Power used during cruise was then calculated using excel, as it was also dependent on the weight guess. The desired endurance time of 2.5 hrs was then used in conjunction with the calculated power used to determine the cruise time BMF. The takeoff, descent, and landing BMFs were assumed to be negligible. The BMFs were then summed and used in the electric sizing equation, along with the takeoff weight guess and the derived empty weight fraction and payload to determine the calculated takeoff weight (Figure 72). This process was repeated until the takeoff weight guess and calculated takeoff weight agreed.

Table 15: Tertiary Values Used in the Electric Flying Wing UAV Sizing

V_v (m/s)	34.93965326	Eq. 20.5
$P_{used,\ climb}$ (kW)	1.74	(0.87 x 2) Data Sheet
$P_{used,\ cruise}$ (kW)	0.051113207	Eq. 20.2

Sizing Calculations for an Unmanned Electric Flying Wing

W_0, Guess (lbs)	8.73		Payload Weight (lbs):	3.0
Calculated Mass (kg)	3.9598407		Calculated Mass (kg):	1.36077
Endurance (hrs)	2.5		Cruise Velocity (m/s):	20
Lift/Drag (L/D)max:	19		Lift/Drag (Cruise) (prop) (L/D):	19
Cruise Alt (ft AGL)	1000		Lift/Drag (Loiter)(prop) (L/D):	16.454
Cruise Alt (m AGL)	304.8		Endurance Time (hrs):	2.50
Warmup and Takeoff	$BMF_{takeoff}$	0	Assumption, Bungie Launch	
BMF, Climb	BMF_{climb}	0.0068005	Eq. 20.9	
BMF, Known Run Time	BMF_{cruise}	0.2061	Eq. 20.6	
Descend/Land	$BMF_{descend}$	0	Negligible, much less than climb	
BMF, Required	$BMF_{required}$	0.2129	Summation of BMF	
	W_e/W_0:	0.4433	Derived from trendline	
Empty Weight	W_e (lbs):	3.87		
	W_0:	8.73	Eq. 20.11	

	Data entry field
	W_0, Calculated

Figure 72: Last Iteration of Initial Electric Flying Wing UAV Sizing

Table 16: Electric Flying Wing UAV Sizing Iterations

Electric Flying Wing UAV Sizing Iterations			
W_0, Guess (lbs)	W_e/W_0	W_e (lbs)	W_0, Calculated (lbs)
5	0.4975	2.4875	10.36
7	0.464	3.248	9.28
8.5	0.4458	3.7893	8.79
8.7	0.4436	3.85932	8.73
8.73	0.4433	3.870009	8.73

The takeoff weight was iterated until the value of 8.73 lbs was reached (Table 16). This value seemed extremely low. There were several reasons why this might be so. One is the bulk of peak power provided by the selected motors. This resulted in extreme vertical velocities greater than the cruise velocity. Another, and probably more significant reason, is the assumed L/D ratio of 19 for cruise. This historical

value was taken from a large-scale aircraft. After initial results from computer modeling, it is apparent that while improved L/D numbers are very achievable with continued improvements, L/D values approaching 19 are unachievable. This is most likely due to the lower Reynold's numbers small-scale, slower aircraft experience.

7.2) Proposed Weight Sizing:

After compiling CFD lift data on the aircraft model, a new value for the lift to drag ratio of 6.75 was obtained and inserted into the spreadsheet. However, with the required 2.5-hour endurance, no solution was possible for any weight. To find a sizing solution, the weight was set to the desired max takeoff weight of 15 pounds and instead, the endurance was iterated using the goal seek function in Excel. This resulted in a reduced endurance of 1.71 hours (Figure 73).

Sizing Calculations for an Unmanned Electric Flying Wing				
W_0, Guess (lbs)	15.00		Payload Weight (lbs):	3.0
Calculated Mass (kg)	6.80385		Calculated Mass (kg):	1.36077
Endurance (hrs)	1.71		Cruise Velocity (m/s):	20
Lift/Drag (L/D)max:	6.75		Lift/Drag (Cruise) (prop) (L/D):	6.75
Cruise Alt (ft AGL)	1000		Lift/Drag (Loiter)(prop) (L/D):	5.8455
Cruise Alt (m AGL)	304.8		Endurance Time (hrs):	1.71
Warmup and Takeoff	$BMF_{takeoff}$	0	Assumption, Bungie Launch	
BMF, Climb	BMF_{climb}	0.007575	Eq. 20.9	
BMF, Known Run Time	BMF_{cruise}	0.3961	Eq. 20.6	
Descend/Land	$BMF_{descend}$	0	Negligible, much less than climb	
BMF, Required	$BMF_{required}$	0.4037	Summation of BMF	
	W_e/W_0:	0.3963	Derived from trendline	
Empty Weight	W_e (lbs):	5.94		
	W_0:	15.00	Eq. 20.11	

Figure 73: Updated Aircraft Sizing Utilizing CFD Results.

7.3) Final Component Weight Sizing

Component	Weight (g)	# of Components	Total Component Weight (g)
AR620 DSMX Receiver	8	1	8
Props 12x10 + spinners	21	2	42
MN4012 KV480 Motors	155	2	310
4S 10 amp hour battery pack	902	2	1804
Servos	26	2	52
Servo Extensions	13.6	4	54.4
Miscellaneous Wiring	10	1	10
Airfoil and Control Surfaces	922	1	922
Carbon Fiber Wing Spurs	11.5	2	23
Fuselage	1033	1	1033
Payload	1360	1	1360
			Gross Aircraft Weight (g):
			5618.4
			Gross Aircraft Weight (lb):
			12.38643701

Figure 74: Component Weight Summary

Figure 74 displays the calculated gross takeoff weight of the aircraft utilizing the weight of each component. The weights of each the avionics components as well as the propellers were sourced from manufacturer or retailer specification. The weight of the fuselage was calculated from the 3D printing slicing program. Finally, the weight of the air foils and control surfaces was calculated through the calculation of an irregular quadrilateral with an approximately equivalent surface area to the airfoils and control surfaces. The total component weight including a payload of 2 lbs. which is a reduction from the previous calculated estimate of 15 lbs. We believe that this is a more accurate weight that previous weights due to the generalized nature of previous sizing methods compared to the specificity of accounting for all components.

7.4) Control Surface Sizing

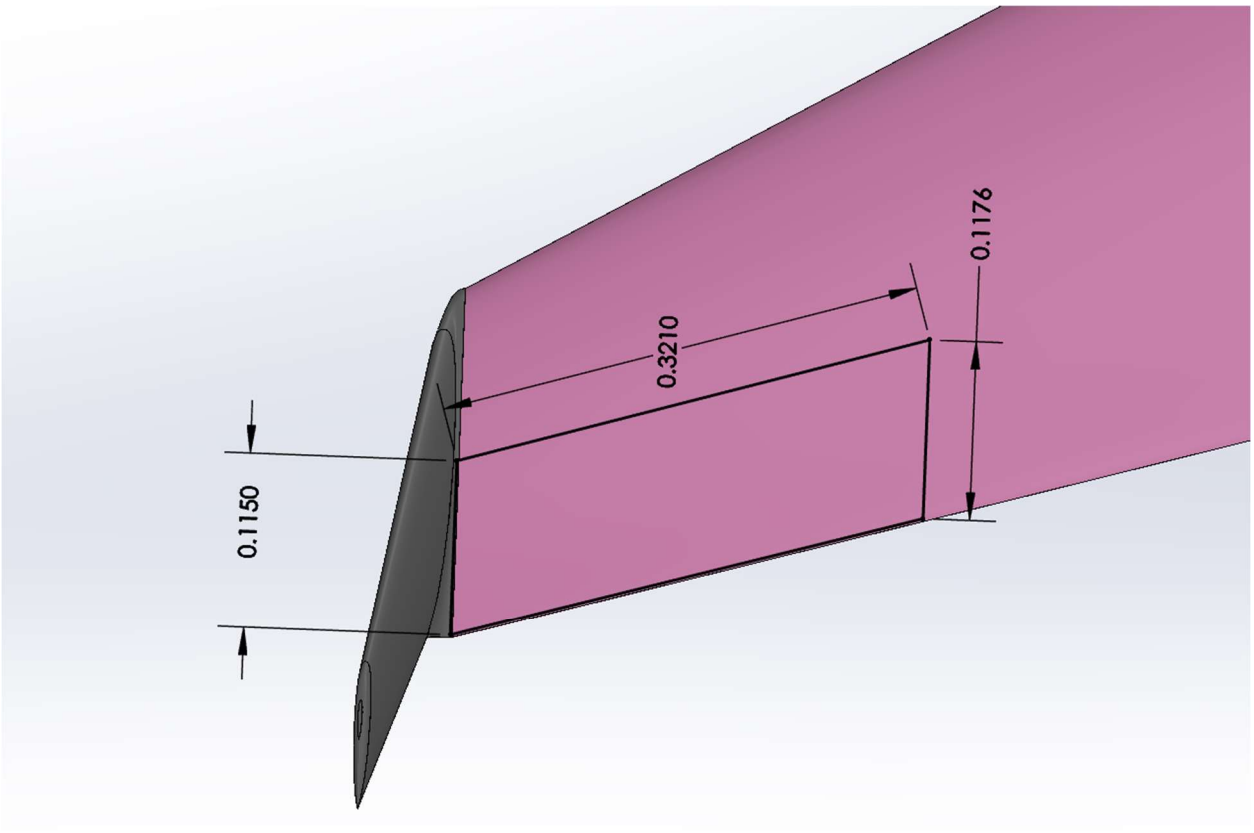

Figure 75:Control Surface Sizing

The control surfaces of the Flying Wing UAV were calculated using methods prescribe by Hamada [10]. For this aircraft which of a similar size as the aircraft described in the paper the following proportions are prescribed an elevon with 50% tip chord, 40% root chord, and 35% mid chord at a distance 40% from the tip of the airfoil. Given the dimensions of our wing the proportions produce a control surface sizing of a tip width of 0.1150m, amid wing width of 0.1176m, and an elevon length of 0.3210m (Figure 75). These dimensions should produce an elevon of sufficient control authority.

Chapter 8: Final Aircraft Design

8.1) Winglet Incorporation

Once all the individual components were selected, they were assembled in Solidworks to produce the model shown below (Figure 74).

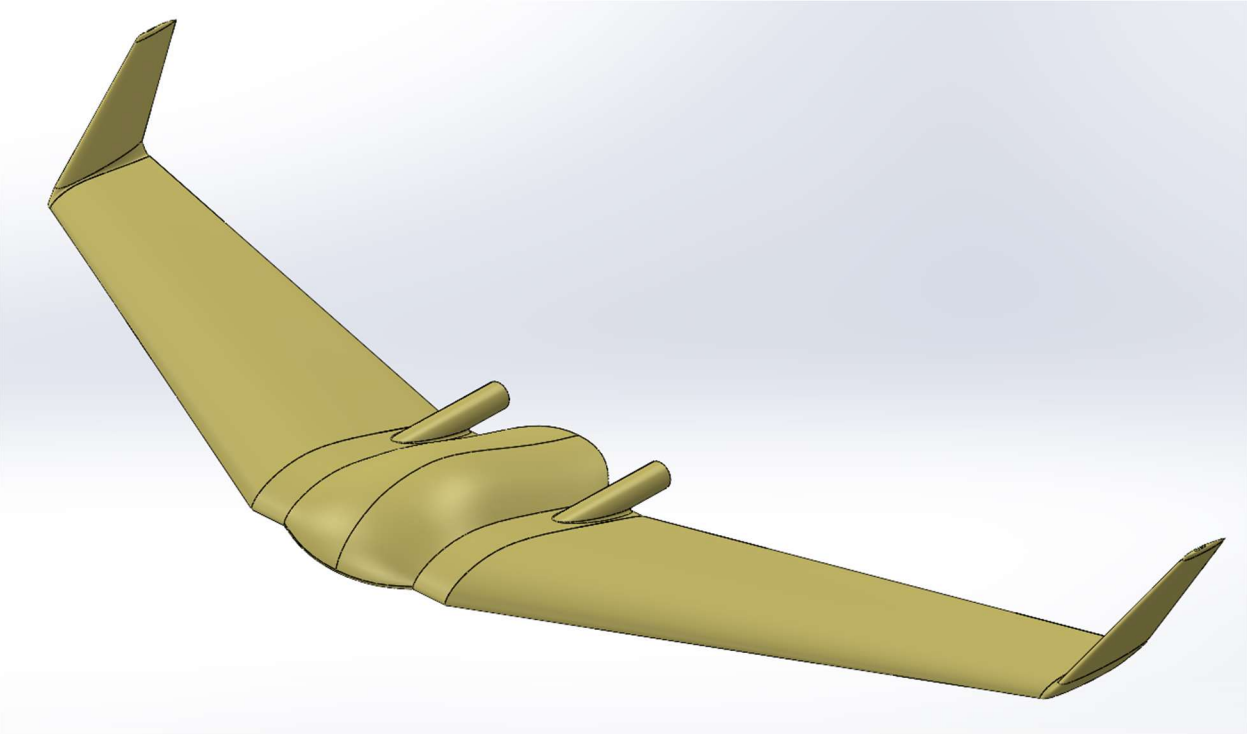

Figure 76: Complete Aircraft Model with Winglets and Motor Mounts.

The winglets were mounted canted outward from the aircraft by 15 degrees (Figure 76) with a 1-degree angle of toe in. The height of the winglet was shortened to save weight and ease manufacturing time, since they will be constructed using a 3D printer. The final winglet height of 6 inches was 2/3 of the tip chord, which did not seem to sacrifice performance. Also, the original winglet height selection of 9 inches was deemed to have a negative cosmetic effect. The winglet height, due to the long tip chord, seemed too tall and did not fit the aircraft well visually.

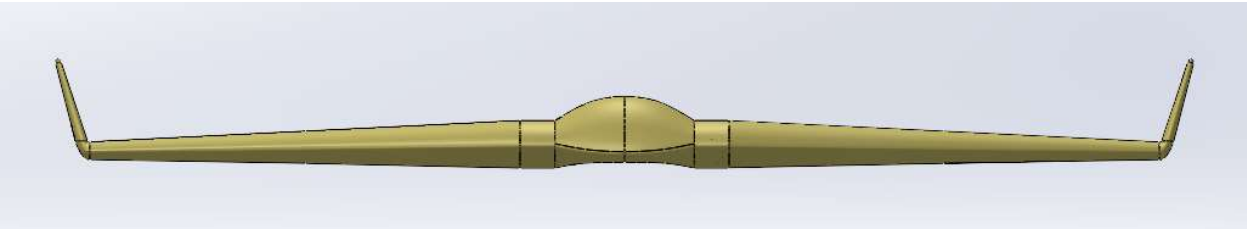

Figure 77: Front View of the Aircraft, Showing Canting of the Winglets

8.2) CFD Analysis of the Completed Model

Once the model was completed, new CFD analyses were conducted to find the new aerodynamic center of the aircraft. With the addition of the winglets, the aerodynamic center moved further back on the aircraft, to 0.270 m from the front of the body from an original location of 0.255 m from the front of the body. This made sense logically, as the change in the aircraft added more flight surfaces to the rear of the aircraft, which would move the aerodynamic center in that direction. Once the new aerodynamic center was located, the final CFD analysis was run using a finer mesh of the computational area, meaning more computational data points and more accurate results.

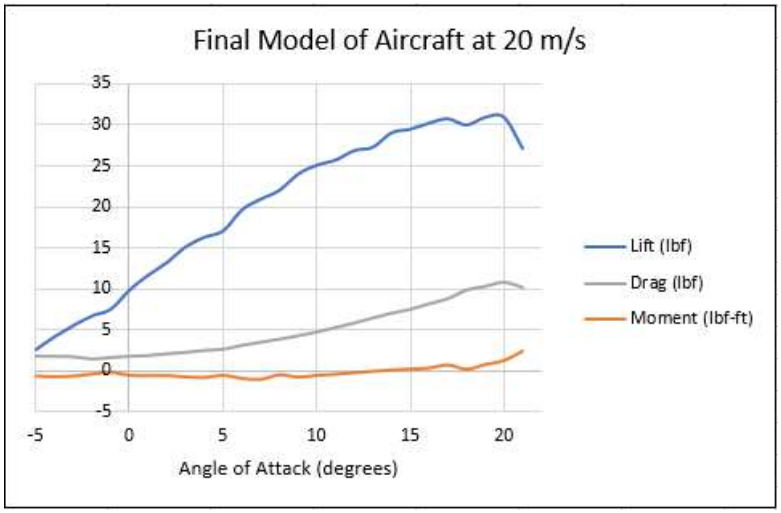

Figure 78: Final Computer Model Performance (CFD).

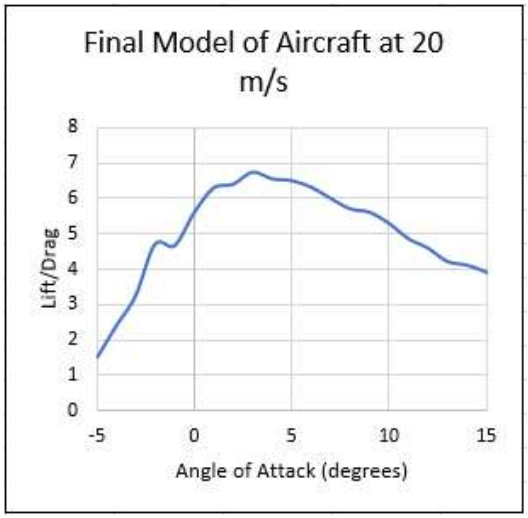

Figure 79: Final Computer Model Lift/Drag Ratio (CFD).

The increase in performance from the winglets was significant (Figure79), improving the L/D ratio by 14.4% at a 3-degree AOA and 22.4% at a 5-degree AOA. Even more significant was the change in AOA required to achieve the required lift at cruise from 5 degrees to 3 degrees (Figure 78). Examined in this way, the level cruise L/D was improved by 26.9% by adding winglets (Figure 80).

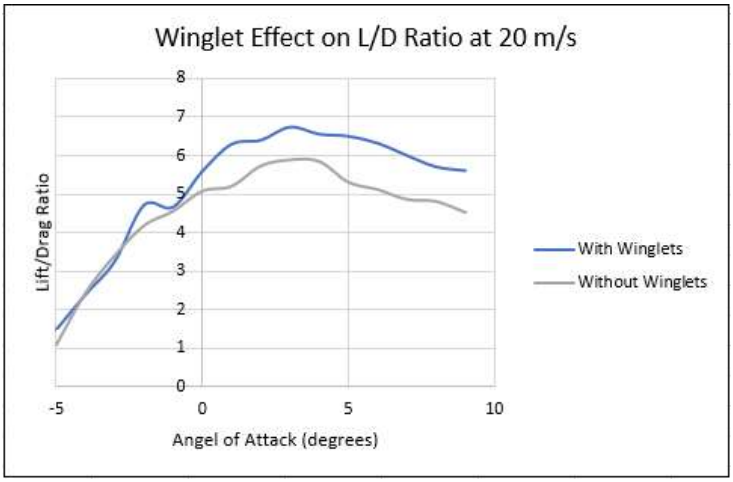

Figure 80: Winglet Effect on Lift/Drag Ratio for the Completed Model (CFD).

The change in the airflow is visibly evident when the CFD models at a 3-degree AOA are compared with each other. The streamline representation of the airflow over and around the winglets produces some small vortices at the winglet tips and small vortex at the base of the winglet/wing tip. The vortex at the wing tip is pushed out and away from the wing by the effects of the winglet (Figure 81), reducing the induced drag. This is in comparison to the large, well-defined vortex produced on the identical wing before the winglet was added (Figure 82).

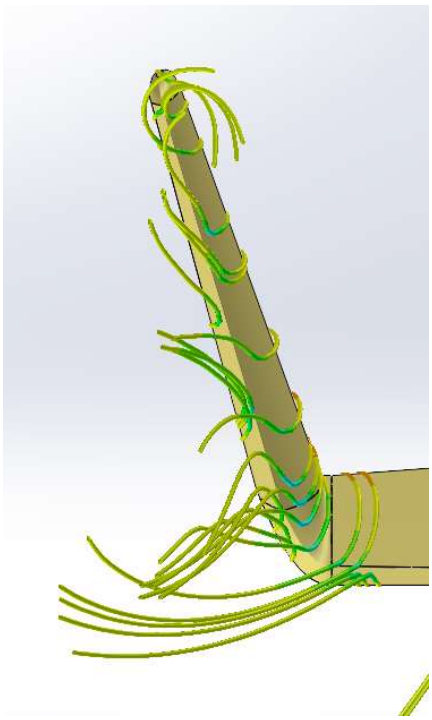

Figure 81: Small, Loose Vortices from a Winglet at a 3-Degree AOA (CFD).

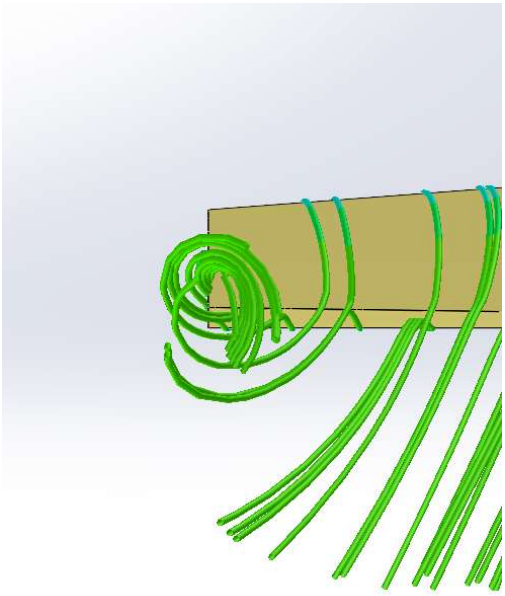

Figure 82: A Well-Defined Wingtip Vortex at a 3-Degree AOA (CFD).

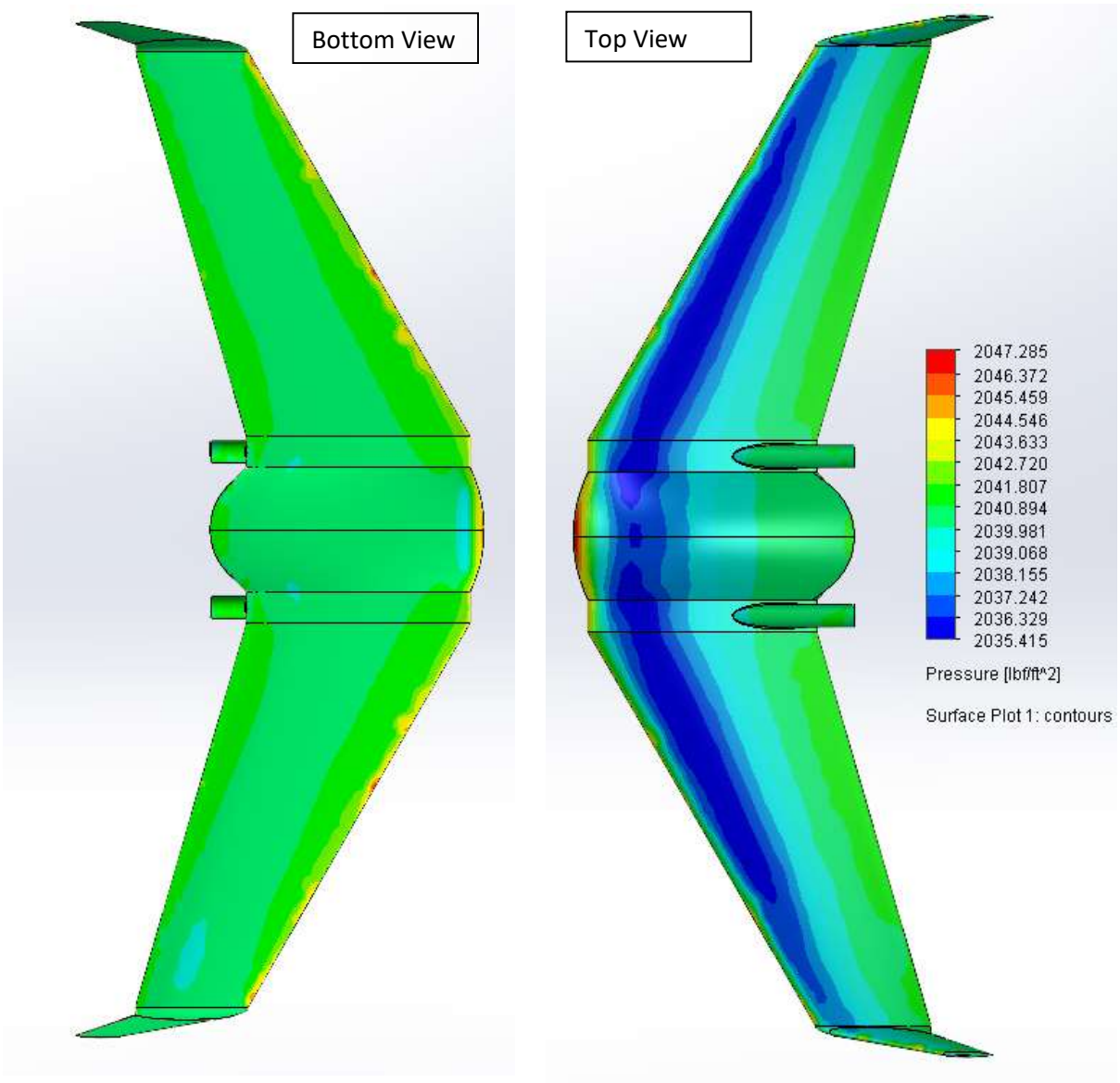

Figure 83: Bottom/Top View Surface Pressure Plots of the Modeled Aircraft (Scale applies to both views) (CFD).

The surface pressure plots (Figure 83) illustrate lift in terms of pressure acting on the aircraft. The figure above shows the higher pressure acting on the bottom of the aircraft and lower pressures acting on the upper portion of the aircraft.

The Figure 84 illustrates an area of the body's design that may need to be refined. In the figure, central streamlines can be seen with their velocities almost coming to a standstill at the rear of the body while also circulating in the area several times before exiting the vicinity of the aircraft. This indicates poor airflow and possible flow separation. Future redesigns should attempt to address this and improve airflow over the rear of the body.

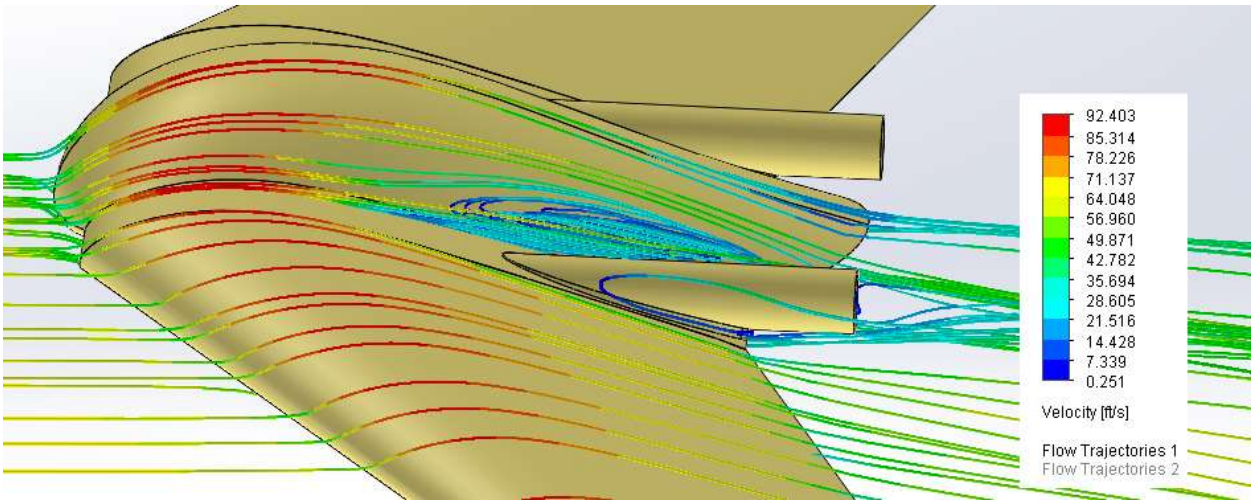

Figure 84: Streamlines Depicting Airflow Over the Body (CFD).

Utilizing the CFD results from the aircraft model, several aircraft characteristics could be derived. A wing area of 7.77 ft^2 was measured from the Solidworks model and used to calculate a maximum wing loading of $1.93\ \frac{lbf}{ft^2}$. The maximum lift from the CFD model was used in conjunction with the wing loading to calculate a stall velocity of $13.9\ \frac{m}{s}$. The following additional aircraft characteristics were also calculated:

- Climb Rate: $18.25\ \frac{m}{s}$
- Range: 123 km

Chapter 9: Center Wing and Components

9.1) Center Wing Body

The center section of the wing (at times referred to as the “fuselage” for ease of description) will house all electrical components except the servos and will also serve as a connection point between the left and right outer wing sections. Though appearing as a single piece once assembled, the center wing will be made up of three separate pieces, the nose, the top hatch, and the primary housing. The fuselage will be 3D printed on a large-volume 3D printer, so careful consideration was given to ensure that the center wing is printer-friendly with respect to its layout and individual pieces. This will allow all three components to be printed without supports to minimize production time, cost, and material waste.

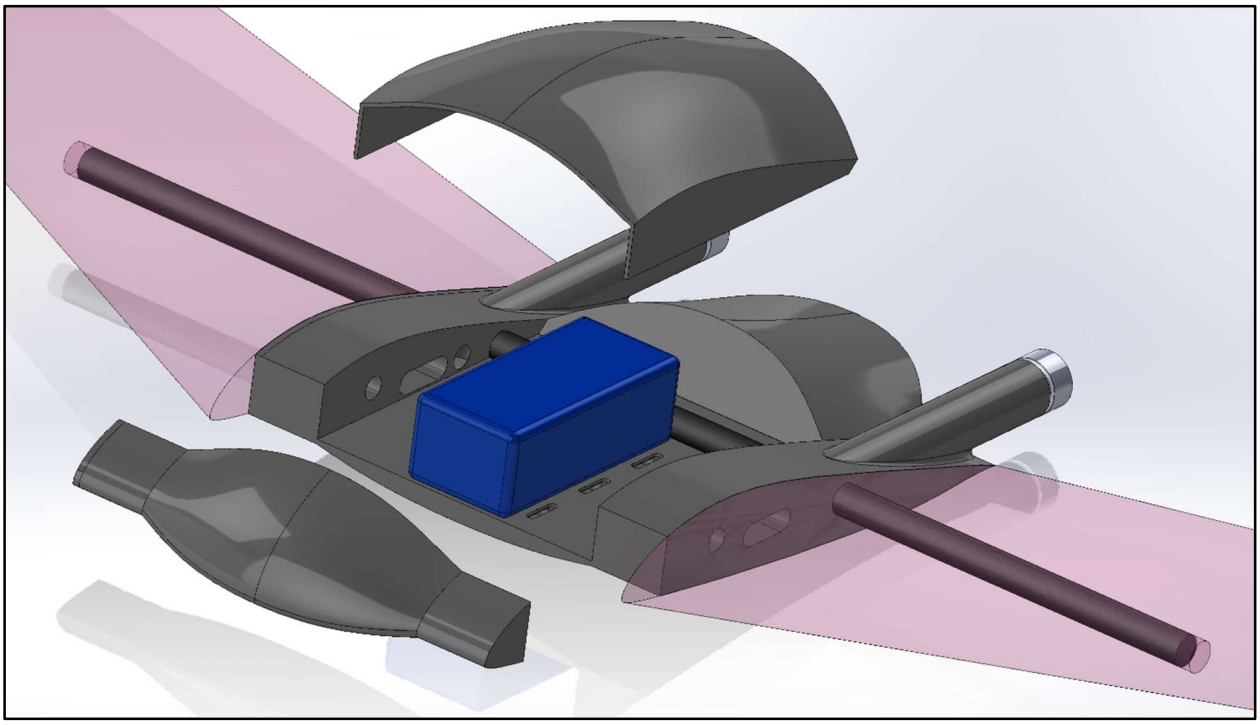

Figure 85: Center Wing Section - Exploded View

Being an electric aircraft, quick access to the battery and other electronics will be crucial. The top hatch is designed to install and remove quickly and will attach to the primary housing with pins and/or nylon bolts, utilizing alignment pegs where necessary. The nose of the aircraft is a separate piece which allows for ease of printing but will also allow the nose section to be customized to fit cameras and other surveillance devices as needed without any additional modification or reprinting to the hatch and primary housing (Figure 85). The nose will be attached to the primary housing with nylon bolts and alignment pegs to allow the user to quickly swap from a solid nose to a camera-compatible nose (Figure 86).

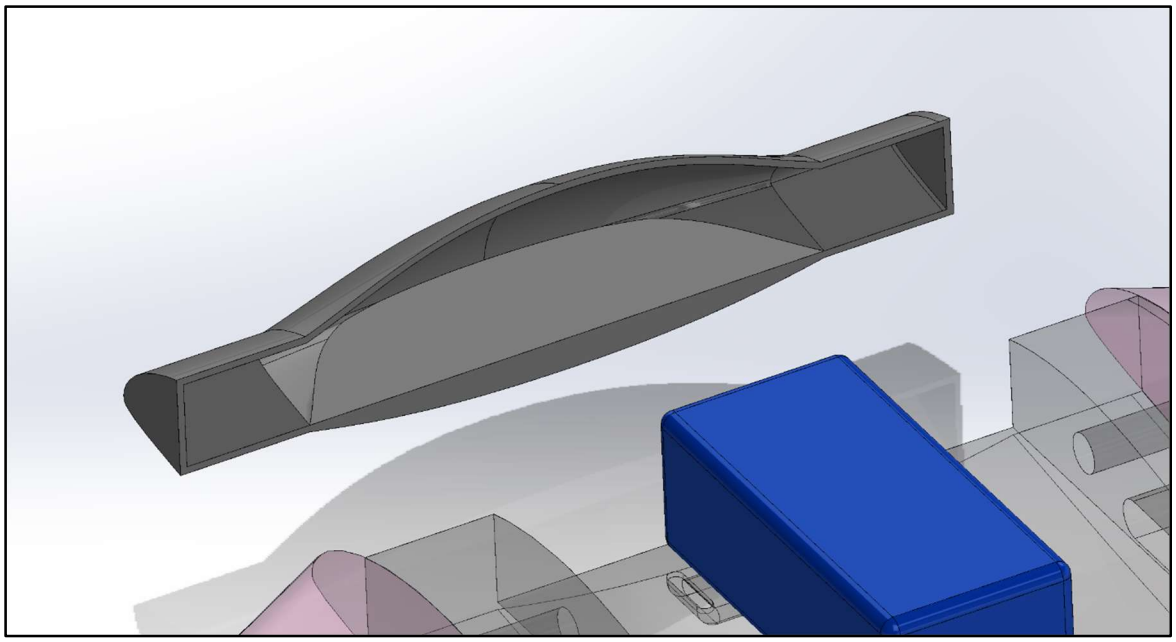

Figure 86: Nose Cowling

Cutouts have been placed along the bottom of the battery compartment to allow for passage of Velcro straps which will hold the battery in place. Cutouts have also been made through both sides of the fuselage to allow for servos wires, spars, and wing attachment bolts (Figure 87). The motor tubes are hollow and provide a pass-through for the motor wires into the electronics bay where the ESCs will be housed.

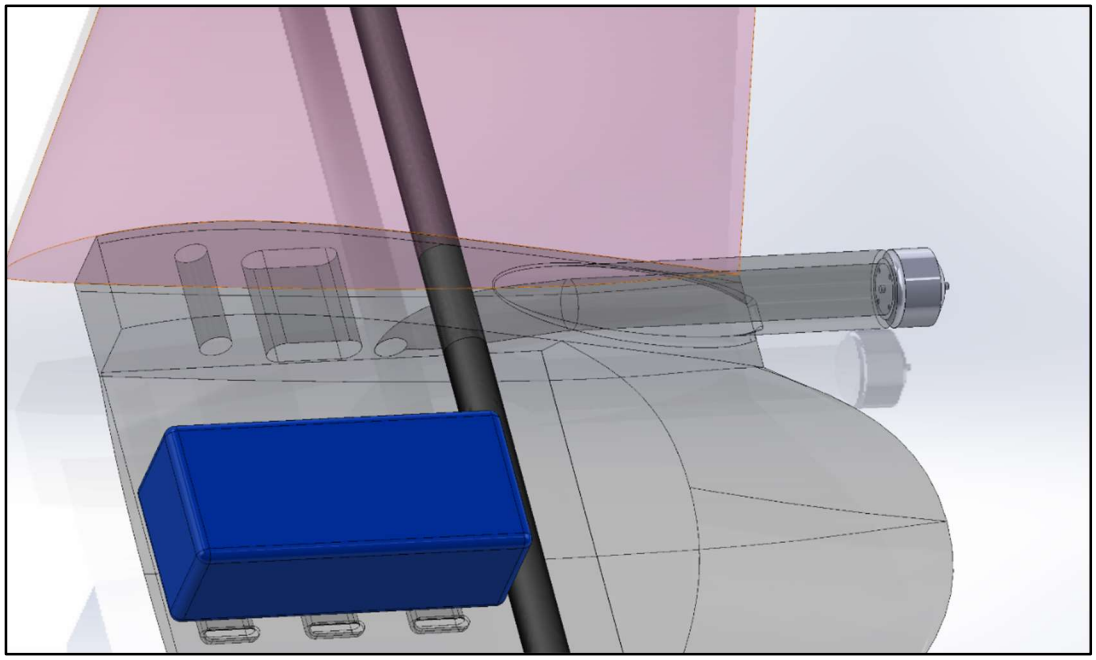

Figure 87: Spar and Wiring Cutouts

9.2) Avionics Selection:

DX6e 6-Channel DSMX Transmitter with AR620:

Specs: Full range AR620 DSMX Receiver, built in telemetry

Source: https://www.horizonhobby.com/product/dx6e-6-channel-dsmx-transmitter-with-ar620/SPM6655.html

Quantity: 1

Figure 88: DX6e 6-Channel DSMX Transmitter with AR620

Aeronaut CAM Folding Propellers:

Specs: 12 x 10 with spinners, made of carbon fiber with reinforced plastic

Source: https://www.espritmodel.com/aeronaut-cam-folding-propellers-rudi-freudenthaler.aspx

Quantity: 2

Figure 89: Aeronaut CAM Folding Propellers (12 x 10)

MN4012 Motor:

Specs: Max Power is 870W, KV rating of 480

Source: https://store-en.tmotor.com/goods.php?id=346

Quantity: 2

Figure 90: MN4012 KV480 Motors

Turnigy High-Capacity Battery:

Specs: 10000 mAh, 4S 12C Lipo Pack, 5.8 lb pack weight

Source: https://hobbyking.com/en_us/turnigy-high-capacity-10000mah-4s-12c-multi-rotor-lipo-pack-w-xt90.html

Quantity: 2

Figure 91: Turnigy High-Capacity Battery

<u>150oz-in, Micro, CLS Servos</u>:

Specs: 150oz-in, 0.057 lb weight

Source: https://www.promodeler.com/DS150CLHV

Quantity: 2

Figure 92: 150oz-in Servos

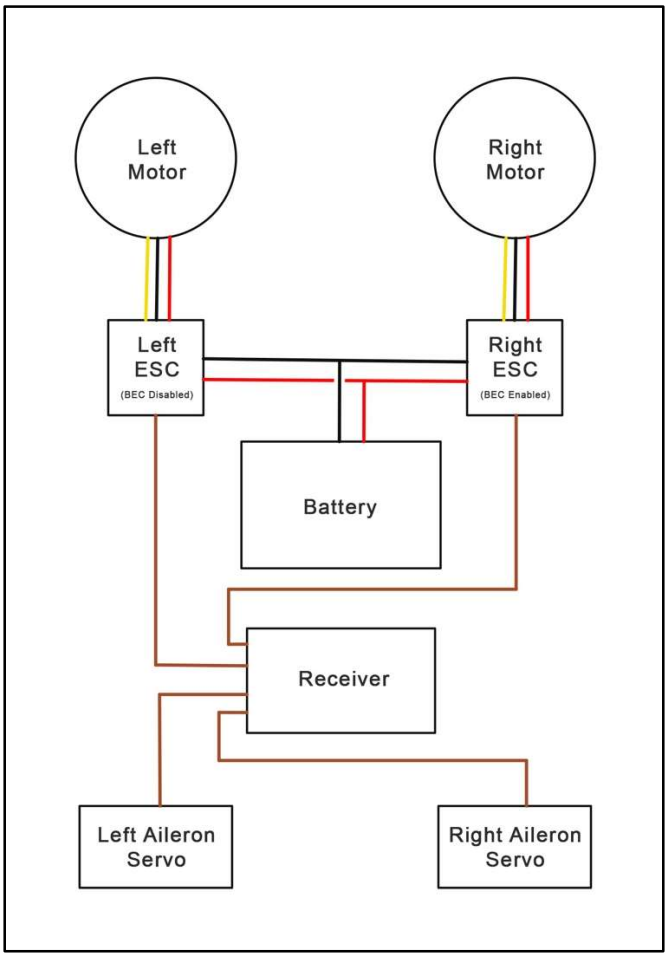

Figure 93: Electronics Schematic

The avionics for the Flying Wing were primarily selected by our sponsoring company. The DX6e 6-Channel DSMX Transmitter with AR620 (Figure 88) was selected for both its operational range which is sufficient for the first iteration of this Aircraft, additionally the built-in telemetry functions provide useful information data to us. The Aeronaut CAM Folding Propellers 12x10 (Figure 89) were selected for two reason. The weight of the propellers given their length and strength is quite low which is helps in keeping the weight of the aircraft low. Additionally, given that the aircraft is intended to belly land the foldability of the props ensures that they will not be damaged by striking the ground upon landing.

The MN4012 Motor (Figure 90) was selected for its low weight and high-power output. This high-power output allows use to more easily hand launch the aircraft. With such a high thrust to weight ratio the aircraft can rapidly gain airspeed to quickly exceed the stall speed after being thrown. The batteries selected Turnigy High-Capacity Battery (Figure 91) provide sufficient power with an acceptable weight while fitting in the geometric constraints of the fuselage. Finally, the 150oz-in, Micro, CLS Servos were selected for the magnitude of torque they can quickly provide (Figure 92). Given that the only control surfaces on this aircraft are the elevons, quick and responsive feedback from them is paramount to the controllability of the aircraft. The electronics schematic of the layout of the avionics is pictured above (Figure 93)

Chapter 10: Wind Tunnel Testing

10.1) 3D Model for Testing

The wind tunnel at KSU has a width of 12 inches at the test section which requires that our model be tested at approximately 15% scale. Due to the small size, winglets on such a model would likely produce negligible results and would also force the model to an even smaller scale. The winglets were neglected from the wind tunnel model in light of these factors. Mounting to the wind tunnel sting also requires that a tube be extruded from the fuselage with the appropriate mounting dimensions. These adaptations will result in absolute values of lift and drag that are skewed from the true lift and drag values seen by the full-scale prototype. The model will be wind tunnel tested for the collection of relative results rather than absolute data.

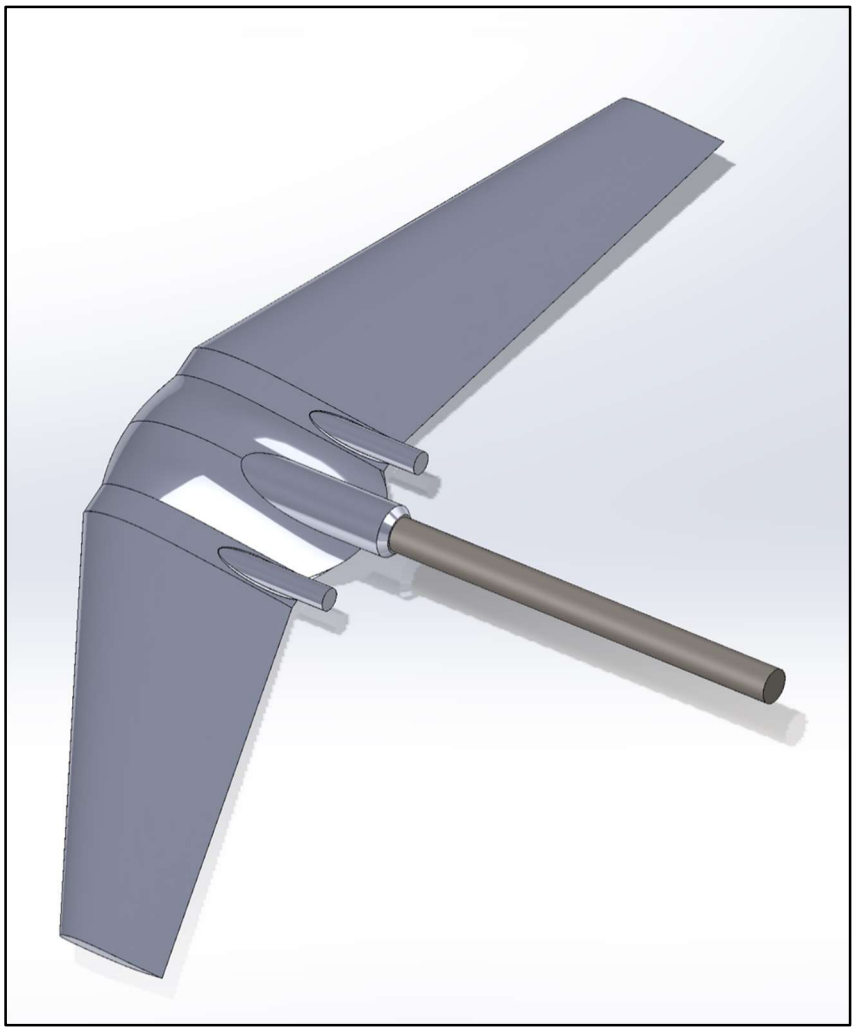

Figure 94: CAD Model of Wind Tunnel Test Prototype with Sting

We determined that the best method for producing a wind tunnel test model would be 3D printing. This production method would also allow us to easily adapt the model for mounting to the wind tunnel sting. Special consideration had to be given to the smoothness of the model's exterior so as not to create turbulent drag around the surface. An attempt was made at printing the model in multiple sections in an effort avoid the use of supports that could leave jagged residual plastic on the model.

Figure 95: Wind Tunnel Test Model V1

Unfortunately, this printing method resulted in a mild gap between the two halves of the wing. While the gap could have been resolved with glue, it is possible that the seam along the length of the mounting tube would make the tube too weak to handle the sustained high wind speeds that will be encountered in the wind tunnel. This method was abandoned, and the model was reprinted on its nose with the help of supports. Some sanding was required to achieve a smooth finish, but it was deemed necessary to achieve adequate strength in the model.

Figure 96: Wind Tunnel Test Model V2 Printed with Tree Supports

Figure 97: Wind Tunnel Test Model V2

Figure 98: The Smooth, Sanded Model

10.2) Wind Tunnel Test Results

During this process, we were assisted by Joshua Hunter, a fellow Kennesaw State University undergraduate student and a member of the KSU Aerial Robotics Team. The model was mounted to the wind tunnel probe using two set screws to fully secure the model. The model felt securely attached to the probe and it was clear of interfering with the probe housing. This was the first time the wind tunnel was being utilized with this probe installed and we took great caution while mounting and removing the model to preserve this new, expensive, piece of equipment. The measurements for the wind tunnel were zeroed out with the model mounted and the wind tunnel off. The testing was conducted under ambient pressure and temperature of 2107 psf (29.9 in Hg) and 75 degrees Fahrenheit. To ensure the safe operation of the wind tunnel, the model was first run through the wind tunnel at the lower speed of 100 mph to slowly ramp up the test to the desired wind tunnel test speed of 120 mph. Since the wind tunnel readings had mild fluctuations, three sets of data were taken for each data point and the results for the three sets were averaged. These averages for each data set were used for future calculations.

As the wind tunnel results were recorded, it was immediately apparent that the drag forces would not be accurate due to the axial force reading from the wind tunnel switching from a positive value at low angles of attack, to a negative value as the angle of attack increased past 2 degrees. We were unable to figure out why the axial force reading would decrease in that way. The remaining data for the lift and drag did not seem flawed, so we proceeded with the testing and processing of the data. Since the wind

tunnel only gave the normal and axial force, along with a measured moment, everything needed to be converted into lift, drag, and the moment around the aerodynamic center of the aircraft. The following equations were utilized:

$$L = N(\cos\alpha) - A(\sin\alpha)$$

$$D = N(\sin\alpha) + A(\cos\alpha)$$

$$P_{m_{ref}} = N\left(\frac{P_m}{N} + A - C\right) \text{ [2]}$$

The results from the wind tunnel can be found below, in Figure 99. The plotted lift data seemed very linear apart from one slight outlier data point at 2 degrees AOA. The plotted drag was likewise linear in slope, but in the wrong direction. The plotted moment data was linear as well, with outliers at -5- and 2-degrees AOA. Although we were disappointed that the data seemed corrupted somehow, it was decided that the lift data appeared like it could be accurate, so we drove forward with the comparison to a CFD model of the wind tunnel test. If the CFD small-scale model test and the wind tunnel test results were similar, it would lend validity to the large scale CFD results for the full-scale model.

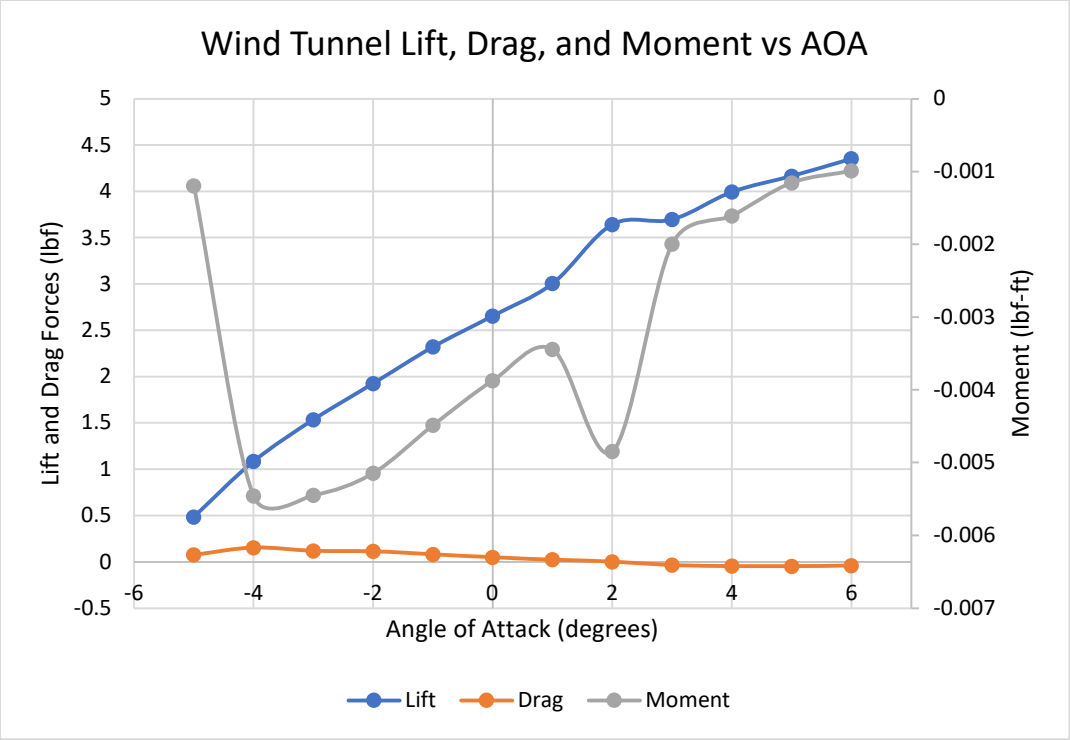

Figure 99: Wind Tunnel Data, Small Scale Model at 120 mph

A CFD simulation of the wind tunnel was conducted with the same Solidworks model that was printed and used in the actual wind tunnel. The CFD was set to run under identical conditions of pressure, temperature, flow velocity, and tunnel size. Figure 100 (below) shows the difference in the drag

between the two methods. As previously mentioned, the wind tunnel results were considered flawed, so this outcome was not unexpected.

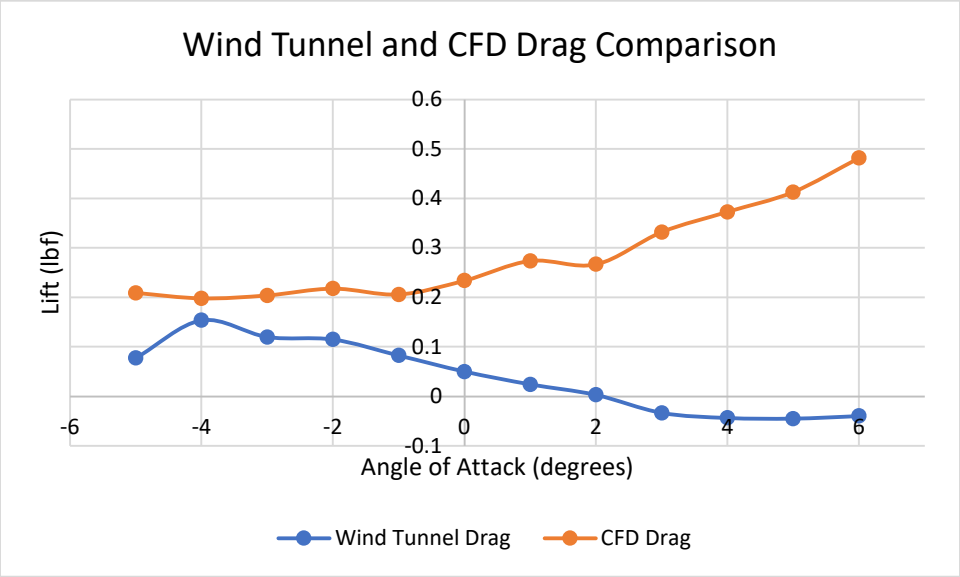

Figure 100: Wind Tunnel and CFD Drag Comparison

As a team, we recognized that the faulty axial force data would corrupt the lift data, however, it was decided that since the axial force and the AOA were so small, the net effect on the lift would be small enough to use the resultant lift data.

When the lift numbers were compared, they were much more similar. However, it was surprising that the wind tunnel numbers were higher than the CFD model (Figure 101, below). We were expecting them to be the same or lower, however we were pleasantly surprised when all the lift numbers for the wind tunnel were higher than the CFD simulation. At a -5-degree AOA, the lift numbers were similar and near zero. However, as the AOA increased, the slopes of both lift curves were close to linear, with the wind tunnel lift data increasing at a faster rate than the CFD lift data. The wind tunnel lift numbers were higher than the CFD lift numbers at all data points. The lift numbers were even higher than the faulty axial force would cause (31% higher at a 6-degree AOA). This implied that a wind tunnel test of the full-scale aircraft would at least meet, if not exceed, the 15-pound lift we achieved in the CFD simulation at a 3-degree AOA.

The raw moment data from the wind tunnel needed to be converted to the moment around the aerodynamic center. This was done using the formula previously listed above, $P_{m_{ref}} = N\left(\frac{P_m}{N} + A - C\right)$. When comparing the wind tunnel and CFD moment results, there is no clear correlation between the two. The wind tunnel results are very close to zero, at -0.005 lbf-ft or less, but the CFD results were generally five times greater or more in magnitude (Figure 102, below). This difference in results in low confidence for our CFD model with regards to the moment data of the aircraft.

Overall, the drag and moment data from the CFD modeling may prove to be inaccurate and lead to catastrophic failure during actual flight testing of the aircraft due to poor longitudinal stability. We will need to proceed slowly and very deliberately to minimize the potential to crash the aircraft during future testing sessions.

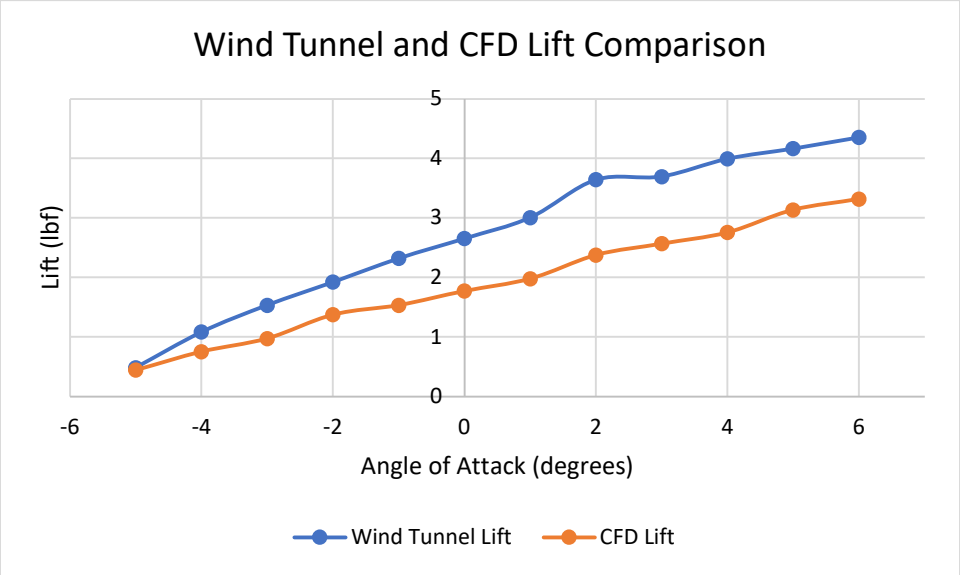

Figure 101: Wind Tunnel and CFD Lift Comparison

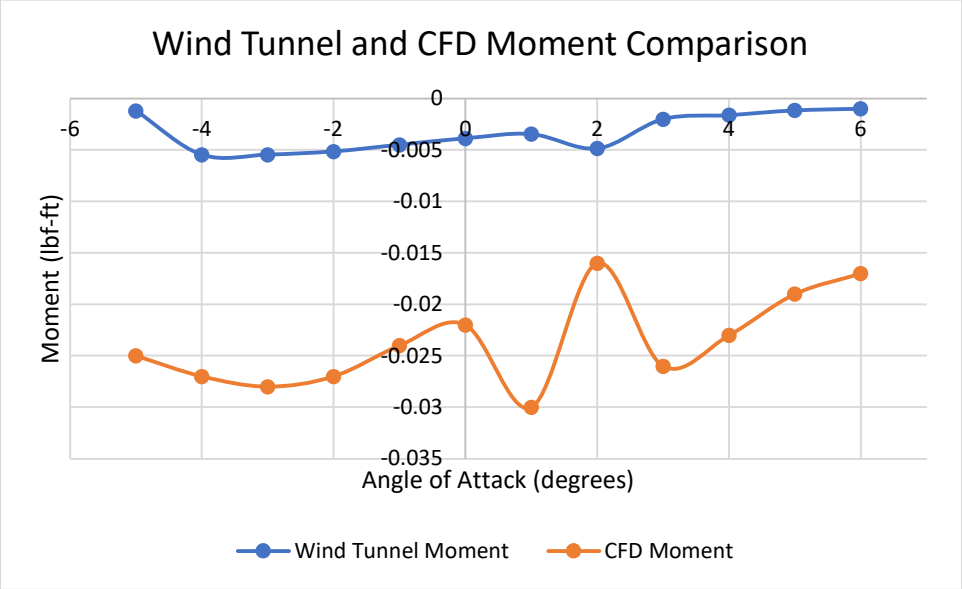

Figure 102: Wind Tunnel and CFD Moment Comparison

Chapter 11: Results and Discussion

While the results will not be validated until the aircraft flies, all the CFD modeling suggests that the design should work and meet most of the design requirements with this first design iteration. The one requirement that we might not meet is the endurance requirement of 2.5 hours, achieving only 68.4% of that goal, theoretically. CFD modeling strongly suggested that the aircraft design would be able to cruise at a maximum weight of 15 lbs at a 3-degree AOA at the required crise speed of 20 m/s while maintaining a stall speed less than 15 m/s. It is currently unknown if the flying wing will reach the maximum required speed of 30 m/s. More simulations would need to be done under 30 m/s flow conditions, along with propellor/motor calculations to see if they could maintain the required thrust. However, it was generally believed by the team that the motors were almost excessively powerful, according to the manufacturer's specification data [14], and would have no trouble achieving the required airspeed.

The ability to manufacture the aircraft is another consideration as a measure of success for this project. Currently, the fuselage has been manufactured, after working on some kinks with the 3-D printing process (Figures 103 and 104, below). However, the hot wire cutting of the foam wings has presented problems due to the combination of taper and twist with the wings. This process is currently being refined and the outlook for producing the wings to specification is positive.

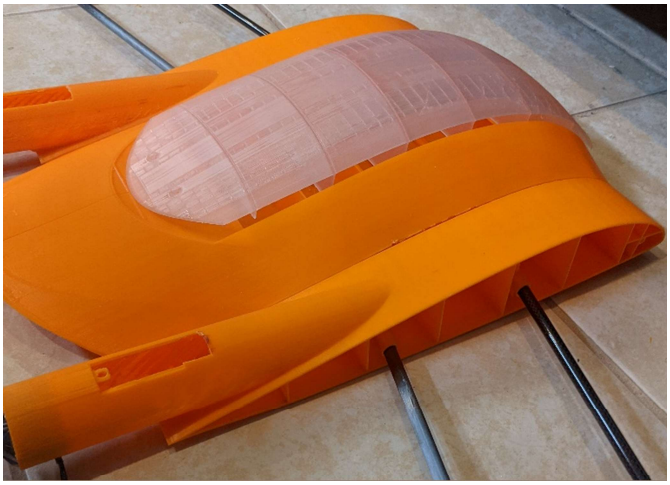

Figure 103: 3-D Printed Aircraft Body Displaying the Access Panel and Wing Root Structure.

Figure 104: 3-D Printed Aircraft Body Displaying a mounted Motor and Battery Fit.

While the current state of the design appears to meet the client's requirements, there is lots of room for refinement. This process was not rushed, but it was a project that could have used a lot more time to test configurations in more detail and with different setups. For example, we did not have time to go back and refine the airfoil selection once we changed the angle of incidence and washout for the wings. If the flight tests prove that the moment is too large and the aircraft is unstable, or if the drag is too great but there is an abundance of lift, airfoil selection can be revisited. There are many other factors that can be addressed to improve efficiency and the overall feeling is that this aircraft should work and should work well, but that its efficiency can be improved by a lot more. With that thought in mind, with improvements to the base design, it may very well be possible to achieve the endurance requirement that this version failed to meet.

Chapter 12: Conclusion and Recommendations

12.1) Conclusion

Our group was tasked with designing an unmanned aerial vehicle (UAV) that would be used for object tracking and surveillance. There were many requirements given to us by our project sponsor, including that the UAV be a flying wing design with an endurance of 2.5 hours, obtain speeds of 30 m/s, have a maximum payload of 15 pounds, and have a successful test flight. We were certainly challenged in our design with the given requirements. Flying wing designs are typically less stable than traditional aircraft so we had to account for those instabilities early on in our design. Additionally, we faced many difficulties in meeting the 2.5-hour endurance that our sponsor requested. Many hours were spent iterating on our initial aircraft design to attempt to meet all the sponsor's needs. However, due to time limitations, we could not get our UAV to fly to for 2.5 hours. Instead, we calculated a maximum endurance of around 1.7 hours. We did find this comparable given our time and resource limitations. While most other requirements were met, we did not get to have a successful test flight. The semester quickly came to an end and we realized that preparing for field testing was going to be too much to accomplish with such a short timeline. Despite not being able to field test prior to the submission of our project, we do plan on field testing the completed model with our sponsor at a later date.

Overall, we are extremely satisfied with our efforts in designing a flying wing UAV. There were many hurdles that we faced over the course of the semester, but we are pleased with where our hard work brought us. The knowledge that we gained from our project will certainly be an asset as we all transition into our engineering careers.

12.2) Recommendations

In the future, it would be desirable to revisit the airfoil selection process to ensure the best possible airfoil selection for minimum lift, stability, and efficiency. We feel that the process of meeting minimum requirements combined with the time constraints of the semester rushed the process somewhat. For example, once we found a wing configuration that worked well and provided the proper lift, we never went back to test the original airfoils on the new wing configuration. It might also be possible to refine the design for greater ease of manufacture, as the current version has presented some difficulty in manufacturing the wings.

In addition, different winglet configurations could also be explored. Designs that protrude below the wing were not desirable for this aircraft due to the belly-landing requirement, but there are still many other winglet designs that could possibly improve performance.

It may also be possible to change the motor/propeller configuration to a single motor setup. This may improve efficiency and allow future designs to meet the endurance requirement. It would be worth examining this option in more detail since it would also be easier to incorporate the motor mount and improve the aerodynamics of the aircraft. The current two-motor setup has aerodynamic inefficiencies where the current motor mounts meet the body of the aircraft. If the two-motor design is retained, this area of the body needs to be revised to improve the airflow over its surface.

The final recommendation for future projects would be to set as few restrictions on the design as possible, limiting design requirements to performance only and not a particular body style. Freedom of design would have enabled the group to explore simpler models that would meet the performance requirements and be much easier to design and manufacture.

References:

[1] "12x8.5F." *APC Propellers*, 27 Jan. 2020, www.apcprop.com/product/12x8-5f/.

[2] AEROLAB 12 x 12 Educational Wind Tunnel System Operating Instructions. AEROLAB.

[3] Airfoil Tools, Feb. 2021, airfoiltools.com/.

[4] "Bramor MSX." *C*, www.c-astral.com/en/unmanned-systems/bramor-msx.

[5] Costa, Alfred, et al. "Design and Construction of a Remote Piloted Flying Wing." Nasa Technical Reports Server, Worcester Polytechnic Institute, 2 May 1994, ntrs.nasa.gov/api/citations/19950006282/downloads/19950006282.pdf.

[6] "EBee X." *SenseFly*, 18 Feb. 2021, www.sensefly.com/drone/ebee-x-fixed-wing-drone/.

[7] Erdozain, et al. IN-FLIGHT RECONFIGURABLE HYBRD UNMANNED AERAL VEHICLE.

[8] Faisandier, Alan, et al. "System Requirements." *Sebokwiki*, Lockheed Martin, 30 Oct. 2020, www.sebokwiki.org/wiki/System_Requirements.

[9] GONGZHANG, HANLIN, and ERIC AXTELIUS. "Aircraft Winglet Design: Increasing the Aerodynamic Efficiency of a Wing." Digitala Vetenskapliga Arkivet, KTH Royal Institute of Technology, 2020, www.diva-portal.org/smash/get/diva2:1440647/FULLTEXT01.pdf.

[10] Hamada, Ahmed, et al. "Design, Build and Fly a Flying Wing." Athens Journal of Technology & Engineering, vol. 5, no. 3, 2018, pp. 223–250., doi:10.30958/ajte.5-3-2.

[11] Hepperle, Martin. Basic Design of Flying Wing Models, www.mh-aerotools.de/airfoils/flywing1.htm.

[12] Kelayeh, Ruhollah Karimi, and Mohammad Hassan Djavareshkian. "Aerodynamic Investigation of Twist Angle Variation Based on Wing Smarting for a Flying Wing." Chinese Journal of Aeronautics, Elsevier, 16 Mar. 2020.

[13] Maughmer, Mark D. "THE DESIGN OF WINGLETS FOR LOW-SPEED AIRCRAFT." Technical Soaring: An International Journal, vol. 30, no. 3, July 2006, pp. 61–73., journals.sfu.ca/ts/index.php/ts/article/view/187/172.

[14] *MN4012 KV480_Navigator Type_Motors_Multirotor_T-MOTOR Store-Official Store for T-Motor Drone Motor,ESC,Propeller*, store-en.tmotor.com/goods.php?id=346.

[15] "NewZeta FX-79 Buffalo FPV 2m Wing INav." Carbonbird.com, www.carbonbird.com/products/zeta-fx-79-buffalo-wing-new-version-inav-au-usa.

[16] P-Themes. “Believer UAV Ready To Fly.” UAV Systems International, uavsystemsinternational.com/products/x8-long-range-surveillance-drone-1.

[17] Piacenza, Joanna. “Increased Support for Buying 'Made in America' Goods.” *Morning Consult*, Morning Consult, 22 Nov. 2017, https://assets.morningconsult.com/wp-uploads/2017/11/made-in-america-2.png

[18] RAYMER, DANIEL. AIRCRAFT DESIGN: a Conceptual Approach. 6th ed., AMER INSTITUTE OF AERONA, 2018.

[19] Siegmann, Hartmut. “Airfoil Database for Tailless and Flying Wings.” For Tailless and Flying Wings, Feb. 2021, www.aerodesign.de/english/profile/profile_s.htm.

[20] “SkyWalker X8 (2.120mm) FPV/UAV Flying Wing KIT.” OneDrone.com - Your One Stop Drone Shop., www.onedrone.com/store/skywalker-x8-2-120mm-fpv-uav-flying-wing-kit.html.

[21] “Turnigy High Capacity 10000mAh 4S 12C Lipo Pack w/XT90.” *Hobbyking*, hobbyking.com/en_us/turnigy-high-capacity-10000mah-4s-12c-multi-rotor-lipo-pack-w-xt90.html?queryID=23e6e294729af4546146030a345ec71b&objectID=78424&indexName=hbk_live_magento_en_us_products.

[22] “Turnigy High Capacity 20000mAh 6S 12C Lipo Pack w/XT90.” *Hobbyking*, hobbyking.com/en_us/turnigy-high-capacity-battery-20000mah-6s-12c-drone-lipo-pack-xt90.html.

[23] “UAV Factory: Penguin C UAS.” *UAV Factory | Penguin C UAS*, uavfactory.com/en/penguin-c-uas.

[24] Van de Kerckhove, Koen. “Special: Horten Flying Wings.” Special: Horten Flying Wings - Nest of Dragons, Van De Kerckhove, Koen, 1 Mar. 2021, www.nestofdragons.net/weird-airplanes/flying-wings/special-horten-flying-wings/.

[25] Witzigreuter, John. “Flying Wing UAV.”

[26] Yaakob, et al. “Development of Multiple Configuration Flying Wing UAV.” International Conference on Computer and Drone Applications, 16 Mar. 2020.

[27] “Zeta FX-61 Phantom FPV Flying Wing V2.” Team Legit, team-legit.com/Zeta-FX-61-Phantom-FPV-Flying-Wing-V2_p_1524.html.

Appendix A: Acknowledgements

The Kennesaw High Altitude Lightweight Inspection Device Team would like to give our gratitude to John Witzigrueter for sponsoring and assisting us with our flying wing UAV design. John has provided us with numerous resources over the course of our project such as access to equipment needed to build our design as well as purchasing the electronics required for the final design of our aircraft. Additionally, John was able to provide valuable feedback at each stage of design processes.

Appendix B: Contact Information

Sponsor:

John Witzigreuter
Inspired Products, LLC.
john@inspiredproductsglobal.com
404-509-1779

Team:

Kristen Padgett
Project Manager, Systems Engineer
Kristennpadgett@outlook.com
770-713-3949

Scott Semmelink
Project Coordinator, Technical Reviewer
Scott.semmelink@gmail.com
910-916-6419

Paul Horne
Technical Aircraft Expert
PJHorne91@gmail.com
470-538-1819

Jared Lasley
Data Analyst, Mathematician
LasleyJared@gmail.com
404-901-4337

Appendix C: Reflections

Paul Horne: This project has helped me to connect my previous knowledge of airfoils and small aircraft electronics to the data and mathematics behind it all. It has also helped me to learn new skills such as modeling airfoils in SolidWorks. This has been my first experience working within client design requirements for an engineering project, and it has given me insight into the importance of prioritizing customer requirements. The vast amount time required in literature research, design optimization, and computational analysis before ever creating a physical model have helped me to better understand the steps required in the engineering design process and the reliance on interdisciplinary teams. The experience in developing a model for wind tunnel testing allowed me the opportunity to hone my skills in 3D print manufacturing and its associated unpredictable tolerances. Lastly, working on this project while simultaneously taking Aircraft Design has helped to solidify the concepts learned in that class.

Scott Semmelink: I enjoy the challenge of solving a problem and I enjoy learning. This project has brought me both. Each time things looked bleak, I have kept pushing and looking for the mistake or what was overlooked or why it was coming out that way when I just know it should not. I just kept trying to solve the puzzle. The task of learning new methods and concepts of both flying wings and electrical aircraft was both frustrating and a joy. I certainly feel like this would have been so much easier if it were only a traditional aircraft with a tail instead of a flying wing. I am anxious about testing of our aircraft. Even though I have poured a lot of hours and research into the design, modeling process, and CFD analysis, I still am unsure if what I did was correct, and I am rarely this unsure. Ultimately there is only one way to find out how well we designed this aircraft, and that is for it to fly.

Jared Lasley: Working on the flying wing UAV has been an insightful experience. I have enjoyed learning to apply the design concepts and techniques that we have been taught through the aerospace engineering minor. Additionally, I have enjoyed being able to put the mathematics I have learned in my major into practice. It is a wonderful feeling after years of learning proofs to be able to design and fabricate a solution to a real-world problem. Further I have learned a great deal about the collaboration required to bring an aircraft to fruition. Between subject matter experts, wind tunnel testing, and customer feedback I can now better appreciate all the moving pieces required to bring projects such as this into reality. Unfortunately, due to time constraints the initial test flight of this aircraft will not be possible before the submission of this paper, however I am excited for the day when it will finally take to the sky.

Kristen Padgett: I have enjoyed getting to work on the design of our flying wing UAV. I find that being the project manager has allowed me to gain great leadership skills that I know will be beneficial as I start my engineering career. Additionally, I have been able to put my field experience and academic experience into use as the system engineer for the team. It has been a pleasure getting to be a part of not only designing a UAV but also constructing a model to test in a wind tunnel. While we did not get to

fabricate and test our design before the competition of this project and report, I do look forward to field testing our final design to see our hard work come to fruition.

Appendix D: Challenges Faced

Meeting Sponsors Needs and Requirements: The requirements given by the sponsor have been somewhat of a challenge for us to meet. Our model currently appears to be capable of meeting most requirements, but we have not been able to meet the endurance requirement of two and a half hours. We believe that with multiple iterations in design, the aircraft design could be optimized the meet the endurance requirement.

Fuselage Sizing to Fit Batteries Given by Sponsor: We had some issues sizing the fuselage due to the sponsors pre-purchased batteries being larger than expected. To compensate for the large batteries, we decided to find a larger airfoil to use for the blended body and wing design. This will allow for ample battery space.

Ambitious Initial Planning: We were very ambitious in our initial planning and did not consider the deadlines being too tight to meet. We ended up having to go back through and redo our schedule a few times to update due to lack of experience in scheduling a project like ours.

Modeling Software in SolidWorks: Solidworks proved to be more difficult to use than anticipated. It was challenging to collaborate as a group while using Solidworks as the main tool for creating our model. It proved to be very time consuming to develop and run our model, with the model being difficult to manipulate while attempting to perform accurate simulations. To overcome this, we watched many video and written tutorials.

One Student with KSU Aero Lab Access: We found it challenging to manage only one group member having access to the aero lab. There were a few occasions where one team member just needed to go in to double check sizing or make sure the 3D model fit on the mount and it was difficult to manage schedules to find a time that worked best for everyone. We do see the need for restrictive access with such expensive equipment but still did list it as a challenge because of the schedule setbacks we faced.

Challenges in Setting Up Wind Tunnel Test Time: When we were looking to access the wind tunnel, the subject matter expert for the wind tunnel was limited in availability. We did find that it was a challenge getting plans solidified to wind tunnel test because of the limited availability. This did end up pushing our overall schedule behind about a week.

Appendix E: Wind Tunnel Testing Data

Measurement	Pitch Angle (deg)	Air speed (mph)	Lift (lbf)	Drag (lbf)	Moment (in-lbf)	Testing Notes
	Input Variables		Measured Variables			
1	-5	100	0.19	0.11	0.37	
2	-5		0.19	0.1	0.37	
3	-5		0.18	0.11	0.36	
1	-4		0.71	0.16	1.31	
2	-4		0.7	0.16	1.31	
3	-4		0.69	0.15	1.28	
1	-3		0.97	0.15	1.85	
2	-3		0.97	0.15	1.86	
3	-3		0.97	0.15	1.85	
1	-2		1.23	0.12	2.38	
2	-2		1.23	0.15	2.38	
3	-2		1.24	0.14	2.4	
1	-1		1.55	0.08	3.03	
2	-1		1.56	0.08	3.05	
3	-1		1.51	0.09	2.95	
1	0		1.73	0.05	3.42	
2	0		1.74	0.05	3.44	
3	0		1.67	0.05	3.29	
1	1		1.97	-0.01	3.91	
2	1		2	-0.01	3.97	
3	1		1.98	-0.01	3.93	
1	2		2.24	-0.08	4.48	
2	2		2.24	-0.09	4.48	
3	2		2.24	-0.09	4.48	
1	3					No data: forgot to measure at this pitch angle
1	4		2.62	-0.29	5.37	
2	4		2.63	-0.3	5.4	
3	4		2.61	-0.3	5.35	
1	5		2.88	-0.38	5.94	
2	5		2.92	-0.39	6.01	
3	5		2.91	-0.39	6	
1	6		2.93	-0.51	6.06	
2	6		2.99	-0.52	6.18	
3	6		2.91	-0.52	6.02	
1	7		3.14	-0.61	6.51	
2	7		3.19	-0.62	6.59	
3	7		3.17	-0.62	6.54	

Measurement	Pitch Angle (deg)	Air speed (mph)	Lift (lbf)	Drag (lbf)	Moment (in-lbf)	Testing Notes
1	-5		0.48	0.16	1	
2	-5		0.47	0.14	0.97	
3	-5		0.48	0.11	0.99	
1	-4		1.07	0.23	2.09	
2	-4		1.07	0.28	2.1	
3	-4		1.07	0.27	2.11	
1	-3		1.54	0.22	3.02	
2	-3		1.52	0.25	2.98	
3	-3		1.52	0.23	2.99	
1	-2		1.92	0.19	3.78	
2	-2		1.9	0.21	3.74	
3	-2		1.94	0.23	3.83	
1	-1		2.33	0.12	4.62	
2	-1		2.35	0.13	4.68	
3	-1		2.28	0.17	4.53	
1	0		2.68	0.02	5.37	
2	0		2.66	0.07	5.33	
3	0		2.63	0.06	5.26	
1	1		3.01	-0.02	6.05	
2	1	120	3.02	-0.07	6.09	
3	1		2.99	-0.06	6.02	
1	2		3.63	-0.18	7.22	
2	2		3.66	-0.16	7.26	
3	2		3.63	-0.19	7.12	
1	3		3.75	-0.31	7.69	
2	3		3.66	-0.29	7.5	
3	3		3.65	-0.32	7.48	
1	4		4.05	-0.43	8.34	
2	4		3.91	-0.42	8.06	
3	4		3.96	-0.46	8.15	
1	5		4.14	-0.55	8.57	
2	5		4.08	-0.56	8.45	
3	5		4.18	-0.56	8.66	
1	6		4.31	-0.66	8.96	
2	6		4.33	-0.71	8.97	
3	6		4.28	-0.67	8.88	
1	7					No data: model kept spinning at this point so we ended the testing
	Maximum pitch angle is +- 30 degrees	Not to exceed 120 mph				

Appendix F: Contributions

Chapter	Contributor
Executive Summary	Jared Lasley
Chapter 1: Flying Wing UAV for Surveillance and Object Tracking	Jared Lasley, Paul Horne
Chapter 2: Literature Review	Paul Horne, Scott Semmelink
Chapter 3: Project Management	Kristen Padgett
Chapter 4: Airfoil Selection	Scott Semmelink, Jared Lasley, Kristen Padgett
Chapter 5: Airfoil Analysis	Scott Semmelink
Chapter 6: Wing Composition and Modeling	Scott Semmelink, Paul Horne
Chapter 7: Weight and Sizing	Scott Semmelink, Jared Lasley
Chapter 8: Final Aircraft Design	Scott Semmelink
Chapter 9: Center Wing and Components	Paul Horne, Jared Lasley
Chapter 10: Wind Tunnel Testing	Paul Horne, Kristen Padgett, Scott Semmelink, Jared Lasley
Chapter 11: Final Thoughts and Recommendations	Paul Horne, Kristen Padgett, Scott Semmelink, Jared Lasley
Conclusion	Kristen Padgett
Appendices	Kristen Padgett

Figure 105: Contributions by Chapter

Kristen Padgett	Primary contributions were constructing requirements, ensuring requirements were being met, developing wants versus needs from the customer, coordinating meetings, coordinating testing plans, developing test procedures, ensuring deadlines were being met, other necessary project management tasks, and helped perform research for airfoils and winglets.
Scott Semmelink	Flying wing theory research, electric aircraft research, aircraft sizing, airfoil selection, wing design and analysis, aircraft body design and analysis, wing-body integration, full-scale modeling, all CFD modeling, locating the aerodynamic center through use of CFD, wind tunnel testing and data analysis.
Jared Lasley	Primary contributions were writing the executive summary, writing the aircraft introductions and justifications, performing market research, performing scholarly research, preliminary airfoil research, winglet research and analysis, component weight calculations, avionics selection rationale, and wind tunnel testing.
Paul Horne	Primary contributions were aiding in the design process through previous radio-controlled electric aircraft experience, literature research, mission profile creation, initial SolidWorks modeling, electronics configuration and schematic, designing and 3D print manufacturing of wind tunnel test model, wind tunnel testing visual documentation, designing of center body fuselage.

Figure 106: Detailed Technical Contributions